MECHANICAL ENGINEERING

MSc Dissertation

A novel method to evaluate synthetic fuel options for gas turbines in terms of O-ring swelling

Author:
Shehzaad Visram

Supervisor:
Adj. Prof. Andy Yates

Co-supervisor:
Dr Chris Woolard

September 2009

DECLARATION

I know that plagiarism is wrong. Plagiarism is to use another's work and pretend that it is one's own.

I have used the **IEEE convention** for citation and referencing. Each significant contribution to, and quotation in this report from the works of other people has been attributed, and has been cited and referenced.

This project and report is my own work.

I have not allowed, and will not allow anyone to copy my work with the intention of passing it off as his or her own work.

Shehzaad Visram

ACKNOWLEDGEMENTS

The author wishes to thank the following people for their time, invaluable advice and support during this research project:

Adj. Prof. Andy Yates - Project supervisor;

Dr Chris Woolard - Project co-supervisor;

Mark Wattrus, for his assistance in designing of the experimental apparatus and general electronics;

Carl Louis Viljoen, Mariam Ajam and Mazwi Ndlovu for their precious time, guidance and knowledge throughout my research project;

Department of Chemistry - Dr Gerhard Venter, for his assistance in computational modelling;

Mr Gavin Tomlinson - SAFL Laboratory Technician;

Many thanks to the UCT Knowledge Commons technical staff member, **Miss Nuroonisa Ismail** for her support in formatting my thesis;

I would like to thank my girlfriend, **Miss Ashwina Dhunnoo** and my parents **Mr and Mrs Visram and family** for their personal advices, encouragement and support in all aspects of my research;

Sasol Technology Fuels Research for sponsoring this research project.

EXECUTIVE SUMMARY

Background

Before 1999, all commercial aviation fuel had been produced from petroleum feedstock. With the growth in demand, it has put significant strain on the availability of jet fuel at Oliver Tambo International Airport (ORTIA). In 2008, Sasol was granted an approval to use fully synthetic jet fuel upon the publication of Defence Standard 91-91, Issue 6 [1]. Sasol's fully synthetic jet fuel is the only fuel in the world which had obtained the necessary approval for commercial use. The DEF STAN had an 8% minimum aromatic limit in the final blend. Sasol produces fully synthetic jet fuel from its Fischer-Tropsch process and the latter is the source of synthesised paraffinic kerosene (SPK). SPK typically contain iso paraffins and small quantities of normal paraffins. However, they do not contain heteroatomic species or aromatic compounds. Advantages of the use of F-T fuels over petroleum-derived fuels include outstanding thermal-oxidative stability characteristics with relatively lower particulate matter (PM) combustion emissions. The lack of aromatics causes a decrease in the tendency of the fuel to swell nitrile O-rings. This is of particular concern as the transition of synthetic fuels to conventional fuels can result in fuel leakage and elastomer shrinkage in fuel distribution systems.

Objectives

The primary focus of this project was to develop a method to evaluate the swelling performance of potential additives that can be blended in synthetic jet fuels. Since an elastomer compression rig that was available at the Sasol Advanced Fuel Laboratory (SAFL) at the University of Cape Town (UCT), it could provide a performance parameter was required to investigate the swelling behaviour of

nitrile elastomers in additised synthetic jet fuels which could be compared to petroleum-derived jet fuel. Once the performance parameter was decided upon, an experimental procedure was developed to investigate the behaviour of nitrile rubbers through switching of fuels.

Experimental Procedure and Apparatus

The elastomer compression rig, which was designed and modified at the SAFL, used a pneumatically driven piston to periodically compress an O-ring in six modules within the constraints of the O-ring groove which was machined to the dimensions for a static flange seal. The tests were conducted for seal swell performance and switch load experiments in (SPK), SPK blended with potential swelling additives and petroleum-derived Jet A-1. Seal swell performance tests were conducted at 50°C for 150 hours while switching of fuels was done after every 48 hours. The standard test method for Rubber Property - Effect of Liquids (ASTM D471-06) [2] was used as a basis for the bench swell experiments which involved weighing of samples before and after immersions in fuel. Computational modelling using density functional theory was performed to predict interaction energies of various model fuel molecules.

Discussion of Results

Measurements in pure solvents that were tested in the current study revealed that oxygenates such as benzyl alcohol displayed the highest percentage mass change, even higher than aromatic hydrocarbons (tetralin and toluene). Oxygenates have a high solubility parameter but this alone cannot account for the observed high swelling of oxygenates. It is rather the low difference in the solubility parameters between the oxygenate and the NBR that can account for high volume swell. This result was consistent with binding energies predicted by molecular modelling (cf. Figure 5.2). The optimised geometry of benzyl alcohol with isobutylnitrile showed a specific interaction (hydrogen bonding) between the hydroxyl group (- OH) of benzyl alcohol and the nitrile group (- CN) of isobutylnitrile.

Nitrile elastomers were shown to swell significantly more in Jet A-1 when compared to SPK. Measurement of static volume swell with additised SPK revealed that concentrations of benzyl alcohol as low as 1-2% is required to achieve greater swell than Jet A-1. The poor swelling behaviour of hexylbenzenes blended in SPK suggested that compounds containing an aromatic ring with a longer saturated group attached to the ring behave intermediately between aliphatic and aromatic compounds. Furthermore, it was suggested that shorter alkylbenzenes (toluene) would require lower concentrations to swell NBR O-ring than the longer alkylbenzenes (hexylbenzenes) used in the current study.

Experimental results from the compression rig expressed in terms of normalised expansion also revealed that Jet A-1 has a better swelling performance compared to SPK. Normalised expansion measurements of SPK additised with 8% toluene indicated similar swelling to Jet A-1 suggesting that toluene has a significant effect on the swelling performance of SPK. SPK additised with tetralin has also revealed similar seal performance to Jet A-1. It was suggested that the swelling performance of SPK is dependent on the concentration of tetralin in the final blend.

The switch load experiments highlighted the difference when switching from Jet A-1 to SPK and vice versa. Nitrile O-ring behaves differently in fuels with different hydrocarbon composition. Shrinkage of an O-ring switching from Jet A-1 to SPK was suggested to be caused by aromatics which had diffused into the polymer during the initial Jet A-1 immersion followed by removal of the same aromatics together with some plasticisers when switched to SPK.

SPK additised with 0.5% benzyl alcohol also resulted in shrinkage of O-rings when the fuel was switched from Jet A-1 to SPK additised with 0.5% benzyl alcohol. Nonetheless, SPK containing 2% benzyl alcohol has an opposite effect to 0.5% benzyl alcohol suggesting that concentration of 2% benzyl alcohol in SPK showed greater swell than the aromatics present in Jet A-1. Results from the elastomer rig displayed some differences in seal performance measurements for additised SPK compared to static measurements. It was suggested that difference in the rubber/solvent ratio and the operating temperature conditions affects the diffusion kinetics of some solvents which are blended in SPK.

Conclusion

A novel method was developed to assess switch load performance of fuels in an elastomer compression rig under dynamic condition as opposed to static switch load measurements. The static switch load measurements were in agreement with the elastomer switch load rig measurements for pure SPK. It was concluded that caution should also be taken when comparing the static switch load measurements to the rig switch load measurements. This is because rig measurements were done in a dynamic environment compare to bench measurements which were conducted in a static environment.

It was suggested that 1-2% benzyl alcohol was enough to act as a potential swelling additive in SPK. Furthermore, it was concluded that SPK blended with low solubility parameter, longer alkylbenzenes such as hexylbenzenes would not provide adequate swelling compared to higher solubility parameter, shorter alkylbenzene such as toluene. Furthermore lower solubility parameter aromatics would require greater quantities for an equal amount of swelling.

CONTENTS

CHAPTER 3

CHAPTER 4

CHAPTER 5

APPENDIX C

APPENDIX D

LIST OF FIGURES

LIST OF TABLES

LIST OF ACRONYMS

BA–	Benzyl Alcohol
CV–	Coefficient of Variation
DFT –	Density Function Theory
Di-EGME –	Diethylene Glycol Monoethyl Ether
DOA –	Dioctyladipate
DoD –	Department of Defence
DOP –	Dioctylphthalate
ECD –	Emission Control Diesel
EVA–	Ethylene co-Vinyl Acetate
FAME –	Fatty Acid Methyl Ester
F-T –	Fischer-Tropsch
FTIR –	Fourier Transform Infrared Spectroscopy
GC-MS –	Gas Chromatography-Mass Spectroscopy
HB –	Hexylbenzene solvent
HNBR –	Hydrogenated Nitrile Rubber
HSP –	Hansen Solubility Parameter
HTFT –	High Temperature Fischer-Tropsch
IPK –	Iso-Paraffinic Kerosene
λ, Lambda –	Normalised expansion
LTFT –	Low Temperature Fischer-Tropsch
MO –	Molecular Orbital

NR –	Natural Rubber
NBR –	Nitrile Rubber
ORTIA –	Oliver R.Tambo International Airport
PM –	Particular Matter
SAFL –	Sasol Advanced Fuel Laboratory
SMDS –	Shell Middle Distillate Synthesis
SPD –	Slurry Phase Distillate
SPK –	Synthesised Paraffinic Kerosene
SSJF –	Semi-Synthetic Jet Fuel
XLD –	Crosslink Density

CHAPTER 1

INTRODUCTION

1.1 Background

Before 1999, all commercial aviation fuel has been produced from petroleum feedstock [3]. As jet travel and consequently jet fuel demand has risen, there was a significant strain put on the availability of jet fuel at Oliver R. Tambo International Airport (ORTIA). As of 1999 the only sources of petroleum-based jet fuel that could meet the demand for jet fuel at ORTIA were the nearby Sasol/Natref refinery in Sasolburg and two coastal refineries, further away in Durban. At the time the Natref refinery had reached its maximum production capacity, while the coastal refineries had serious logistical constraints given their geographic location with respect to Johannesburg [4]. In 1999, Sasol was granted an approval to blend synthetic kerosene up to 50% with a Merox-treated jet fuel from petroleum derived sources to make a semi-synthetic Jet A-1 aviation kerosene under DEF STAN 91-91/Issue 3 [4]. In 2008, Sasol was granted a further approval to produce fully synthetic jet fuel upon the publication of Defence Standard 91-91, Issue 6 [1]. Sasol's fully synthetic jet fuel is the only fuel in the world which has currently obtained the necessary approval for commercial use. A significant requirement in DEF STAN 91-91, is that both the fully and semi-synthetic jet fuel must meet a specification of a minimum 8% aromatic compounds in the final blend [1]. The figure below shows a picture of Sasol's Tiger jet with a South African Airways (SAA) Boeing.

Figure 1.1: A L29 Sasol Tiger jet with the SAA's Boeing 747-200, "Lebombo" in the background

Fischer-Tropsch (F-T) fuels typically contain iso- and normal paraffins and do not contain heteroatomic species or aromatic compounds. Some of the advantages of F-T fuels over petroleum-derived fuels are their outstanding thermal-oxidative stability characteristics and relatively low particulate matter (PM) combustion emissions [5]. F-T fuels have displayed a reduction of emissions such as soot and sulphurous oxides. This is the result of an absence of aromatics, sulphur and heteroatomic compounds in the fuel.

On the other hand, the absence of aromatics causes a decrease in the tendency of the fuel to swell nitrile O-rings. This is of particular concern as the transition of synthetic fuels to conventional fuels could result in elastomer shrinkage in fuel distribution systems leading to fuel leakage and possible engine fires [6].

One of the ways to reduce this potential seal swell problem is to blend a suitable amount of aromatic compounds with the synthetic fuel in order to enhance its swelling characteristics.

This route, however, would increase both the production cost and the susceptibility of the fuel to generate soot. A natural question that then arises is which aromatics should be used. In particular, do all aromatics impart similar swelling behaviour to O-rings, or do some aromatics swell more than others? Consequently could some aromatic compounds be blended in lower quantities, possibly even below the DEF STAN limit to produce sufficient O-ring seal swell [6].

1.2 Project Objectives

The following were the objectives of this project:

- To study the literature on potential swelling additives and their compatibility with synthetic jet fuels.
- To explore potential swelling additives that could be blended into synthetic jet fuels.
- To study the performance parameters of an elastomer compression rig that was built specifically for this project.
- To investigate the swelling performance of an additised synthetic jet fuel and compare with a commercial jet fuel.
- To perform experiments which involve switching of fuels between additised synthetic jet fuel and conventional jet fuel (switch load).

1.3 Project Scope and Limitations

The project covers work done on nitrile O-rings and solvents (potential additives). Sasol Synfuels and the Natref crude oil refinery supplied the required Merox petroleum derived and synthetic fuels. The scope of the project does not cover the design and modification of the elastomer compression rig, which was supplied by Sasol Advanced Fuel Laboratory (SAFL). However, the project does include the development of experimental procedure for switch load experiments. The latter was conducted on the elastomer rig and compared with the ASTM-Bench swell experiments.

1.4 Layout of this Report

Chapter Two begins with a literature review on the characteristics of synthetic jet fuel, fluid compatibility and existing literature on the physical properties and diffusion of solvents through an elastomeric material. This is followed by theories relating to solubility parameter and Flory-Rehner in **Chapter Three**. Experimental procedures and apparatus used in obtaining the mechanical and chemical data are presented in **Chapter Four**. The results obtained during experiments are presented in **Chapter Five** and are analysed and discussed in **Chapter Six.** Conclusions based on these findings are drawn in **Chapter Seven**. Recommendations on the future work are presented in **Chapter Eight**.

CHAPTER 2

LITERATURE REVIEW

This chapter reviews the literature regarding Low Temperature Fischer-Tropsch (LTFT) synthetic derived jet fuel and elastomer compatibility. This is a key research area for the synthetic jet fuel to be considered as "fit for purpose". It further discusses the theory underlying solubility parameters and its influence on the solvent-polymer thermodynamics.

2.1 Synthetic Jet Fuel from Fischer-Tropsch Processes

Aviation fuel used in jet engines predominantly consists of hydrocarbon compounds which contain 10-15 carbon atoms, typically in linear or slightly branched chains. Jet fuel is obtained from fractional distillation of crude oil by keeping the cut between 150°C and 275°C. It is also called kerosene. A kerosene cut may also be produced as a synthetic fuel from a synthesis process first developed in the 1920s known as Fischer-Tropsch [7]. Recently the United States Department of Defence (DoD) have been motivated to explore the use of F-T fuels in their aircraft as an alternative to crude-derived products. Interest in F-T fuels was raised because it could help alleviate energy dependence on the import of crude oil from distant (and possibly politically unstable) sources [8]. Coal-derived synthetic fuels for automotive purposes have been a reality since the early 1970s at Sasol in South Africa [7]. The F-T technology used involves either a High

Temperature Fischer-Tropsch (HTFT) process or a Low Temperature Fischer-Tropsch (LTFT) process. HTFT operates at temperatures between 310-340°C. The HTFT process is completed through various steps which involved the reforming of natural gas or gasification of coal to produce synthesis gas (hydrogen and carbon monoxide). In the HTFT process the synthesis gas (carbon monoxide and hydrogen) is converted over an iron based catalyst to an olefinic syncrude fraction (F-T syncrude). This fraction is then distilled into naphtha and distillate fractions. Following a further hydrotreatment, it is distilled to produce two distillates in the boiling range of diesel, viz. a light hydrotreated distillate and a heavy cracked diesel [9]. By contrast, the Sasol Slurry Phase Distillate (SPD) LTFT technology operates at lower temperatures which are usually between 210-260°C. Here the syngas is converted over an iron or cobalt catalyst to produce a mixture of straight chain paraffins, olefins and oxygenates (F-T syncrude). The Sasol SPD process incorporates three major processing steps towards the final synthetic fuel. The first step is the reforming of natural gas or gasification of coal to syngas which is then followed by the conversion of syngas to F-T syncrude. The F-T syncrude is then upgraded in the final step to the middle distillate using a hydroconversion and iso-cracking process. The third step is very important for the final product as it hydro-cracks the heavy hydrocarbons chains while the olefins and oxygenates are hydro-treated to paraffins [9].

LTFT fuel has a relatively high hydrogen to carbon ratio with ultra-low sulfur levels and almost zero aromatics. The low levels of aromatics and sulfur lead to significantly lower particulate matter (PM) combustion emissions than conventional petroleum-derived fuels [9]. This makes F-T distillate fuels ideally suited for environmental reasons [10].

One of the streams identified for the production of synthetic jet fuel is iso-paraffinic kerosene (IPK). Two other kerosene streams which contain fractions in the appropriate boiling range, hydrogenated distillate (lighter components) and hydrogenated naphtha (heavier components), are currently used to make diesel and gasoline fuel. Such streams could be blended at ratios which would meet the specification requirements for synthetic jet fuel [3]. Below is a schematic of Sasol's semi synthetic jet fuel production. Note that blending with petroleum-based jet fuel is omitted.

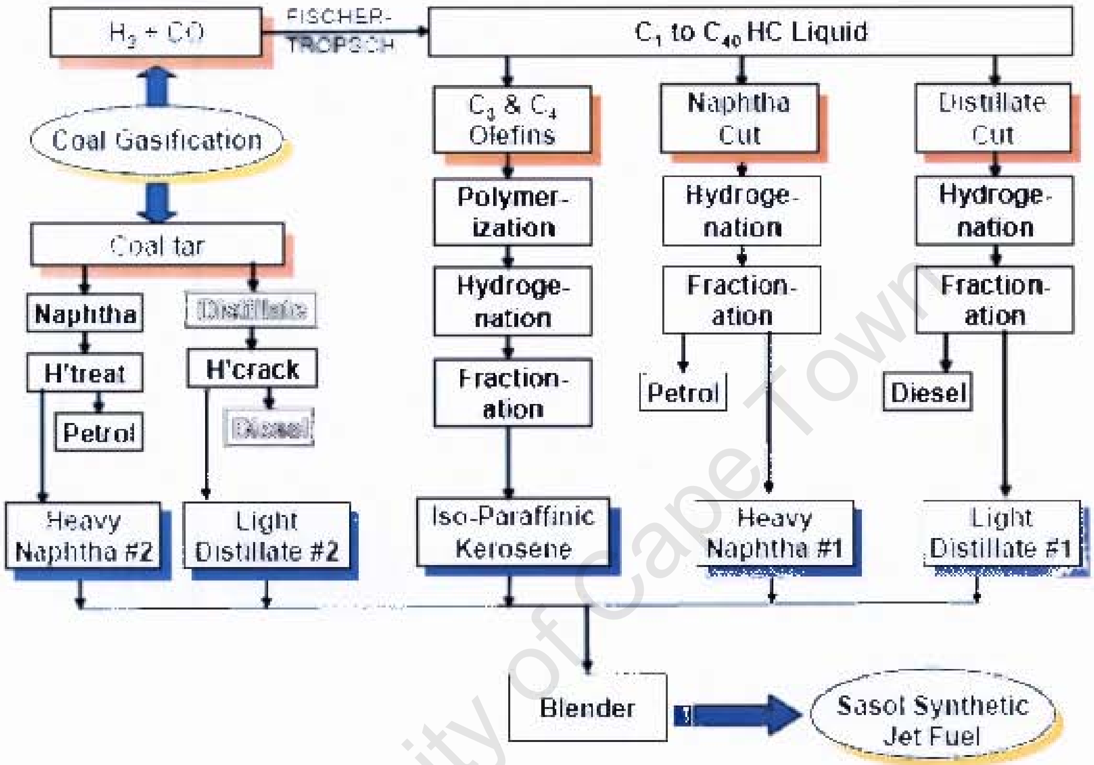

Figure 2.1: Sasol's semi synthetic jet fuel production scheme [3]

2.1.1 Historical Issues and Concerns with Synthetic Kerosene as Jet fuel

Sasol first considered introducing iso-paraffinic kerosene as a jet fuel in the 1980s. There were a few concerns at that time which were raised by the aviation industry. Some of those concerns were [4]:

- low lubricity
- no aromatics and hence poor seal swell
- low fuel density and hence low energy density

Lack of hetero-atoms such as sulfur species in the fuel reduces the tendency of the fuel to lubricate fuel distribution parts such as fuel pumps and fuel injectors. Lack of aromatic species reduces the ability of the fuel to swell elastomer seals such as O-rings. This is of particular concern as the transition of synthetic fuels to conventional fuels could result elastomer shrinkage in fuel distribution systems, in turn leading to fuel leakage and possible engine fires [6]. Fuel density is also important for the design and operations of aircraft. Most F-T fuels, as indicated earlier, are iso-paraffins and/or normal paraffins with no aromatic compounds. The lack of the latter results in such fuels failing to meet the required density specifications of 775kg/m^3 at 15°C [3].

2.1.2 Synthesised Paraffinic Kerosene (SPK)

Initially, SPK was known as Iso-Paraffinic Kerosene (IPK) which is the dominant blending component in SSJF. In an HTFT scheme, IPK is obtained from a specific range of olefins that have been distilled from the F-T syncrude. The process of producing IPK of the appropriate boiling range as jet fuel is to put the olefins through a polymerisation unit followed by hydrotreating and distillation [4].

As its name suggests, IPK is dominated by iso-paraffins, although it does contain some normal paraffins and even cycloparaffins. The carbon number distribution ranges between 10-13 carbon atoms. Consequently, the aviation industry has lately used a more appropriate name for IPK as Synthesised Paraffinic Kerosene (SPK), which makes a provision for all the synthetic paraffins contained in the kerosene [11]. Figure 2.2 below shows how the paraffinic hydrocarbons in a component of Sasol's synthetic F-T jet fuel are distributed.

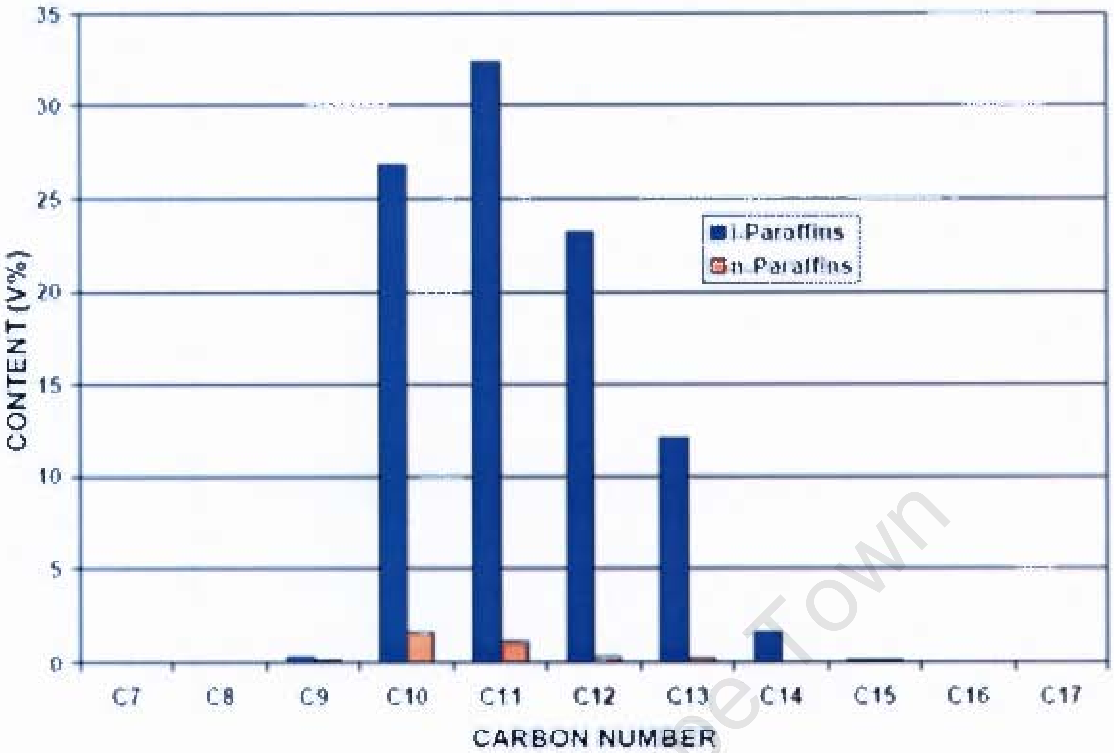

Figure 2.2: Volume percent of paraffinic hydrocarbons in synthetic jet fuel [4]

2.1.3 Other Synthetic Jet Fuels for Gas Turbine Engines

S-5 fuel is a fully saturated paraffinic hydrocarbon. It is a high flash point synthetic F-T jet fuel produced by the Syntroleum Corporation. They use their gas-to-liquids LTFT technology that converts natural gas into hydrocarbon fuel. S-5 fuel contains no aromatics. This is a representative of synthetic fuel that is produced from F-T process utilizing low temperature reactors [12]. It is more n-paraffinic in nature.

JP-900 is another synthetic fuel that is produced by hydrotreating of coal-tar/petroleum blends followed by hydrogenation at moderate temperatures. It is named for its high temperature stability (up to 900°F). The manufacturing process was first demonstrated in a pilot plant at the PARC Technical Services [13]. JP-900 is a thermally stable, coal derived fuel which contains no monoaromatics and heteroatomic compounds. Instead it contains cycloalkanes and a small quantity of two ring hydro-aromatics. JP-900 fuel is denser than typical jet fuels. High density cycloalkanes and hydro-aromatics compensate for volume-limited aircrafts. It has been reported that these multicyclic compounds provide thermal stability and also stabilise other fuel species by donating hydrogen to the reactive free radicals generated during oxidative decomposition reactions [13].

2.2 Conventional Petroleum Jet Fuel (Jet A-1)

The most common jet fuel used by the commercial aviation industry is Jet A-1. Jet A-1 is a U.S civil aviation turbine fuel found in the kerosene boiling range. Jet A-1 has a boiling range of approximately 149°C to 290°C. Furthermore it must have freezing point below -47°C [14].

The carbon distribution of Jet A-1 lies typically between 8 and 16 carbon atoms. Jet A-1 is a mixture of iso-paraffins, normal-paraffins and aromatics. The Jet A-1 that Sasol currently produces at its Natref refinery contains approximately between 18% aromatic species [2]. Figure 2.3 shows how the hydrocarbons are distributed in petroleum derived Jet A-1.

There are a number of other jet fuels that are usually used for military applications. The United States Department of Defence (DoD) (Army Air Force) uses a single kerosene based fuel in almost all of its gas turbine applications as long as they meet the Jet Propulsion 8 (JP-8) specifications. JP-8 is similar to Jet A-1 except for additional additive requirement such as icing inhibitors [8, 14]. On the other hand, JP-5 Jet fuel is designed by the U.S Navy to meet the operational safety requirements for aircraft carriers. In particular JP-5 therefore has a higher flash point.

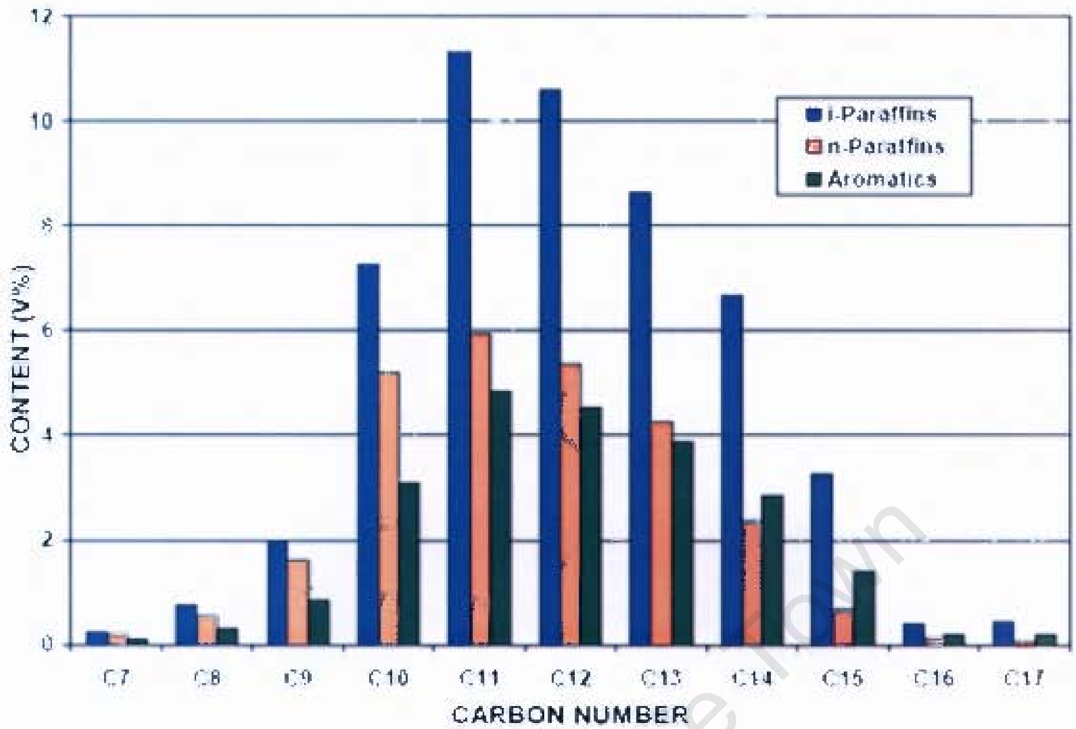

Figure 2.3: Volume percent of paraffinic hydrocarbons and aromatic hydrocarbons in a typical commercial jet fuel [4]

2.2.1 Characterisation of Jet Fuels using GC-MS Analysis

Gas Chromatography-Mass Spectroscopy (GC-MS) analysis has been used to identify various organic compounds present in fuels. Many compounds in petroleum- and coal-derived fuel, however, are difficult to identify because of their similar mass spectra. There is thus a need to identify the hydrocarbons in conventional and coal-derived jet fuel, especially those that are responsible for thermal stability, high density and swelling behaviour for future high performance gas turbine engines.

Experimental work was conducted at Pennsylvania State University, which used a temperature dependent retention time analysis. This technique provided a detailed identification of two JP-8 jet fuels, namely coal-derived (JP-8C) and petroleum-derived (JP-8P) [15]. It was clearly shown from the GC-MS analysis that the saturate fraction of JP-8P is dominated by straight chain alkanes ranging from C9-C14. Branched and cycloalkanes were also present within the fraction. It was shown that the aromatic fraction was dominated by alkylbenzenes. These alkylbenzenes were mostly short substituted benzenes instead of the long chain alkylbenzenes. There was also a polyaromatic fraction present which was dominated by naphthalene and alkylnaphthalenes.

The results showed that the petroleum derived jet fuel (JP-8P) was significantly different than the coal derived jet fuel (JP-8C). The latter consisted primarily of mono-, di- and tricyclic alkanes and hydro-aromatics while the former has straight and branched chain alkanes. [15].

2.3 Polymeric Materials

A polymer is a large molecule constructed from smaller structural units called monomers. These units are covalently bonded together in a variety of conceivable patterns. When only one species of a monomer is used to build a macromolecule, the product is called a homopolymer. However, if the chains are composed of two types of monomer unit, the material is known as a copolymer [16].

Polymers may be divided into three major categories according to their structure and properties. These are thermoplastics, thermosets and elastomers (also termed rubbers).

Elastomeric materials are used throughout the fuel distribution system and equipment as seals, coatings for hoses, gaskets and in other various applications. A seal is an elastomer compound which is used to prevent the loss of fluid or gas. O-rings and gaskets are the two major sealing equipments used in fuel systems [17]. Generally, elastomers have varying degrees of resistance and sensitivity to fuels and fluids. Physical properties such as hardness are influenced by the addition of compounding ingredients such as fillers and plasticisers. When an elastomer is exposed to fuel and fluids, changes in physical properties and importantly volume may occur [18].

2.3.1 Nitrile Rubber (NBR)

Nitrile rubber is a random copolymer of butadiene and acrylonitrile which belongs to a complex group of unsaturated elastomers. Figure 2.4 is a representation of the structure of monomeric units in nitrile rubber. Oil and heat resistance is the most important property of nitrile rubber. The individual properties of the nitrile rubber vary considerably with the ratio of acrylonitrile to butadiene. The polybutadiene segments contribute to the softness and flexibility of the rubber while the presence of polyacrylonitrile segments strongly influence the fuel resistance [6].

Depending on the ratio of acrylonitrile to butadiene , the properties of NBR such as oil and solvent resistance differ significantly [19]. Overall, these properties increase as the acrylonitrile content of the elastomer increases. The service temperatures of nitrile rubbers lie between -30 to 100°C. At high temperatures, however, nitrile rubbers have poor ozone and thermal ageing due to the reactivity of the double bonds present in the polybutadiene segments [19].

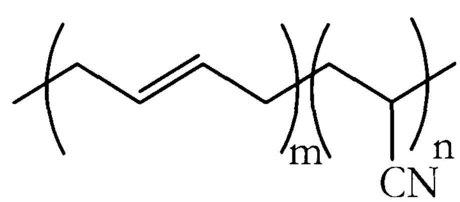

Figure 2.4: Chemical structure of the repeating units of nitrile rubber [19]

2.3.2 Plasticisers

A plasticiser is a high boiling point organic solvent incorporated into an elastomer to increase the flexibility, reduce viscosity, control volume swell, improve low-temperature properties and most importantly allow easy processing of the elastomer. Various oils are also added to the rubber compound to improve processing and to lower cost without affecting the physical properties of the rubber. Good compatibility between the elastomer and the oil is essential. Paraffinic oils are more compatible with the more saturated elastomers while aromatic oils are more compatible with polar rubbers such as nitrile rubber [20].

Plasticisers produce different plasticisation in different rubbers depending on the nature of the interactions between the polymer and the plasticiser and those between the polymer units itself. The majority of nitrile rubbers are plasticised with monomeric esters as opposed to polymeric esters. Polymeric ester plasticisers are used for high performance applications which require high heat ageing and extraction resistance while monomeric ester plasticisers are used for general performance applications. Nitrile rubber plasticisers contain polar and non-polar structural groups. The polar component would typically be a carboxylic ester functionality group and the non-polar component would be an aliphatic chain of an ester group [21].

The permanence of plasticisers in an elastomer depends upon the relative polarity and molecular weight of the plasticiser. Plasticisers having branched structures in their polymeric backbone tend to entangle with the polymer matrix and therefore resist extraction by the solvents. Furthermore, high molecular weight plasticisers tend to have less mobility and thus are more difficult to be extracted from the rubber. Figure 2.5 shows typical nitrile rubber monomeric ester plasticisers such as dioctyladipate (DOA) and dioctylphthalate (DOP) [21].

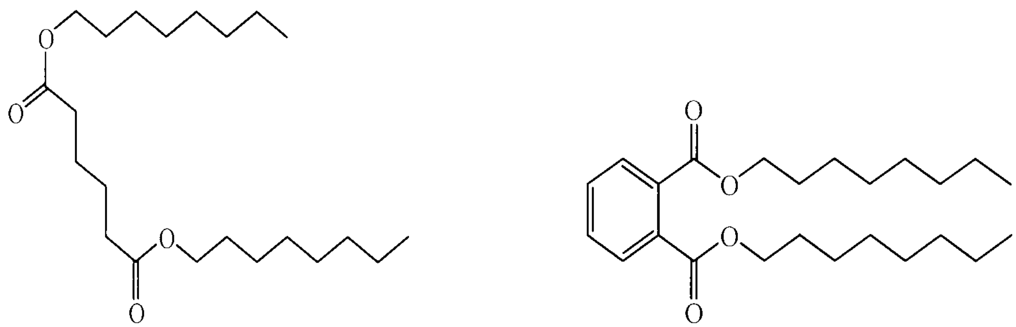

Figure 2.5: Structural components of monomeric ester plasticiser in nitrile rubber [21]

2.4 Rubber-Solvent Transport Phenomena

The transport process through a polymer membrane involves diffusion, sorption and permeation of solvent molecules. The concentration gradient of the solvent between that inside the polymer membrane and that in the pure solvent (or solution) outside is the main reason behind the transport process. The chemical potential between the two phases eventually equalises and equilibrium is reached. The factors contributing to the transport behaviour of solvent in a polymer membrane are discussed below [22].

2.4.1 Nature of the Polymer

Depending on the nature of the polymer, different polymers have different transport processes for a given solvent molecule. This is due to the individual structure and properties of a given polymer. Free volume and chain mobility of a polymer are two of the properties which affect transport behaviour of a given penetrant. Chain mobility of a polymer is affected by the unsaturation of the polymer backbone, degree of cross-linking, nature of the substituents and glass transition temperature. Polymer backbones with high unsaturation display better chain mobility compared to those with saturated backbones. Furthermore, a high degree of crosslinking decreases the diffusivity of penetrant molecules. Polar and bulky substituents influence the transport behaviour of polymers by having lower diffusivities into the polymer [22].

Figure 2.6 shows a study that was conducted to investigate the effect of increasing crosslink density for a hydrogenated nitrile rubber (HNBR) immersed in toluene. HNBR, vulcanized to different extents. Additional crosslinks affect the rate of solvent uptake and reduced the equilibrium level of solvent uptake. [23].

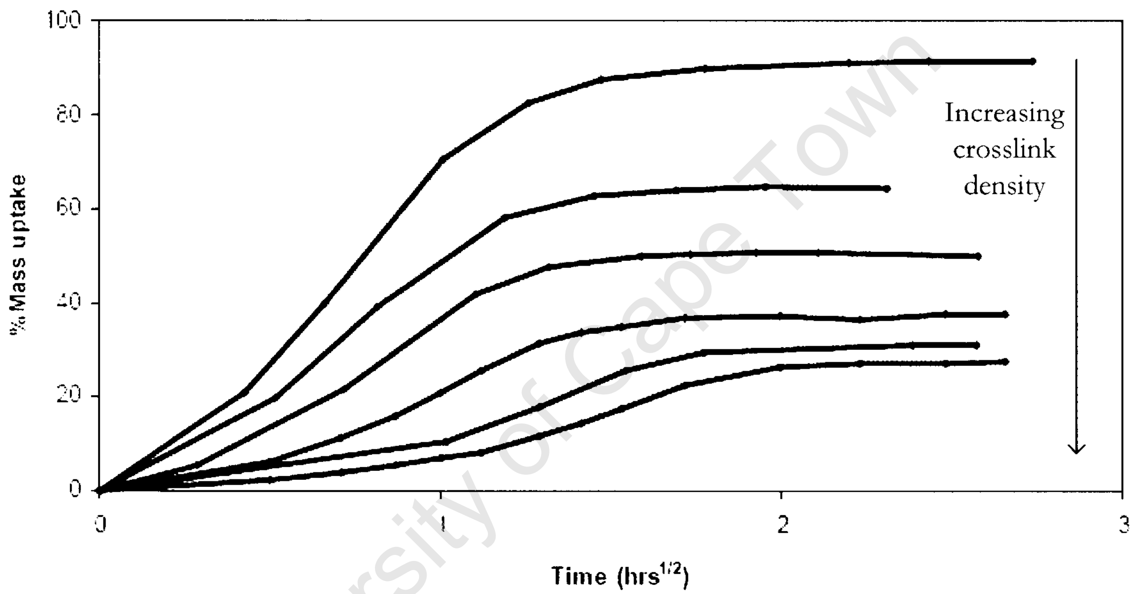

Figure 2.6: The effect of crosslink density on an HNBR rubber immersed in toluene [23]

2.4.2 Nature of Crosslinks

A polymer with the same crosslink density but different types of crosslinks has an effect on the transport behaviour of solvent molecules. A study was performed to investigate the diffusion of hydrocarbons through a natural rubber membrane with different types of crosslinks. The membrane was subjected to swelling in various hydrocarbon solvents. The type of network that is formed during vulcanisation determined the flexibility of polymer chains. The polymer structure with high chain flexibilities imparted maximum solvent uptake [22].

2.4.3 Nature of Penetrant

The size (and by implication molecular weight), shape and chemical nature of the penetrant molecule can influence the transport behaviour in polymer membranes. An increase in the size of molecules can cause a decrease in diffusivity. A study was conducted whereby alkanes from heptane to dodecane were allowed to diffuse through the polymer membrane. It was shown that equilibrium uptake decreased with an increase in the chain length [22]. In a different study p-xylene displayed the lowest solvent uptake while benzene showed a maximum. This study is shown in Figure 2.7 below.

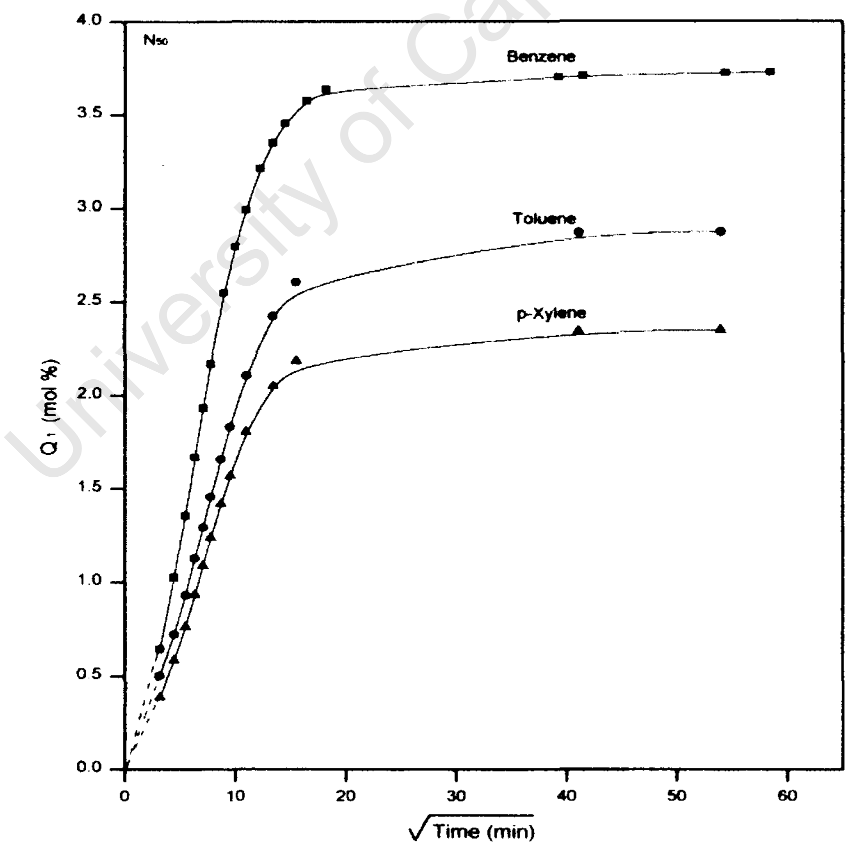

Figure 2.7: Sorption behaviour of organic molecules through a NBR/NR polymer blend [24]

Toluene showed an intermediate uptake of solvent. This result suggested that with an increase in molecular size of the penetrant molecule, there is a decrease in equilibrium uptake of solvent [24].

In a related study, it was also shown that the rate of swelling of nitrile rubber in aromatic hydrocarbons decreased with molar volume: toluene> xylene> 1,3,5 trimethylbenzene [25].

2.4.4 Temperature

The effect of temperature on molar equilibrium sorption coefficient is described by the Van't Hoff equation below:

$$\log K_s = \Delta S / (2.303R) - \Delta H / (2.303RT)$$

In the above equation, K_s is the sorption rate constant, ΔS and ΔH are the entropy and enthalpy of sorption respectively and R is the universal gas constant. Mathai and Thomas conducted a study on the diffusion process of xylene in NBR/EVA blends at temperatures of 23°C, 60 °C and 75°C. It was observed that an increase in temperature caused an increase in the initial rate of diffusion. The equilibrium uptake increased with an increase in temperature. This is attributed to an increase in chain mobility at higher temperature [25].

2.5 Fluid Compatibility

Fluid compatibility of elastomers can be explained via physical and chemical interactions between an elastomer and solvent [26]. When an amorphous polymer is mixed with a suitable solvent, it behaves like a liquid by dispersing in the solvent. A good solvent is classified as one that is highly compatible with the polymer. The liquid-polymer interactions expand the polymer chains from its unperturbed dimension. On the other hand, for a poor solvent the interactions are fewer and the chain expansion is restricted [16].

The effects of typical physical interactions of fluids on vulcanised elastomers result in:

- Fluid absorption
- Extraction of soluble components from the elastomer

The magnitude of the effects depends on the environmental fluid, the elastomer and the temperature conditions.

On the other hand, chemical reactions with the elastomer may result in degradation of elastomeric compounds either by attacking the polymer backbone or some of its compounding ingredients [27]. Elastomers can be attacked by chemically aggressive solvents which can alter the chemical structure of the elastomer. This chemical structure change might be irreversible and the properties are permanently affected (often detrimentally). The polymer backbone offers numerous sites for chemical attack, for example the acrylonitrile group can be attacked by molecular oxygen at high temperature. At lower temperatures the unsaturated double bond sites within a polymer is prone to attack, leading to the possibility of extra crosslinking and age hardening [22].

2.5.1 Fluid Absorption

The free internal volume in the amorphous regions, of elastomers enables high molecular chains to move easily when fluid is absorbed inside the polymer. The free volume is not eliminated after fluid absorption. Instead kinetic movements of the chain segments allow some regeneration of free space causing the polymer to swell [23].

Volume swell has detrimental effects on the physical properties of the rubber such as modulus, hardness and tensile strength. Excessive volume swell greater than 20% can cause negative effects by significant deterioration of physical properties while lower levels of swell often prove beneficial provided sufficient sealing contact stress is maintained [26].

Laboratory tests were conducted by Muzzell *et al.* [18] to determine the change in the physical properties of nitrile elastomers in various fuels at 40°C. The O-rings were immersed in a fuel with different aromatics content shown in Figure 2.8. It was concluded from the results that that NBR swells in the presence of aromatic hydrocarbons. The test fuels included S-5 fuel, JP-5 which contained 18% aromatics, Emission Control Diesel (ECD-1) with 19% aromatics and ultra low sulfur content. A150 is an aromatic solvent which was blended into the S-5 fuel. The results show an overall trend of increased mass change (swelling) as the fuel aromatic content increased. i.e. the greatest amount of swell was measured for S-5 +25% A150. It was also shown that nitrile O-rings immersed in JP-5 reached a change in mass approaching that of S-5 + 25% A150, even though less aromatics are present in the JP-5 fuel compared to S-5 + A150. These non-linear responses of swell of nitrile O-rings can be attributed not only to the concentration of aromatics present in the fuel, but also to specific type of aromatics [12]. This refers to the effect of degree of alkylation on benzene rings and the molecular weight of the alkylated substituted mono-aromatics rings [18].

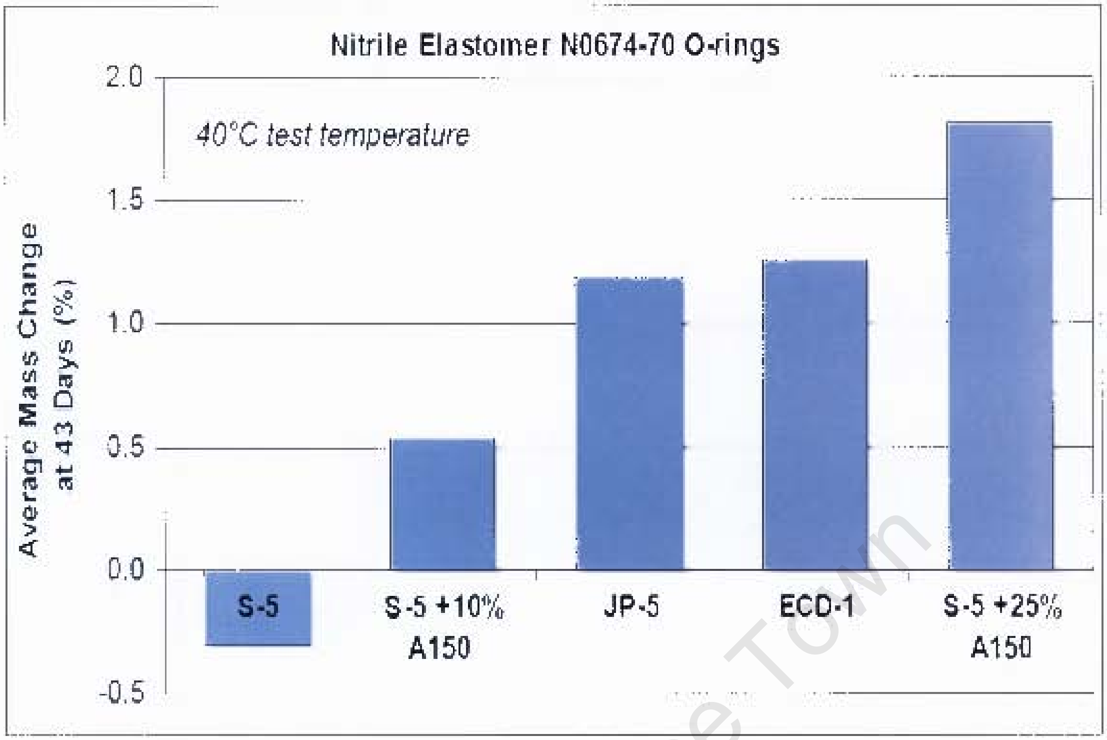

Figure 2.8: Average mass change after 43 days of immersion for nitrile 70 O-rings [18]

Elastomer compatibility tests were also reported by Moses and Roets [3] on elastomers which are typically used for sealing applications. The elastomers tested were nitrile, fluorocarbon (Viton) and fluorosilicone rubbers. Of these materials, NBR is very responsive to fuel chemistry due to the aromatic solvent activity on the nitrile plasticiser.

One of the reasons that aromatics are limited to 25% in a typical jet fuel is to prevent the fuel from acting as a strong solvent on nitrile elastomers especially the solvent activity of aromatics on the plasticisers used in nitrile elastomers [3]. On the other hand, aromatics are considered necessary in jet fuel to swell elastomer, and this swell is used by the designers to ensure a better seal to prevent seal leakage. Therefore, a minimum of 8% aromatics is required for a fully synthetic jet fuel in DEF STAN 91-91/Issue 6 [1].

Further research was conducted by Moses and Roets to investigate the swelling behaviour of O-rings. The results show that Viton and fluorosilicon O-rings swelled very little as expected. These authors studied four blends of synthetic kerosene with different amounts of aromatics in the range 8-17%. It was strongly suggested that the swelling of nitrile O-ring was related to the aromatic content in the fuel [10]. Furthermore, it was suggested that both the synthetic blends of jet fuel and petroleum derived Jet A-1 swell to a dynamically allowable limit [10]. The synthetic fuel blend 4, shown in the Figure 2.9 has 16.9% aromatics. These aromatics were primarily single ring aromatics but also contained di-aromatics to a certain extent. This shows that the aromatic chemistry in that blend of fuel is of similar manner compared to a typical jet fuel [28].

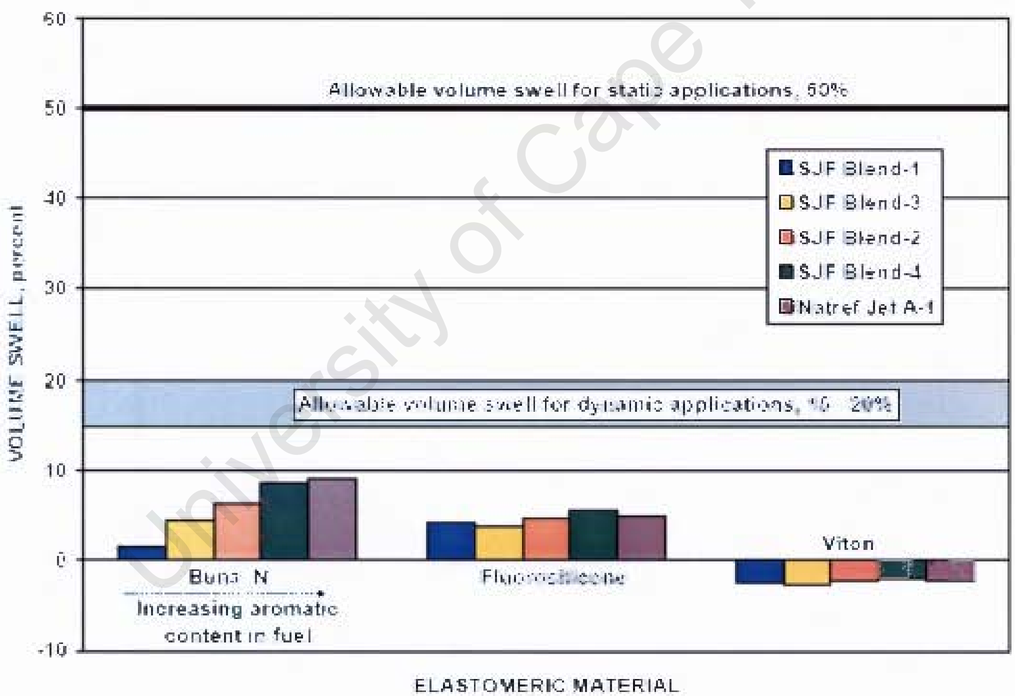

Figure 2.9: Effect of Sasol synthetic jet fuel with different level of aromatics on volume swells of fuel system elastomers [3]

Optical dilatometry has been used in many elastomer swell experiments to monitor the swelling behaviour of nitrile O-rings as a function of time. It was concluded from the results that a very naphthenic coal-based fuel containing as little as 1.6% tetralin showed similar swelling characteristics as petroleum-derived jet fuel, while F-T fuel which contained no aromatics and polar compounds showed very little swell. The results suggest that cycloalkanes such as decalin, hydrogenated aromatics such as tetralin and substituted tetralins, may exhibit good swelling behaviour compared to acyclic compounds [13]. The Figure 2.10 below shows that swelling behaviour of coal based naphthenic fuel.

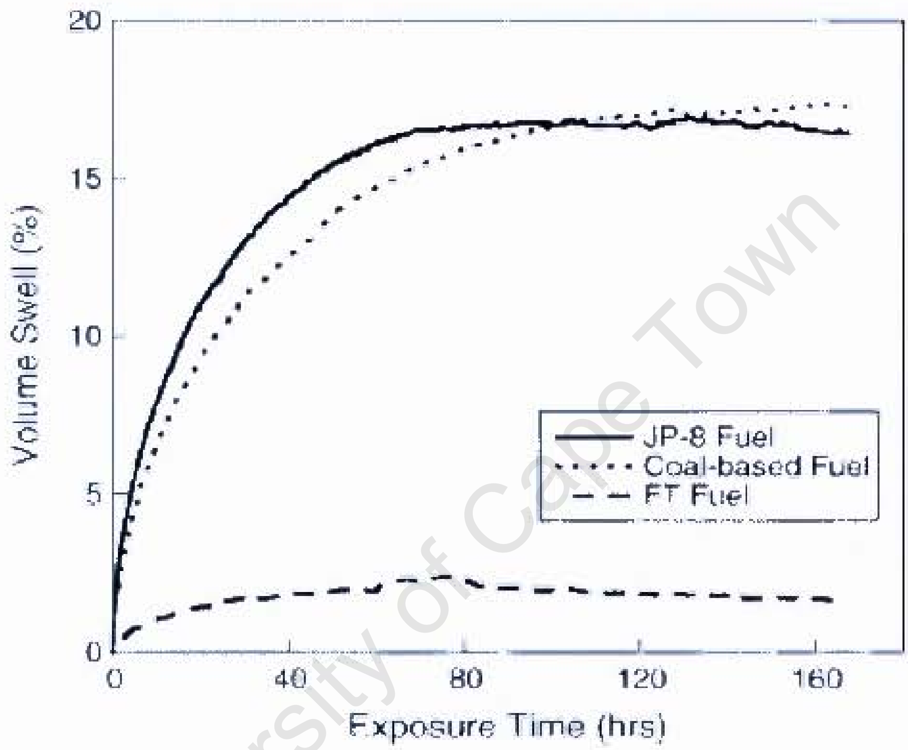

Figure 2.10: Volume swell versus time for nitrile O-rings aged in JP-900, F-T fuels and JP-8 fuel at room temperature [13]

2.5.2 Extraction of Plasticisers

Elastomer shrinkage occurs as a result of constituents such as processing oils, plasticisers and protective systems being leached out from the rubber. This can cause a loss of seal stress, an increase in hardness and a decrease in the ageing characteristics of an elastomer [29].

To illustrate this effect, data is presented for nylon-11 immersed in methanol. Even though Nylon-11 is not an elastomer, similar effects may be observed in elastomer systems and the example is presented here as illustration. Nylon-11 was found to reach an absorption peak before it eventually started to shrink after a long period of immersion. This suggests that there are two processes that occur during solvent uptake, one is the absorption of solvent and other is leaching out of plasticiser. An approach to equilibrium behaviour was obtained when the plasticiser was first extracted and the sample was re-immersed in the alcohol [23].

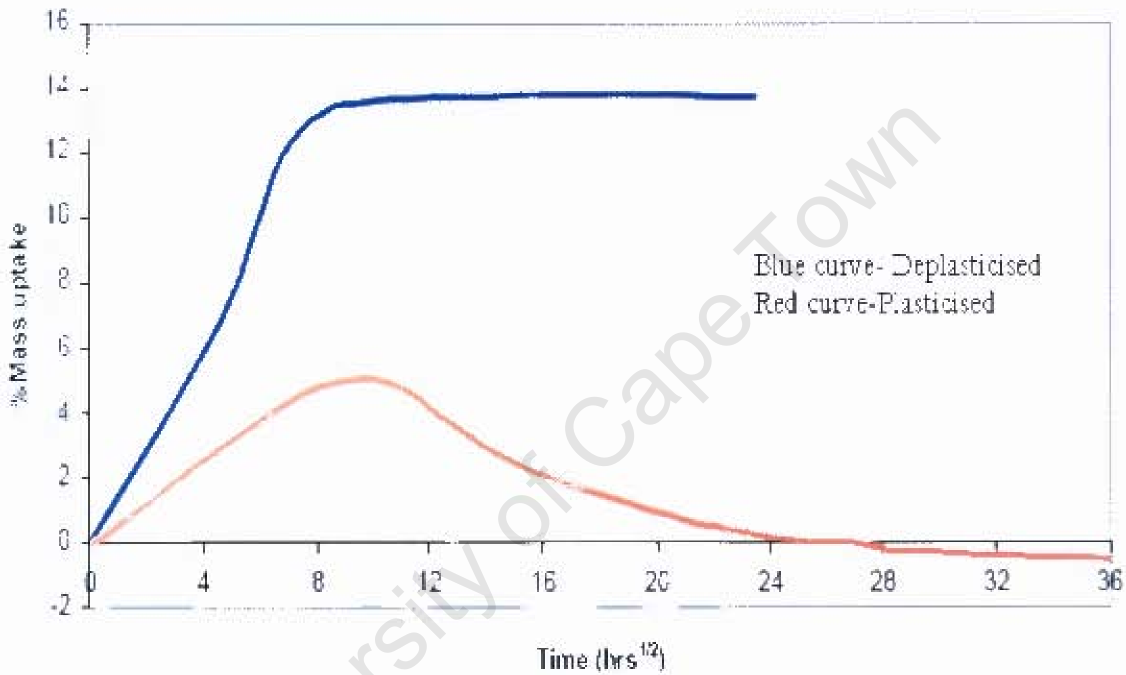

Figure 2.11: Nylon-methanol immersion at room temperature. Lower curve is plasticised material, upper curve is de-plasticised polymer [23]

Conventional jet fuel typically extracts plasticisers from rubbers [30]. However, there has been a concern about the removal of plasticiser from nitrile O-rings when exposed to synthetic and additised synthetic jet fuels. This was shown in an experiment where dry O-rings were soaked in JP-5, synthetic fuel and 1% benzyl alcohol additised synthetic fuel. The O-rings were thermally desorbed and analysed for the compounds that were extracted. Most of the species which are released are those that were used during the manufacturing process such as stabilisers and processing aids. When species were extracted from O-rings soaked in S-5 additised with benzyl alcohol, the main extractable species were found to be plasticisers such as dibutylphthlate [30].

2.6 Switch Loading

The development of synthetic jet fuel that is "fit for purpose" requires adequate response of petroleum fuel-wetted elastomers. Changes in physical properties may result from the elastomer being exposed to fuel and fluids [31]. Aromatic species in the fuel tend to get absorbed into the elastomer seal causing it to increase in volume (swell). However, if the same seal is subjected to a fuel containing a much reduced level of aromatic species, the seal tends to decrease in size (shrink). This reduction is size may result in poor sealing performance and possibly to seal leakage [18]. This shrinkage will not cause a leak if the elastomer is still flexible. However, for an aged elastomer which has lost its elasticity, leakage may occur more readily. It is therefore not the low aromatic fuel *per se* that causes the fuel system to leak but it is the change from higher to lower aromatic fuel that may cause such leaks [9].

In an experiment performed at the US Army REDCOM-Tank Automotive Research, Development and Engineering Centre, it was shown that nitrile O-rings and nitrile coupons have different responses when switched back and forth between fuel pairs of different aromatic contents (cf. Figure 2.12). Nitrile coupons are rectangular in shape cut from a nitrile material sheets [31]. JP-5 and S-5 were two such pairs. Nitrile O-rings showed a decrease in mass when exposed to S-5 suggesting that it may be leaching out something from the elastomer (typically plasticisers and processing aids) while it showed an increase in mass when exposed to JP-5. Switching from S-5 to JP-5 showed a significant increase in volume change. Upon switching back to S-5, it had decreased in volume lower than the first immersion. This pattern of decreasing swell levels occurred for all fuels and was expected to continue when additional round of switch loading is carried out for the O-rings. The swelling behaviour of the two fuel pairs moving back and forth was greater for fuels pairs with large differences in aromatic content while it was less for smaller difference in aromatic content [18]. It was also observed that nitrile coupons swell a lot more than nitrile O-rings despite a lower surface area to volume ratio. It was suggested that this could be due to the fact that nitrile coupons have cut edges that enhance further diffusion of fuel molecule [31]. Figure 2.13 shows the effect of aromatic content in the fuel during a switch load experiment.

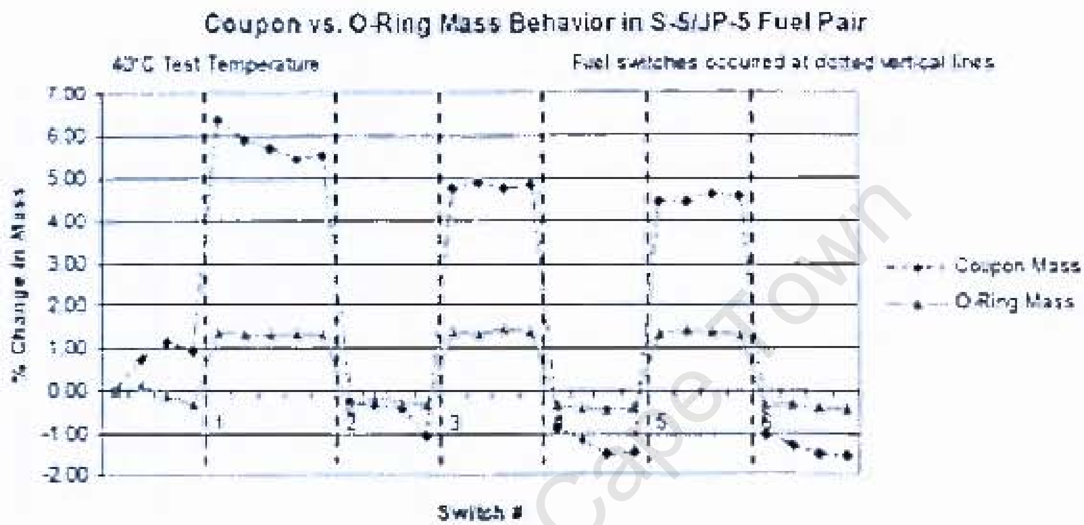

Figure 2.12: Comparison of mass change in S-5/ JP-5 fuel pair switch load [18]

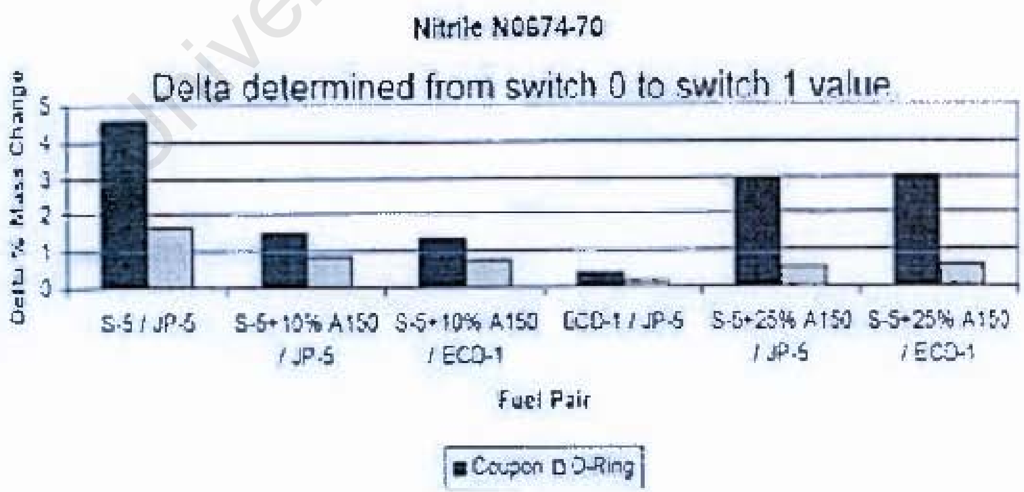

Figure 2.13: Difference in swelling behaviour of fuel pair switch loaded with different aromatic content [18]

A similar study was conducted to investigate the performance of NBR dumbbells exposed to zero aromatic LTFT diesel, HTFT diesel and crude-oil derived including Swedish EC-1 UK EN590 diesel, and US No.2 diesel. The NBR dumbbells were pre-conditioned in highly aromatic US No.2 diesel for 166h at 50°C and thereafter subsequently introduced to the fuels mentioned above for another one week at 50°C. The study resulted in the pre-conditioned swollen NBR shrinking and to losing weight when introduced to a low aromatic candidate fuel. Similar to the other candidate fuel, the dumbbells exposed to LTFT diesel returned back to their swollen condition during switch loading to a highly aromatic fuel. The figure 2.14 below shows the performance of NBR in a mixed fuel after the last switchover being either the candidate fuel or a highly aromatic diesel [32].

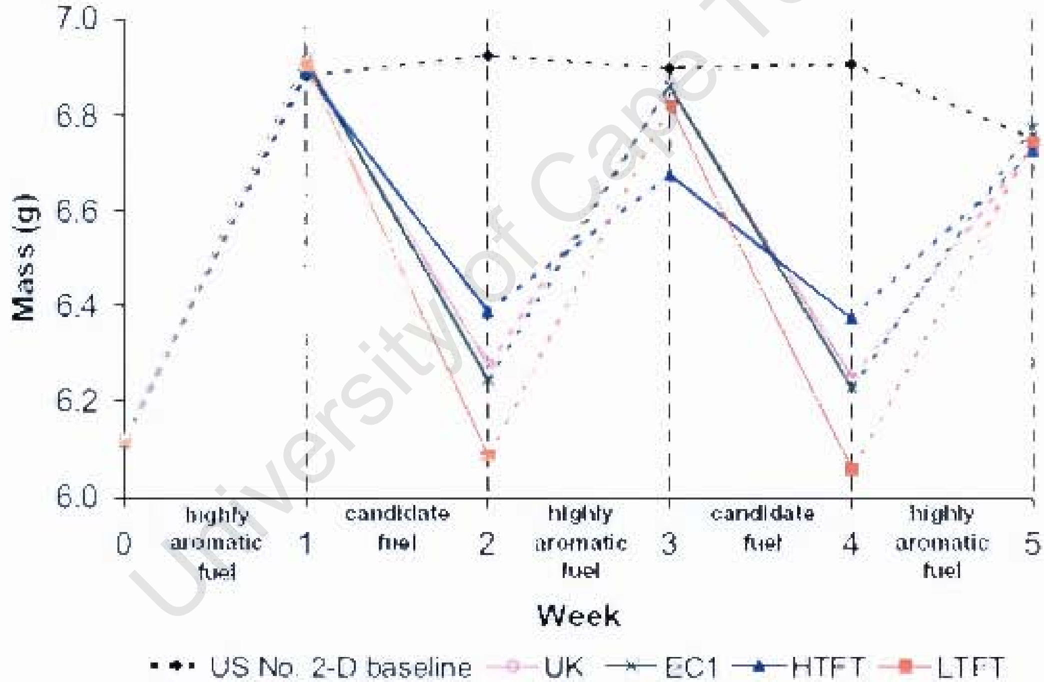

Figure 2.14: Percentage difference in the performance of NBR in a mixed fuel scenario [32]

2.7 Potential Swelling Additives

There is a need to determine alternative options for inducing seal swell by introducing an additive at a low concentration. A potential swelling additive should induce similar swelling to the conventional jet fuel, should not alter the fuel properties, should function at very low concentration and finally should cause no harm to the environment. These additives would restore the seal swell functionality of the synthetic fuels and should allow the fuel to be used interchangeably with conventional petroleum-derived fuels [33]. The competition between inter-molecular and intra-molecular bonds within a rubber and rubber-solvent system explains the mechanism of swelling in rubbers. The understanding of the swelling process is related to the interactions between the rubber and the solvent [33].

An experiment was conducted by Link *et al.* [33] with nitrile O-rings suspended in the test fuel (either synthetic, petroleum-derived fuel or synthetic fuel spiked at concentration up to 1 vol% solvent) for a period of 48h. O-rings swelled approximately 16% in conventional jet fuel. This value was used as a baseline to conduct experiment with spiked aromatics in synthetic fuel. The different aromatics present in conventional jet fuel were characterised by a GC-MS. This technique identified species with a high polarity such as alkylbenzenes [33].

Aromatics typically have smaller molar volume than normal alkanes. Furthermore they have a high hydrogen bonding character resulting in an interaction with the cyano sites within the nitrile rubber. This was shown in an experiment where tetralin, xylene, toluene, ethylbenzene and butylbenzene were blended to up to 40 vol% with Jet-A-1, and immersed for up to sixteen days at 70°C. The results show an abnormally large volume increase. It was thought to be due to peroxide formation in tetralin but the results were similar for other aromatic blends indicating that it is the presence of aromatics causing the increase in volume [34]. It has been found that introducing distillate boiling alkyl aromatics and cycloparaffins to distillate fuels improves the swelling properties of distillate fuels provided that the distillate fuel is produced from F-T process. In an experiment, F-T blends of isopropyl benzene (alkyl aromatic) and isopropylcyclohexane (cycloparaffins) were examined for their seal swell properties. It was concluded that adding alkyl aromatics and cycloparaffins improved the swelling behaviour in a manner similar to conventional fuels. However, smaller amounts of alkyl aromatics were needed to acquire the same volume change compared to cycloparaffins [10].

A further study was performed and found that nitrile elastomer preferentially absorbed fuel components in the order: aliphatics< aromatics< di-aromatics< di-EGME. Di-ethylene glycol mono-ethyl ether (Di-EGME) is a glycol based icing inhibitor for JP-5 fuels [13].

It is also known that partitioning of the fuel into the elastomer depends on the polarity and hydrogen donor ability of the fuel component. Normal and branched alkanes are non-polar and have almost negligible hydrogen donor ability while alkyl benzenes have variable polarity and are weak hydrogen donors. The polarity and hydrogen donor ability of alkylnaphthenes is greater than alkylbenzenes. This result was shown in a study to investigate the concentration and type of aromatic hydrocarbons blended in synthetic fuel to give the desired seals swell. The Figure 2.15 below shows the % volume swell as a function of aromatic content.

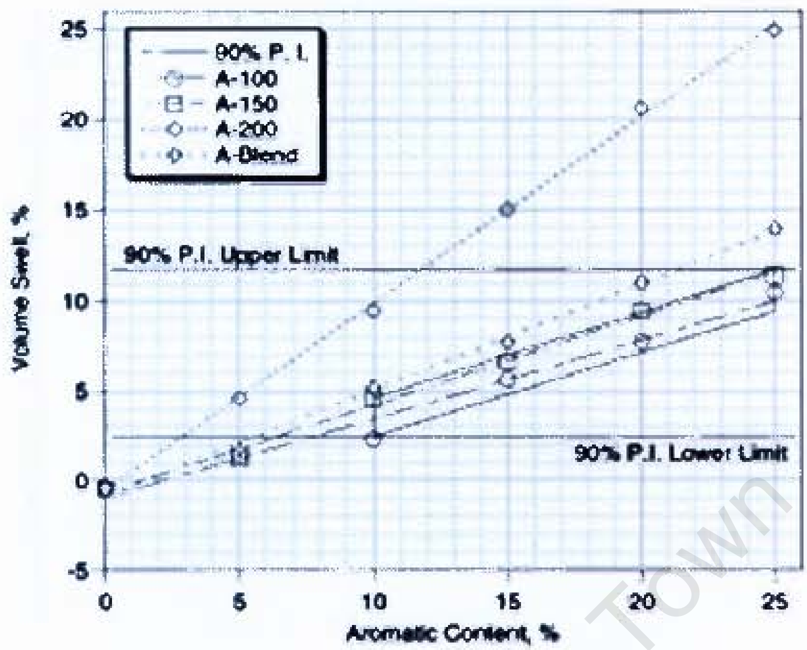

Figure 2.15: Comparison of volume swells of nitrile O-rings as a function of aromatic type and concentration [5]

It would require less amounts of highly naphthenic fuel to give the required seal swell than blending a highly alkylated benzene fuel [5]. Alkyl substitution was shown to reduce the polarity and hydrogen-bonding character of benzene compounds. This is because the carbon-hydrogen (C-H) bonds of the alkyl group of the alkylated benzene are much less polar than those of the aromatic ring itself and thus not able to hydrogen bond with the cyano group within the nitrile rubber [6].

The following compounds show a decrease in Hansen hydrogen-bonding and polarity in the order benzene, toluene, ethylbenzene, n-propylbenzene and n-amylbenzene for the reasons mentioned earlier in the chapter. Figure 2.16 below shows the structure of benzene and alkyl benzenes used to investigate the effect of increasing the alkyl chain length of single substituted benzene.

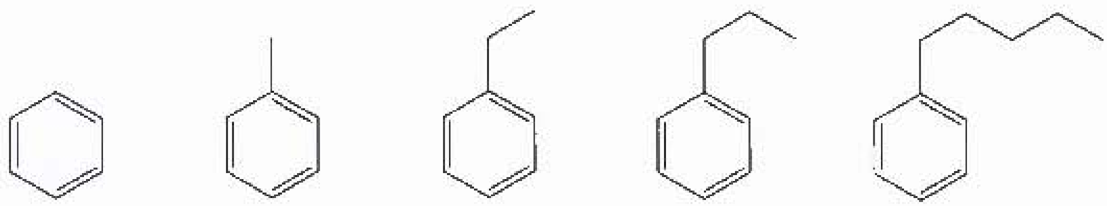

Figure 2.16: Alkylbenzene structures

It was also suggested that benzene not only diffused into the polymer but has also extracted material from the polymer resulting in a loss of volume swell [6]. The Figure 2.17 below shows the % volume swell of nitrile rubber aged with 10% aromatic species whose structures are presented above in Figure 2.16.

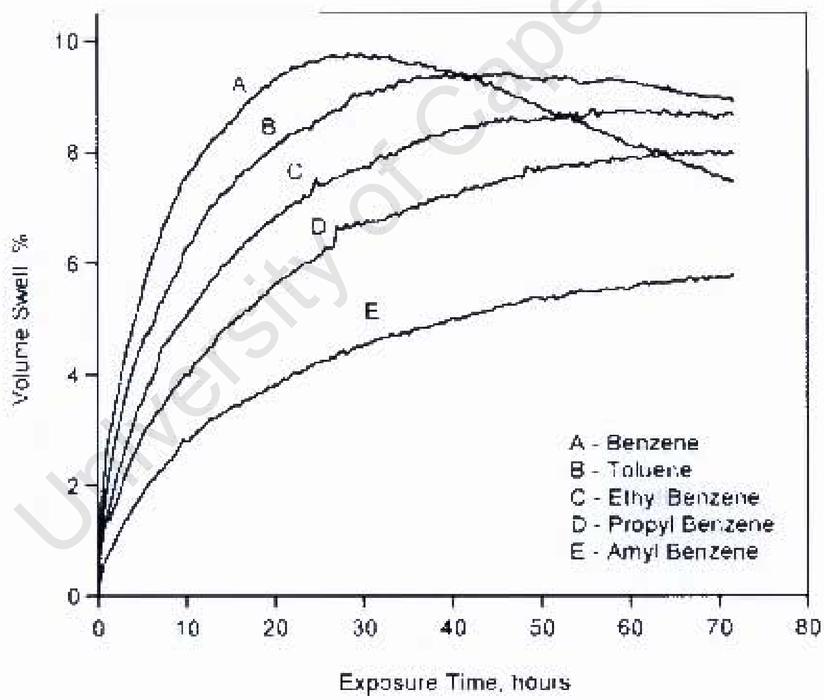

Figure 2.17: Volume swell as a function of time for nitrile rubber aged with S-5 plus 10% v/v of each individual aromatic species at room temperature [6]

Di-aromatics typically have higher hydrogen bonding character than mono-aromatics suggesting that they would have higher swelling behaviour than mono-aromatics. This was shown in an experiment where decalin, tetralin and naphthalene were examined. It appeared that decalin and tetralin did not swell as much as naphthalene [33]. Further studies have been conducted at the Cummins Engine Co with diesel fuel [35]. The study indicated that di-aromatics were most effective in swelling nitrile rubber compared to decalin and tetralin. It was also shown on the seal swell study of Shell Middle Distillate Synthesis (SMDS) diesel that di and tri aromatics have the greatest influence on seal swell [26].

In an experiment conducted at Pennsylvania State University, JP-900 fuel was shown to swell similar to a JP-8 fuel which has approximately 17% aromatic (di-aromatics inclusive). The result suggested that JP-900 which entirely contains decalin and its derivatives have shown excellent swelling characteristics despite it containing no di-aromatics [13]. This suggested that di-aromatics present in JP-8 fuel required lower concentrations for the same degree as swell as decalin in JP-900 fuel.

2.8 Prediction of Binding Energies

The swelling behaviour of polymers can be examined by using weight gain immersion experiments but this provides no direct mechanistic information about the swelling process at the molecular level. The swelling process results from the competition between the intermolecular forces within a polymer compared to the forces between the polymer and the solvent.

Molecular modelling is a useful tool for predicting interaction energies of solvent molecules and polymers. This modelling tool predicts distinctive bonding energies that can be used to identify the functional groups which are responsible within a solvent molecule to induce swelling characteristics in polymer membranes. Molecular Orbital (MO) calculations include optimised geometries, binding energies, vibrational frequency and electrostatic potential estimations. These calculations have shown good correlation with the polymer swelling behaviour and thus can be used to predict the polymer-fuel species interactions [36].

A study has been conducted by Alfonso and Cugini [37] using molecular modelling of a model polymer, isobutylnitrile interacting with variety of model fuel molecules. The theory used for this modelling is called second order Moller-Plesset (MP2) theory. It uses computer software called Gaussian. Full Optimised geometries for various combinations were carried out with the MP2 theory. It was concluded that the C-H group of the solvent hydrocarbons always points towards the cyano (CN) group. It was also shown that the interaction of the aromatic species was greater than the unsaturated and saturated species. This was attributed to the dipole-dipole interaction between the CN fragment and the solvent molecule [37].

Density Function Theory (DFT) on the other hand, also predicts interaction energies between molecules but it is restricted to polar and hydrogen bonded complexes. The calculations are very poor for weak and dispersion interactions [37]. These calculations can be verified experimentally using Fourier Transform Infrared Spectroscopy (FTIR). In one analysis, nitrile rubbers were aged with a variety of fuel species and the measured absorption peaks were associated with the cyano group with and without the interactions [36]. The Figure 2.18 below shows the optimised geometries of various fuel molecules and the nitrile polymer.

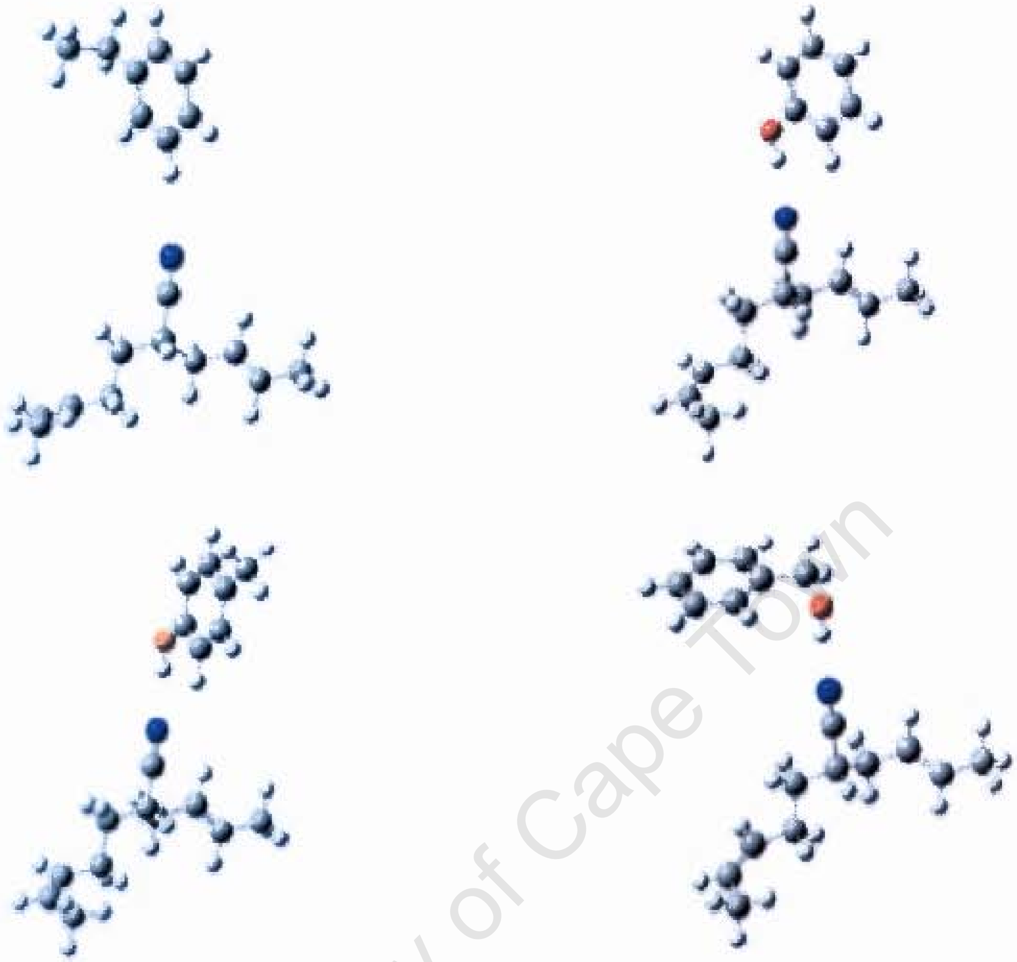

Figure 2.18: Optimised geometry structures of model polymer and fuel species complexes. White, gray, blue, and red indicating hydrogen, carbon, nitrogen, and oxygen respectively [36]

For polymer-fuel species interactions, it is important to determine the binding energy. This is the minimum energy required to be in a stable configuration. For a polymer-ethylbenzene complex, the interaction of the C-H group with the cyano group in the model polymer is weaker compared to a benzyl alcohol-polymer complex. In the benzyl alcohol-polymer complex, the interaction between the OH group in the benzyl alcohol and the cyano group in the model polymer is the strongest. In general, binding energy and vibrational frequency shift were shown to be the strongest for phenol followed by methyl phenol, phenyl methanol, straight chain and cyclic alcohol and ethylbenzene [36]. The above trend is shown in Figure 2.19.

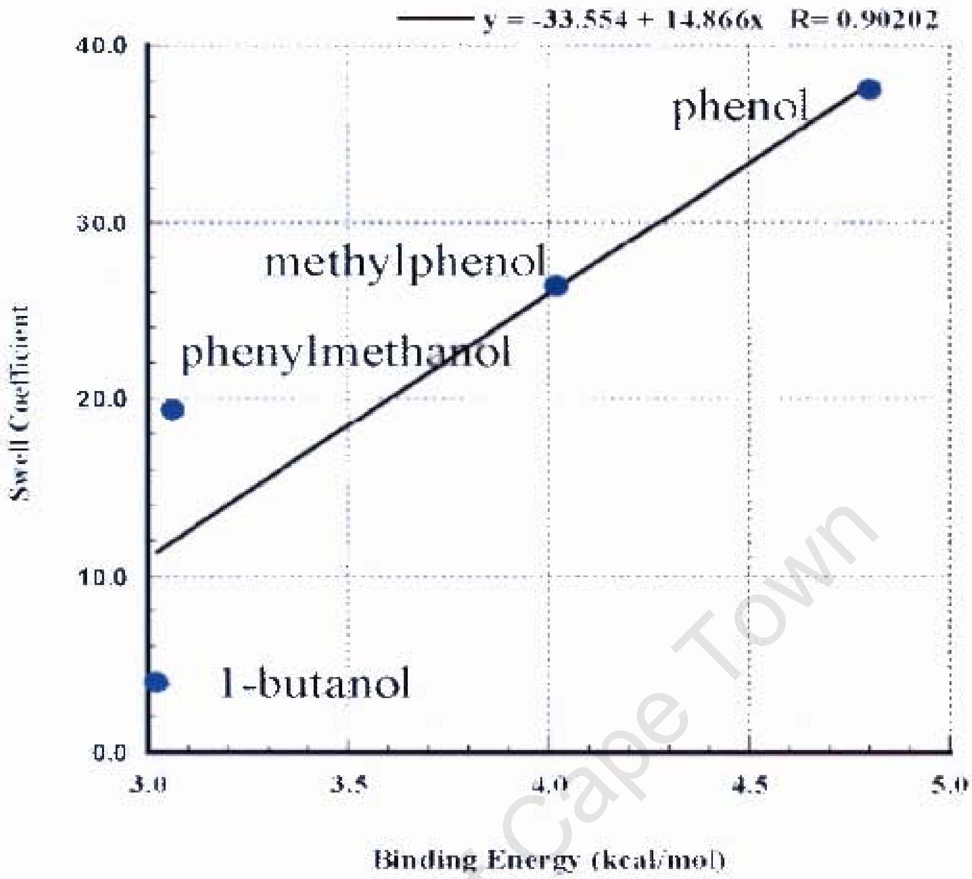

Figure 2.19: Swell coefficient versus binding energy [36]

Aromatic alcohol compounds including benzyl alcohol, naphthol and phenols show high swelling capabilities as compared to the conventional jet fuel. Toxicity and products of thermal deposits are one of the concerns that have to be considered when choosing an additive. Phenols have been implicated in oxidative instability mechanisms which means they are likely not to be useful swelling additive [33]. Previous research in computation modelling has also predicted that the highest degree of interaction between a potential swelling additive and the nitrile monomer would be provided by species having an aromatic ring along with a polar constituent [33]. Table 2.1 below shows the predicted interaction energies and volume swell of S-5 with potential swelling additives.

Table 2.1: Interaction energies and free swell of nitrile O-rings with selected species [38]

Test species	Interaction Energy (kcal/mol)	Volume swell (%)
S-5 + decalin (1%)	-1.9	0.8 ± 0.1
S-5 + naphthalene (1%)	-1.4	1.2 ± 0.5
S-5 + 1-naphthol (1%)	-6.6	13.3 ± 0.6
S-5 + phenol (1%)	-6.2	15.4 ± 1.0
S-5 + benzyl alcohol (1%)	-7.1	17.5 ± 0.4
S-5 + 5,6,7,8-tetrahydro-1-naphthol (1%)	-6.2	7.3 ± 0.4

Apart from toxicity, there are also concerns about the compatibility of some of the proposed additives with the fuel matrix. Octanol has to be used as a co-solvent for naphthol. This militates against the use of naphthol as an additive in the fuel. Benzyl alcohol is less toxic and fuels spiked with 1% benzyl alcohol showed similar swell as the petroleum derived fuel [38].

CHAPTER 3

THEORY

3.1 Hildebrand Solubility Parameter Theory

The solubility parameter was first proposed by Hildebrand and Scott [39, 40]. The Hildebrand solubility parameter is defined as the square root of the cohesive energy density. This may be obtained using the heat of vaporisation, ΔH_{Vap} and the molar volume V as shown in the equation below.

$$\delta^2 = E/V = (\Delta H - RT)/V$$

where, E is the energy of vaporisation. The solubility parameter is an important quantity as it is based on the strength of the intermolecular forces holding two molecules in a liquid phase. Hildebrand's rule of solubility suggests that if the parameters of two molecules/materials are similar, then they should be mutually soluble.

Thermodynamics requires that the free energy of mixing must be zero or negative for the solution process to occur spontaneously. Below is an equation for the free energy of mixing of two solvents.

$$\Delta G_{mix} = \Delta H_{mix} - T\Delta S_{mix}$$

where ΔG_{mix} is the free energy of mixing, ΔH_{mix} is the heat of mixing, T is the absolute temperature and ΔS_{mix} is the entropy change. The entropy term (ΔS_{mix}) is assumed to be small and positive. This is because unlike solvent molecules, monomer units in polymers are linked; thereby reducing the number of available configurations in solution. This is in turn decreases the increase of disorder and thus the increase in entropy upon mixing [16]. Hence, the enthalpy term determine the sign of ΔG_{mix} The equation below gives the heat of mixing as proposed by Hildebrand and Scott [40]:

$$\Delta H = \phi_1\phi_2 V(\delta_1 - \delta_2)^2$$

where $\phi_1\phi_2$ are the volume fractions of solvent and polymer. Since ΔS_{mix} is positive, this suggests that if ΔH_{mix} is positive then it should be reduced as much as possible to ensure a negative ΔG_{mix}.

Therefore, for a high likelihood of mixing of two components, the solubility parameters of the individual components should be similar.

3.1.1 Hansen Solubility Parameter for Selected Polymers

The use of the Hildebrand parameter is limited to regular solutions and does not account for association between molecules, such as polar and hydrogen-bonding interactions. The solubility parameter theory was modified by Hansen [41], who introduced the so called Hansen Solubility Parameter (HSP). This is related to the total energy of vaporisation of a liquid, consisting of factors for dispersion forces, permanent dipole-dipole forces and hydrogen bonding. The equation below describes the total energy of vaporisation as the sum of the individual energies [41]

$$E_{Total} = E_d + E_p + E_h$$

where E_d, E_p and E_h are the energies of dispersive, dipole-dipole and hydrogen bonding respectively.

Dividing the energies by molar volume gives the square of the total solubility parameter as the sum of the squares of the Hansen contributing factors [41].

$$\delta_t^2 = \delta_d^2 + \delta_p^2 + \delta_h^2$$

Solubility parameters of polymers are mostly used to describe the intermolecular bonding within a material. The polybutadiene chain segments are largely non-polar with relatively weak intermolecular forces of attraction between the olefinic groups. In contrast, the polyacrylonitrile chain segments have strong intermolecular forces of attraction between the polar cyano groups. These intermolecular bonding effects can be described using individual components of the total Hansen solubility parameters for the individual monomers and the copolymer as a whole. The total solubility parameter is dependent on the chemical structure of the polymer. NBR is a very polar polymer with high hydrogen bonding character and thus, it was suggested that it would have a high polar and hydrogen bonding Hansen solubility parameters [41]. A typical JP-5 fuel contains aromatic species whose individual solubility parameters compare more favourably with the solubility parameters of the nitrile polymer than the bulk of the fuel. This explains why aromatic species preferably interact with the nitrile polymer than any other fuel hydrocarbons [6]. Table 3.1 below shows the Hansen solubility parameters for one such polymer. There are large variabilities in the individual solubility parameter values. Different sources report different values of solubility parameter. An example of such discrepancy is shown in the literature [42] both stating different values of individual solubility parameters.

Table 3.1: Hansen solubility parameters of nitrile polymer with poly-acrylonitrile-co-butadiene estimated using volume additivity (30% poly-acrylonitrile[b]) [6] and poly-acrylonitrile-co-butadiene[c] reported in literature [42]

polymer	δ_D	δ_P	δ_H
poly(acrylonitrile)	18.2	16.2	6.8
poly(butadiene)	17.0	0.0	1.0
poly(acrylonitrile-*co*-butadiene)[b]	17.4	4.9	2.7
poly(acrylonitrile-*co*-butadiene)[c]	19.8	17.8	3.2

3.1.2 Variation, Assumptions and Limitations within HSP

There may be a local variation in the HSP of some polymers which are not homopolymers. Some solvents tend to interact with the polymer and locate themselves in the regions with similar solubility parameter. This causes clustering of solvents around the functional groups of some polymers or additives inside the polymer which are different from the bulk polymer. This is theorized to happen especially in copolymers which have different functional groups associated with different monomers [41].

Solubility parameters have several assumptions which are not taken into consideration. These include diffusion dominated systems in which solute molecules diffuse in and out of the polymer membrane. The size and shapes of solvent molecules have an effect on diffusion dominated system. This effect tends to disturb the solvent-polymer equilibrium. The importance of entropy in polymer-solvent is also typically ignored [41].

Solubility parameters predicted the affinity of solvents and polymers from the properties of pure substances and ignored the presence of competitive solutes. This is one of the limitations that are often ignored in binary solutions. In a binary solution, if solvent A, with solubility parameter $\delta_{1D}, \delta_{1H}, \delta_{1P}$ and which swells the polymer to a polymer ratio of Q_A. The solvent A is then mixed with solvent B, with solubility parameter $\delta_{2D}, \delta_{2H}, \delta_{2P}$ which swells to a polymer ratio of Q_B.The following equation was used to relate the energy of mixing to swell Q [43]:

$$\log Q_{\max} / Q = \beta V_1 \Delta E_{mix} / \phi_1 \phi_r V_m$$

where β is a function of the solubility parameter of the rubber and the degree of crosslinking. The relationship between solubility parameter and the energy of mixing was mentioned earlier in the section. Therefore, the Hildebrand blending rule holds for all three components [43].

$$\delta_{ij} = \phi_i \delta_i + \phi_j \delta_j$$

3.2 Flory-Rehner Equation

3.2.1 Heat of Mixing: Enthalpy Energy Term

The swelling of a crosslinked polymer is the result of the interaction of the solvent with the polymer molecules. Entropic effects mean that mixing (of which swelling is an example) is favourable but this is an offset by enthalpic effects which are usually endothermic.

The enthalpic term in the mixing equation is usually represented by [16]:

$$\Delta H^M = n_1 RT \chi_{H12} \phi_1 \phi_2$$

where 1 refers to the solvent and 2 to the polymer, ϕ is the volume fraction, n_1 is the number of moles of solvent and χ_{H12} is the enthalpic component of the polymer-solvent interaction parameter. The smaller this latter term, the greater the degree of swelling that is observed.

3.2.2 The Relationship Between Crosslink Density and Swelling

Theoretical treatment of the free energy of mixing and that for expansion of a polymer indicates that at equilibrium swelling, the total free energy of mixing must be zero and the two terms must balance [44].

Such a treatment produces equations of the following form. The derivation is for a crosslinked system of functionality 4 (i.e. each crosslink joins 2 chains and hence has 4 chain segments radiating from it). This is typical for most crosslinked elastomers.

The crosslink density (XLD) is thus:

$$\mathrm{XLD} = \frac{\rho_r}{2M_c} = \frac{-\left[\ln(1-\phi_{rc})+\phi_{rc}+\chi_{12}\phi_{rc}^{2}\right]}{2V_1\left(A\eta\phi_{rc}^{1/3}-B\phi_{rc}\right)}$$

where

XLD	=	crosslink density (i.e. number of crosslinks per unit volume)
ρr	=	density of the rubber
Mc	=	the average molar mass of polymer segments between crosslink
ϕ_{rc}	=	the volume fraction of rubber in the swollen sample at equilibrium
χ_{12}	=	polymer/solvent interaction parameter
η	=	ratio of the rms length of the chain-end distance in the crosslinked network to free chains. For most situations this is 1.
V_1	=	the molar volume of the solvent

A, B = constants depending on the theoretical treatment used

A number of theoretical treatments which usually differ in the treatment of the free energy of expansion lead to the following values for A and B:

Table 3.2: Theoretical values of A and B for the cross-link density equation

A	B	Source
1	½	[45], [46]
½	0	[47]
1	0	[48], [49]
1	1	[50]

The most accepted of these treatments and hence the most widely used [51] is that of Flory and Wall [46], although the resultant equation above is known as the Flory-Rehner equation based on an earlier treatment in which the entropic contribution to swelling was derived [52]. The Treloar equation [48], [49] is actually an older form of the Flory-Wall theory and may be viewed as an approximation of the latter. At high crosslink densities and low degrees of swelling, the two theories approximate to each other.

Furthermore, it should be noted that if the equation based on the theory of James and Guth [47] is used, the apparent crosslink density is half of that found using the Treloar equation.

The Flory-Rehner equation is non-linear in nature but a mathematical solver may be used to calculate ϕ_{rc}. This is the inverse of Q, the swelling ratio, which is the ratio of the swollen volume to the unswollen volume.

The following conclusions can be drawn from the theory:

- Significantly, the degree of swelling Q decreases as χ_{12} increases, i.e. Q will be maximized when χ_{12} is minimized.

- Q decreases as the crosslink density and the hardness of the rubber compound increases.

- The degree of swelling increases significantly as the molar volume of the solvent decreases. Because $V_1 = M_1/\rho_1$, this could be the consequence of a decrease in molar mass and/or an increase in density.

- The swelling ratio increases slightly as temperature rises. Nevertheless, a seal's overall volume will decrease with increasing temperature, owing to thermal contraction of the elastomer due to entropic effects.

3.2.3 Interaction Parameter

The Flory-Rehner equation is derived for an unfilled, unplasticised elastomer. Nevertheless, the influence of the above factors on Q remains similar when more sophisticated models are developed for equilibrium swelling in filled and plasticised systems.

In order to use the Flory-Rehner equation, a value for χ_{12} is needed. Where experimental determinations have been made, these can be used but with unknown or composite solvents, a value needs to be estimated. This can be achieved using the relationship proposed by Shvarts [53]:

$$\chi_{12} \quad = \quad \kappa + \frac{V_1}{RT}(\delta_1 - \delta_2)^2$$

where

κ = entropic contribution to the interaction parameter. 0.34 has been found to be an accurate value for this term for many polymer-hydrocarbon solvent systems. This term is introduced as a correction to account for the combinatorial entropy to χ_{12} [41]

V_1 = molar volume of the solvent

δ_1,δ_2 = solubility parameters for the solvent and polymer respectively

It can readily be appreciated that χ_{12} will decrease and hence swelling will increase as δ_1 and δ_2 approach each other in value. The more matched the solubility parameter of solvent and polymers are, the greater will be the degree of swelling.

Where electrostatic (polar and hydrogen-bonded) interactions are likely, an improvement to the estimation of χ_{12} has been proposed [54]:

$$\chi_{12} = \alpha \frac{V_1}{RT}\left[(\delta_{d1}-\delta_{d2})^2 + 0.25(\delta_{p_1}-\delta_{p2})^2 + 0.25(\delta_{h_1}-\delta_{h2})^2\right]$$

where

V_1 = molar volume of the solvent

δ_d, δ_p, δ_h = the dispersive, polar and hydrogen-bonded contributions to the solubility parameter as defined by Hansen

α = a universal fitting parameter obtained by fitting across a range of polymer-solvent systems. A best estimate of 0.6 was obtained

It can be seen that in this form, χ_{12} will be minimized and hence swelling maximized when the differences between the individual Hansen parameters for polymer and solvent are minimized.

This form of χ_{12} has, however, not yet found wide acceptance in elastomer circles because of the uncertainties associated with the determination of α and its applicability to less polar systems given that no general purpose elastomers were used in its estimation. There are also significant uncertainties in the individual Hansen solubility parameters causing large overall uncertainties. This is especially true for the parameters reported for polymers.

Flory-Rehner theory has been applied to swelling of nitrile rubbers in blends of toluene and iso-octane. It was believed that nitrile rubber swell aggressively in toluene while it does not in iso-octane. Toluene activity was estimated using Flory-Rehner equation [55]. It was concluded that Flory-Rehner theory could be used to estimate the swelling behaviour of an elastomer in a mixture of solvents. The figure below shows the swelling data for nitrile rubber in toluene-iso-octane solution and compared with the data from values estimated using the Flory-Rehner equation.

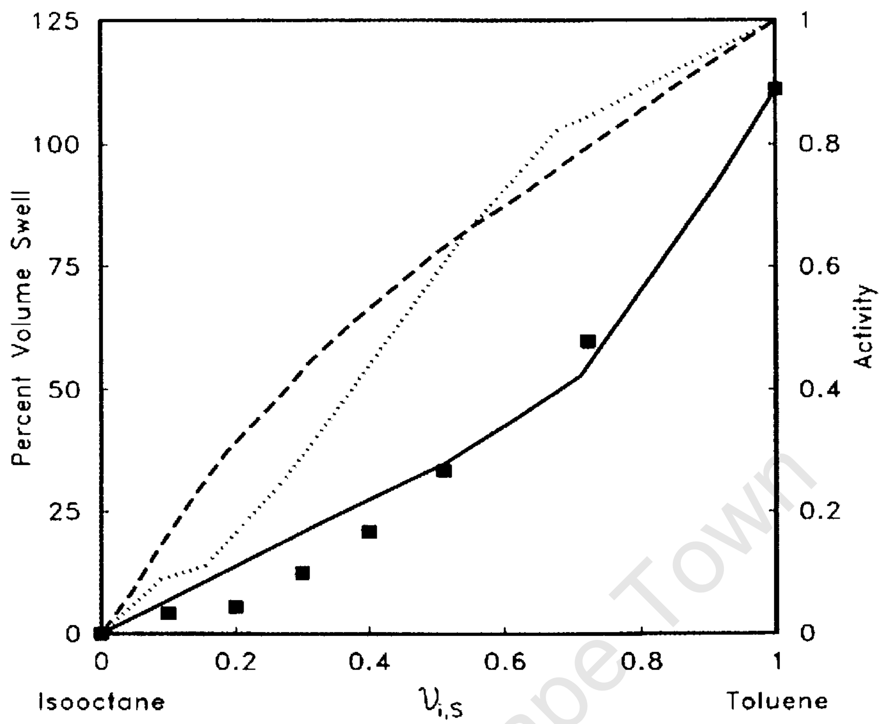

Figure 3.1: Ambient swelling data of nitrile rubber in toluene-iso-octane solution. Data points (square dots) represents actual swell data, the solid line represent predicted swell and the dashed lines are the activity of toluene in pure solvent and elastomer [55]

3.3 Using Flory-Rehner Equation to Illustrate Theoretical Aspects of Volume Swell

The Flory-Rehner equation was used to predict the volume fraction of the rubber in a swollen sample at equilibrium. The swelling data was then plotted against the solubility parameters for solvents of different molar volumes, crosslink densities and temperatures. Referring to Figure 3.2, volume swelling can be seen to increase with solubility parameter (δ) until a maximum at a solubility parameter corresponding to that of NBR. This is because the interaction parameter, χ, is minimised at this point. Thereafter, the volume swell decreased with increase difference between the solubility parameters. Referring to the same Figure, volume swelling was shown to be highest for solvents with a small molar volume. It was reported by George and Thomas [21] that reduced free volume and less chain mobility would decrease the diffusion of solvent molecules into the rubber, hence reduce swelling [22]. On the other hand, increasing the size (high molar volume) and shape of solvent molecules decreases the diffusion kinetics of solvent molecules into the rubber as well as the equilibrium swell achieved [22]. This is in agreement with the predictions presented in Figure 3.2

Furthermore, referring to Figure 3.3, crosslink density displayed a similar trend to molar volume in terms of volume swelling and solubility parameter. Crosslinking of polymer chains is achieved either due to thermal ageing or vulcanization. Vulcanization is a process used for crosslinking polymer chains using compounds which could interact with the polymer chains on either sides of the chain. Typical compounds used for vulcanization are sulfur and hydrogen peroxides. The resulting crosslinked polymer would have less chain mobility and reduced free volume.

On the other hand, temperature shows very little effect on percentage volume swell. This is shown in Figure 3.4. It is suggested that temperature has very small effect on the equilibrium swelling Q although it may have a significant effect on the rates of diffusions (both of fuel into and plasticiser out of the rubber).

The dotted lines in the graphs below indicate the solubility parameter values of SPK (green) and Jet A-1 (black). Chemical composition data for SPK and Jet A-1 were used to estimate the solubility parameters of these fuels. Detailed calculation of the solubility parameter of Jet A-1 and SPK are provided in Appendix A.

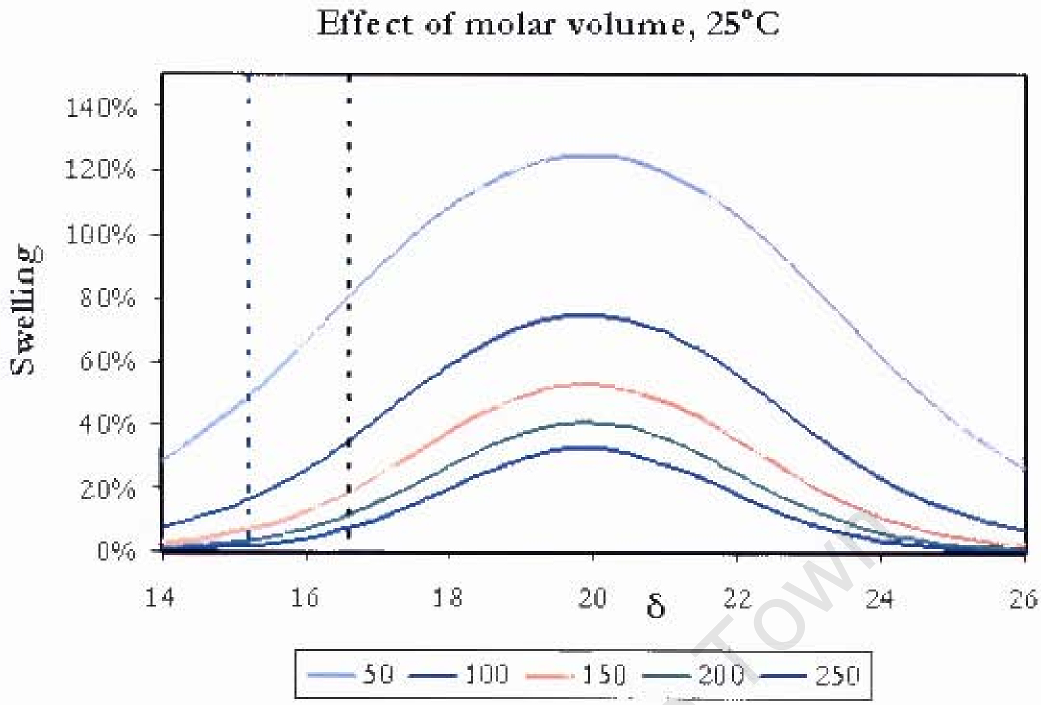

Figure 3.2: Effect of molar volume on volume swelling

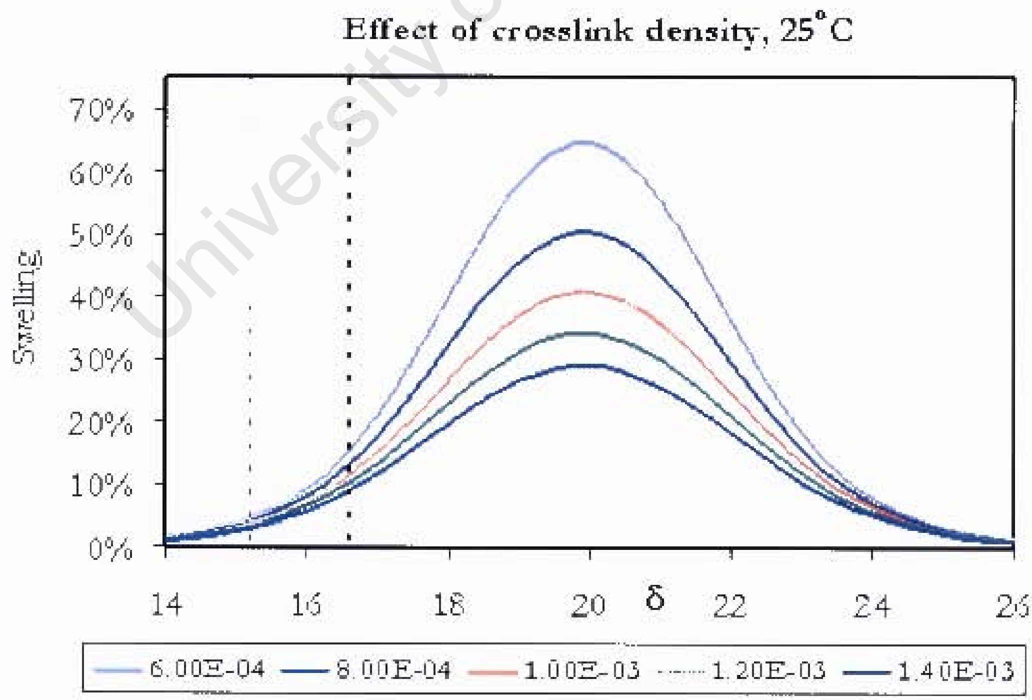

Figure 3.3: Effect of Crosslink density of volume swelling

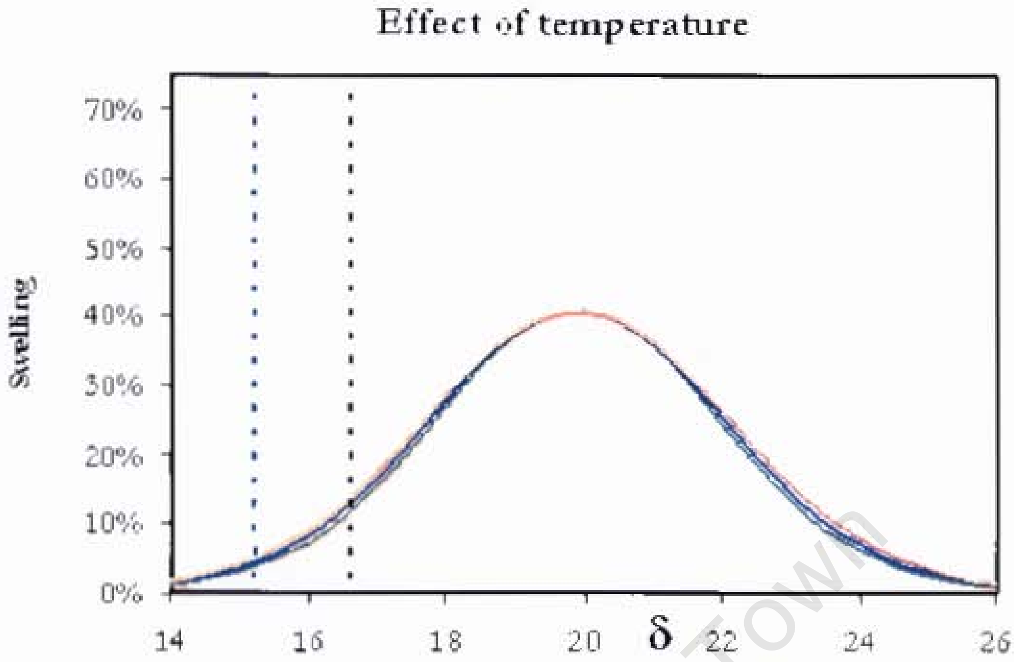

Figure 3.4: Effect of temperature at the same crosslink density on volume swelling

CHAPTER 4

EXPERIMENTAL AND COMPUTATIONAL PROCEDURE AND APPARATUS

The following chapter is a summary of the experimental procedures and apparatus that were used to perform the experiments. The test operating procedures for the elastomer compression rig can be found in appendix C.

4.1 Elastomer Compression Rig

The elastomer compression rig at SAFL, University of Cape Town, was used to investigate the seal swell performance of NBR O-rings in SPK, additised SPK and Jet A-1. The rig was further modified and re-designed to perform switch load experiments. Lab view software was used to capture data at regular time intervals.

Figure 4.1 is a picture of the elastomer compression rig showing all the various components including the data capture software.

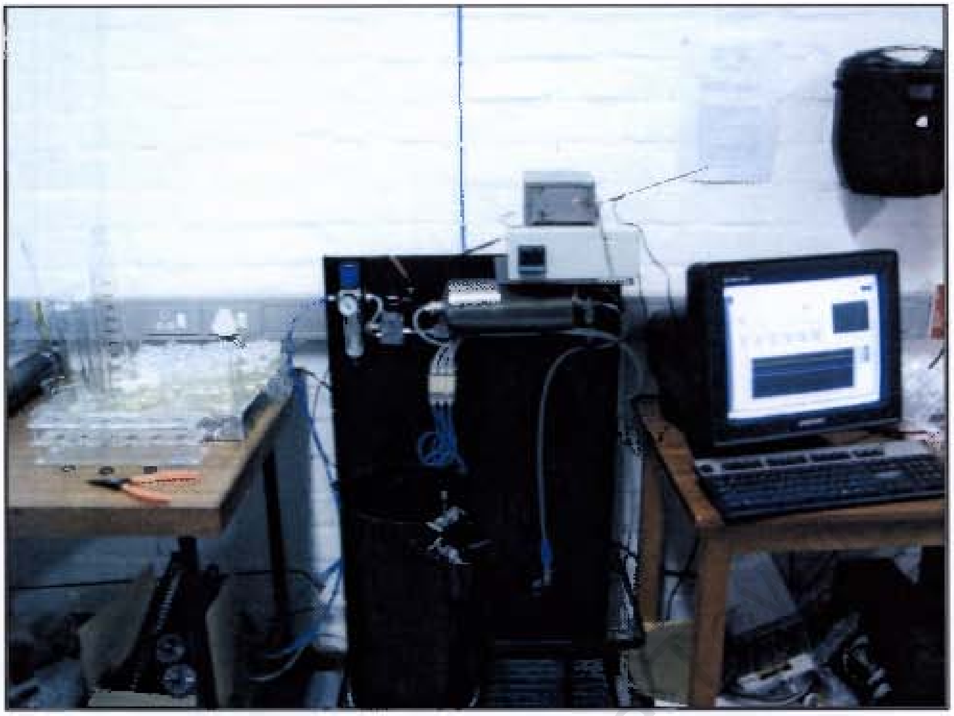

Figure 4.1: Elastomer compression rig showing the various rig components

4.1.1 Rig Assembly

The elastomer compression rig has six modules submerged in an oil bath. Each module has a cylinder base which required approximately 70ml of fuel in order to soak the O-rings. A pneumatically driven piston was used to apply a force by pushing onto the anvil, which then compresses the O-ring. The O-ring was compressed to a position until the anvil used to compress the O-ring makes a contact with the metal sleeve holding the O ring. This position of maximum displacement (X_{max}) was captured. The piston force is then gradually lifted to enable the O-ring to decompress. When the applied compressive force reached zero, another displacement reading was captured, X_{min}. The difference between the maximum limit X_{max} and the rest position X_{min}, ΔX, is a measure of the extent to which the O-ring is compressed. ΔX together with the O-ring groove depth can be used to calculate the thickness of the O-ring at any point during fuel exposure. The equation below describes the calculation of the O-ring thickness.

$$\text{O-ring thickness} = \text{groove depth} + \Delta X$$

$$\Delta X = |(X_{min} - X_{max})|$$

By monitoring changes in the O-ring thickness with time, swelling could be monitored in a dynamic environment as fuel entered the O ring and plasticiser leached out.

The O-ring grooves in each module were machined to the dimensions for a static flange seal. The NBR O-rings used for the tests had an average diameter of 20 mm and 2.5 mm thickness. The displacement readings in each module were taken using a proximity transducer. The temperature of the oil bath was regulated using a thermocouple. All the tests were conducted at 50°C. The tests were run for 150h for the seal performance tests and 48h between every switch load. Figure 4.2 shows the schematic diagram of the operation of the elastomer compression rig.

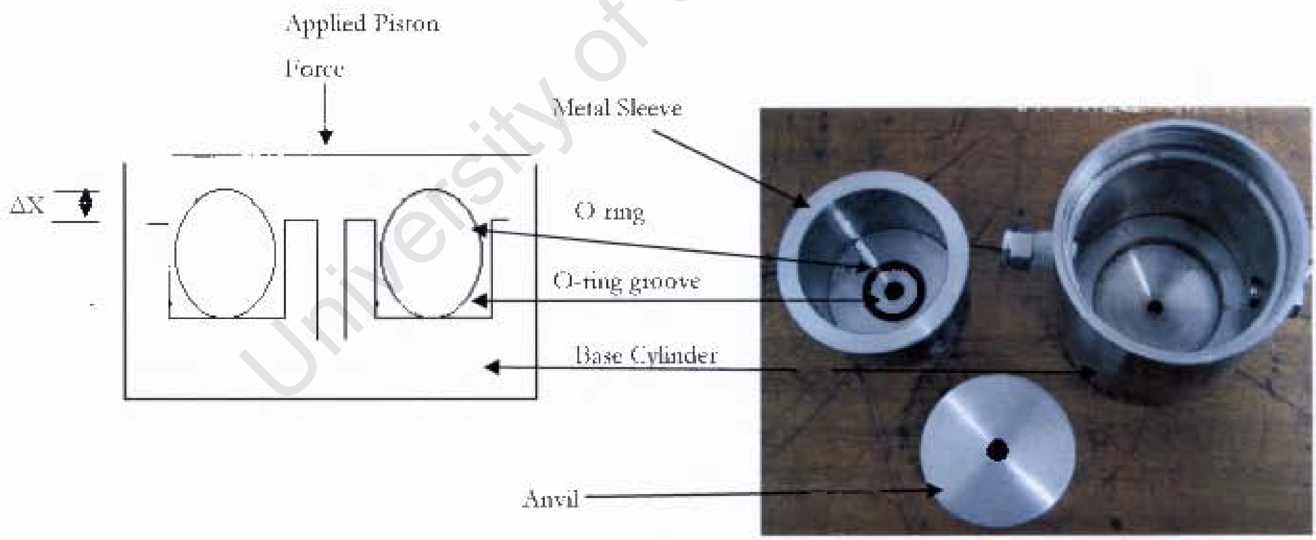

Figure 4.2: Schematic of rig operation showing the O-ring groove and base cylinder

A central hole in the apparatus allowed the O-rings to remain fuel wetted at all times

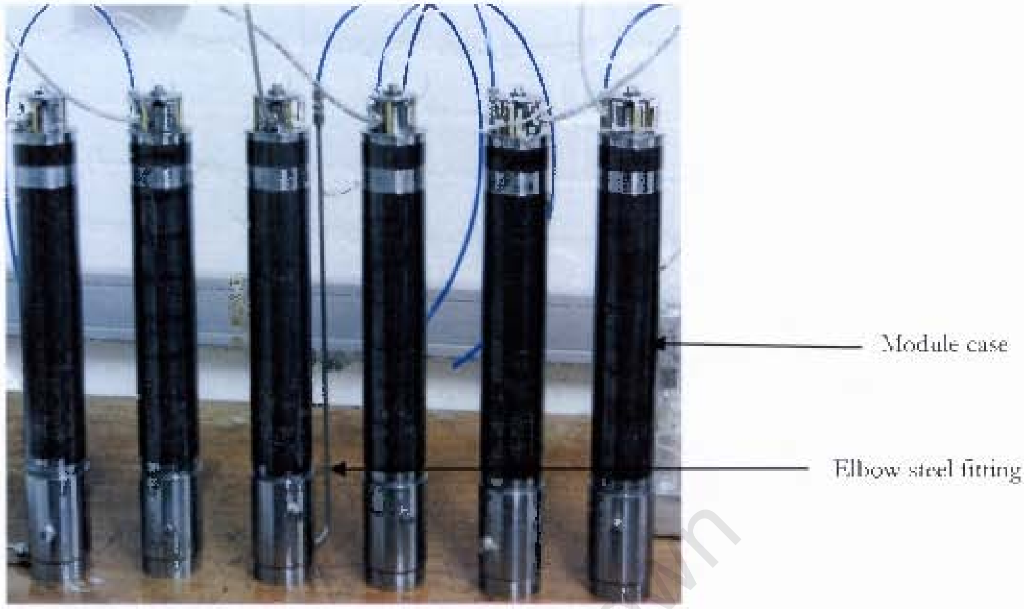

Figure 4.3: Cylinder base with elbow steel fitting, transducer attached to each module case

Figure 4.3, above, shows the elbow fitting that was included in the redesign so that switch load experiments could be performed.

4.1.2 Data Capture

Lab View was used to capture data of pressure and displacement at any given point in time. The increase in pressure of the piston compresses the O-ring to its maximum and thus X-max is recorded. The latter happens when the flange has closed down fully onto the O-ring. It is then followed by a decrease in pressure to zero, thus X-min is recorded. Breakaway pressure was logged as being the pressure corresponding to the position of 0.04mm away from the maximum displacement. Note that although the recorded displacements are negative this is a result of the zero position being arbitrary. The difference (ΔX) between X-max and X-min is what is important in this study and it is the same irrespective of the zero position. Figure 4.4 below shows the pressure trace for the loading and unloading.

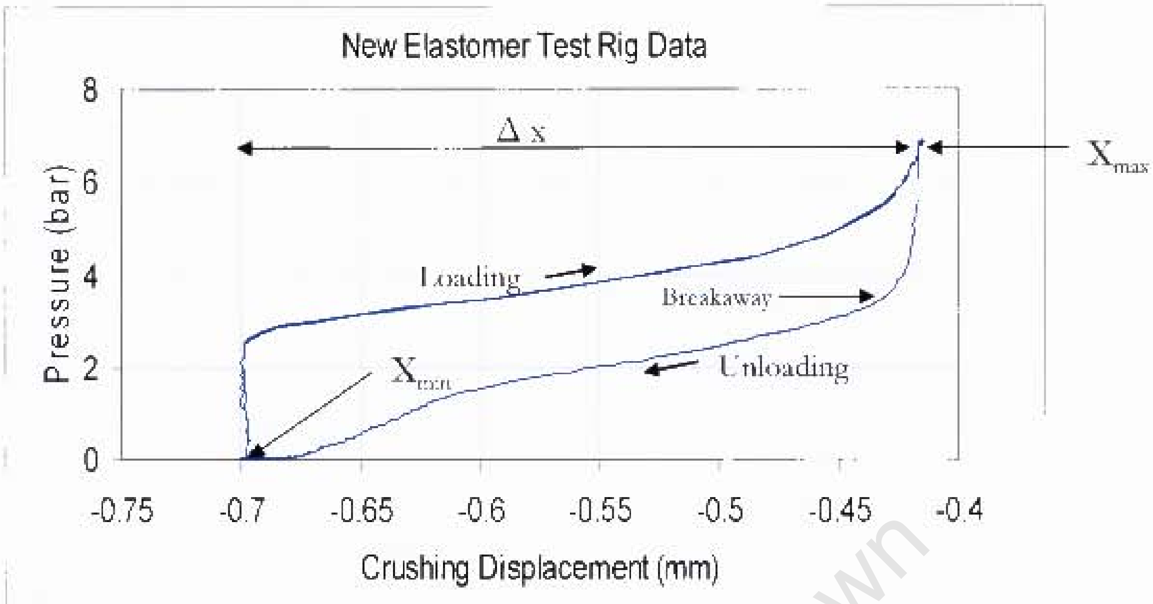

Figure 4.4: Pressure-displacement hysteresis during compression

4.1.3 Switch-load Test Procedure

The test modules were modified for the switch-load experiments. The cylinder base was re-designed to include an elbow steel fitting that was attached to a 6mm hose pipe allowing the fuel to be extracted and the cylinder refilled with a replacement test fuel. A syringe was used to flush out and refill with a new fuel during each switch-load test. Each base cylinder required approximately 80ml of fuel to soak the O-rings. Each switch load test was performed after 48h of operation. Figure 4.5 below shows the switch load set up in an oil bath.

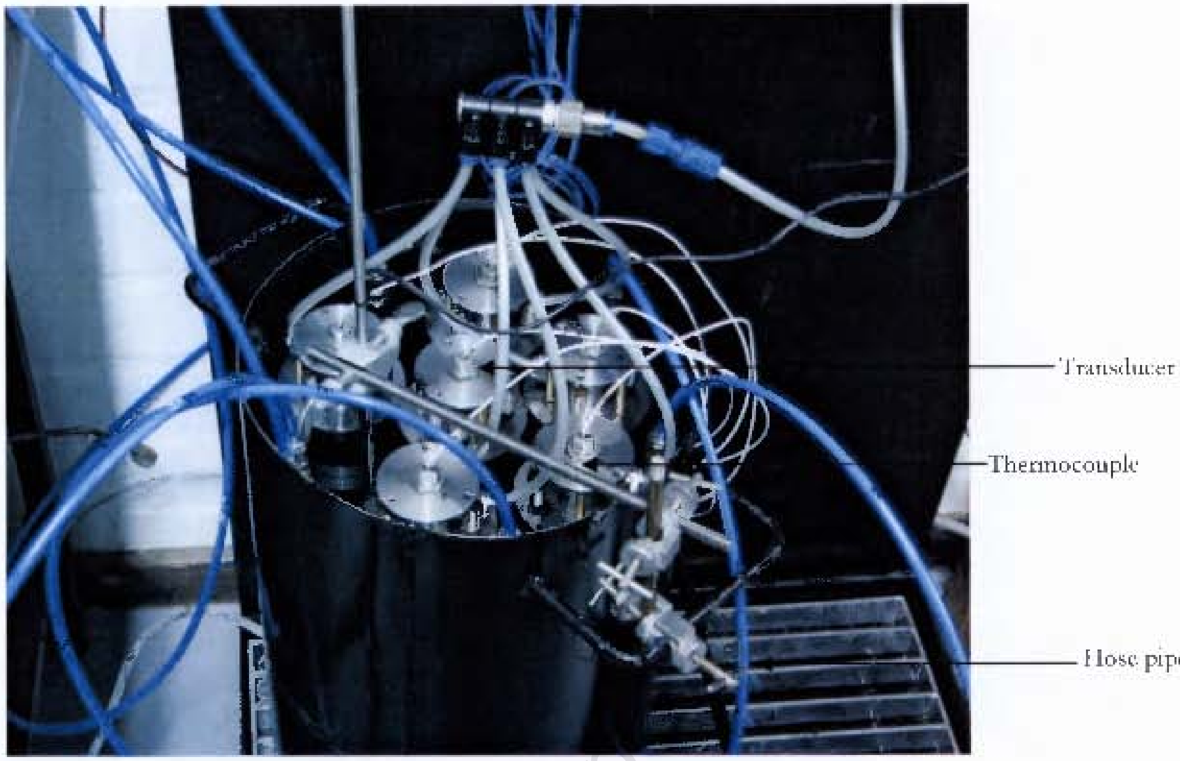

Figure 4.5: Modified design for switch-load with elbow steel fitting and attached hose pipe

4.2 ASTM Bench-Swell Procedure

The standard ASTM test method for Rubber Property - Effect of Liquids (ASTM D471-06) [2] was used as a guide for the bench swell procedure. The volume of the solvent was calculated using a rubber to solvent ratio of 40 and was approximately 15ml. The rubber samples were measured using a Mettler Toledo AT20 microbalance weighing scale with an accuracy of ± 2μg. The O-ring samples were cut in half to fit the 8mm glass vials for the immersion tests.

The samples were weighed before and after immersing in the solvent. In this study, plasticisers were not removed prior to immersion of fluid. The experiment was allowed to run for 48h in order to maximise the difference in swelling between the two fuels. The tests were conducted at room temperature (23°C).

Switch-load bench tests were also conducted for 48h after which the fuels were interchanged. The mass of NBR O-ring was measured before and after immersion in each fuel. Because of uncertainty over the extent of plasticiser extraction, results in this study are presented as mass changes rather than volume changes since the calculation of the latter would require detailed knowledge of the mass of plasticiser extracted.

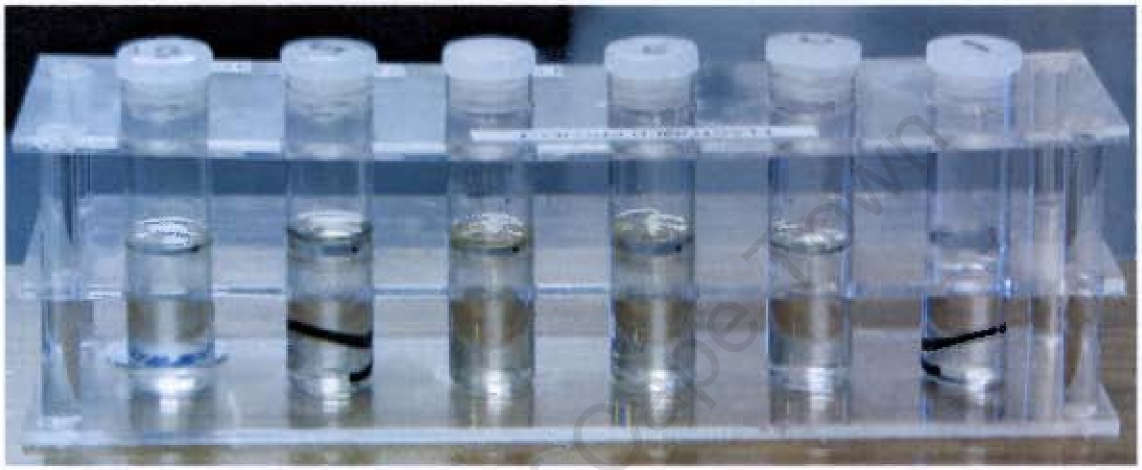

Figure 4.6: Immersion test layout for ASTM bench swell experiments

4.2.1 Test solvents and Rubber Samples

The bench-swell experiments and switch load experiments were conducted on a range of pure solvents and blends of additised SPK fuel. Commercial nitrile rubber O-rings with Shore hardness of 70 and 90 were supplied by Bearing Man Limited in Cape Town. The solvents were supplied by Kimix Chemical and Laboratory Suppliers in Cape Town. The solvents were chosen from a range of solvents that were reported in literature [6, 10, 24, 25, 27, 33, 34, 36, 38, 43, 55, 56]. The idea was to compare the swelling behaviour of hydrocarbon families which are present in a typical jet fuel.

The following are the hydrocarbon groups investigated:

- Paraffins which include straight chain, branched chain, mono-cyclic paraffins, bi-cyclic paraffins and hydro-aromatics
- Aromatics include alkyl benzenes
- Alcohols included a straight chain alcohols (n-butanol) and an aromatic alcohols (benzyl alcohol)

A titration experiment was performed for SPK, with alcohols under consideration i.e. n-butanol and benzyl alcohol. The outcome of this study showed that blending more than 2% of the above alcohols into SPK were not possible because these alcohols became immiscible (phase change) in SPK above this concentration.

Table 4.1: List of solvents and blended fuel

Hydrocarbon Group	Solvent (grade)	% Solvent Blended (by volume) in SPK
Straight chain paraffin	n-octane (99%)	
Branched chain paraffin	iso-octane	
Monocyclic paraffin	dimethylcyclohexane (97%)	
Bicyclic paraffin	decalin (98%)	
Hydro-aromatic	tetralin (98%)	4% and 8%
Alkylbenzene	Toluene (99.5%), blend of hexylbenzene isomers	4% and 8 %(toluene), 4%, 8% and 18 % (hexylbenzene)
Straight chain alcohol	n-butanol (98%)	2%
Aromatic alcohol	benzyl alcohol (99.5%)	0.5%, 1% and 2%

4.3 Computational Modelling

Computational modelling was done at the Department of Chemistry, University of Cape Town by Dr Gerhard Venter. Calculations were performed using density functional theory at the M05-2X/6-311G** [36] level of theory using the Gaussian 03 software package.

Isobutylnitrile was used as a model polymer to predict the chemical interaction with a variety of model fuel molecules. It was assumed that only the cyano moiety of the model polymer interacts with the model fuel molecules while the butadiene double bond moiety has negligible interaction. This assumption was based on the difference between the individual Hansen solubility parameters. This compound has been used as a model for interactions with nitrile rubber in previous studies [36, 37]. The calculations were obtained for stationary gas phase interactions. Figure 4.7 below shows the cyano moiety of the isobutylnitrile model polymer.

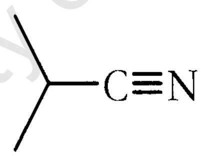

Figure 4.7: Model structure of isobutylnitrile showing the acrylonitrile group

The charge distribution, binding energies and vibrational frequency shifts corresponding to the cyano-group stretching mode were calculated. B3LYP [36] has been successfully employed to assess the geometries, energies and vibrational spectra of hydrogen-bonded complexes. The interaction energy between two molecules, A and B is defined as

$$E_{int} = E\ (AB) - E\ (A) - E\ (B)$$

where E(AB) is the energy of the complex and E(A) and E(B) are the energies of the fragments in the geometry within the complex [25].

CHAPTER 5

RESULTS

5.1 Static (bench) Seal Swell Experiments

Bench swelling experiments were conducted to investigate the swelling behaviour of NBR O-rings in jet fuel and SPK additised fuels as a function of time. It was observed that swelling was dependent on the composition of fuel. Maximum swell was reached followed by a decrease in swell.

5.1.1 Swelling as a Function of Time (Time swell Experiment)

Figure 5.1 shows the percentage mass change of NBR O-rings as a function of time when immersed in Jet A-1 and SPK. The percentage mass change of NBR O-rings reaches approximately 7% in Jet A-1 compared to SPK which has shown little change in percentage mass change.

Both fuels pass through maximum followed by a decrease in mass. However, SPK does not show as large a decrease in mass compared to Jet A-1. The figure includes error bars representing a 95% confidence interval of the mean percentage mass change. NBR 70 represents NBR O-rings with 70 shore hardness.

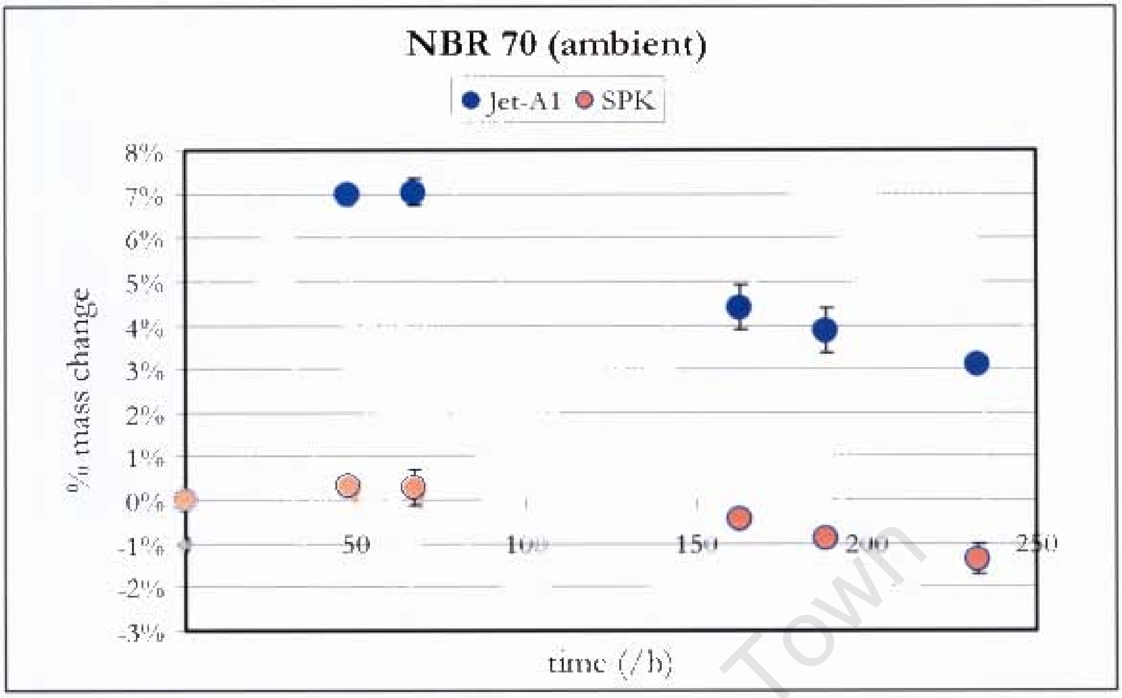

Figure 5.1 Time dependent percentage mass change of NBR O-rings immersed in SPK and Jet A-1 at 23°C

5.1.2 Pure Solvent Swelling

Pure solvents were used to investigate the swelling behaviour of NBR O-rings. The solvents chosen were major components of a typical jet fuel except the oxygenates, benzyl alcohol and n-butanol.

Figure 5.2 shows the percentage mass increase of NBR O-rings immersed in pure solvents for 48h at 23°C. The graph clearly shows that benzyl alcohol followed by toluene and tetralin swelled considerably more than Jet A-1. Iso-octane displayed the least swelling. It can be inferred that non-polar paraffins diffuse less into the polar nitrile rubber and this can be observed for iso-octane. The iso-octane swelling result explains the poor swelling behaviour of iso-paraffinic SPK fuels. Bicyclic paraffins on the other hand, swell to a similar extent as Jet A-1. This explains why thermally stable JP-900 fuel which is entirely dominated by bi-cyclic paraffins have similar swell to Jet A-1. This is in agreement with the results of Balster *et al.* [13].

The relatively poor swelling behaviour of n-butanol suggest that not all oxygenates have similar swelling behaviour. n-Butanol has a total solubility parameter of approximately 23.2 while benzyl alcohol has a total solubility parameter of approximately 23.8. However, n-butanol has a dispersion solubility parameter of 16.0 which is lower than 18.4 for benzyl alcohol. Similarly, it has polarity solubility parameters of 5.7 which is lower than 6.3 for benzyl alcohol [41]. It is inferred that aromatic ring in benzyl alcohol has a preferential interaction compared to long paraffinic chain of n-butanol. This suggests that molecular structure and Hansen polarity thus play a major role in rubber-solvent interaction.

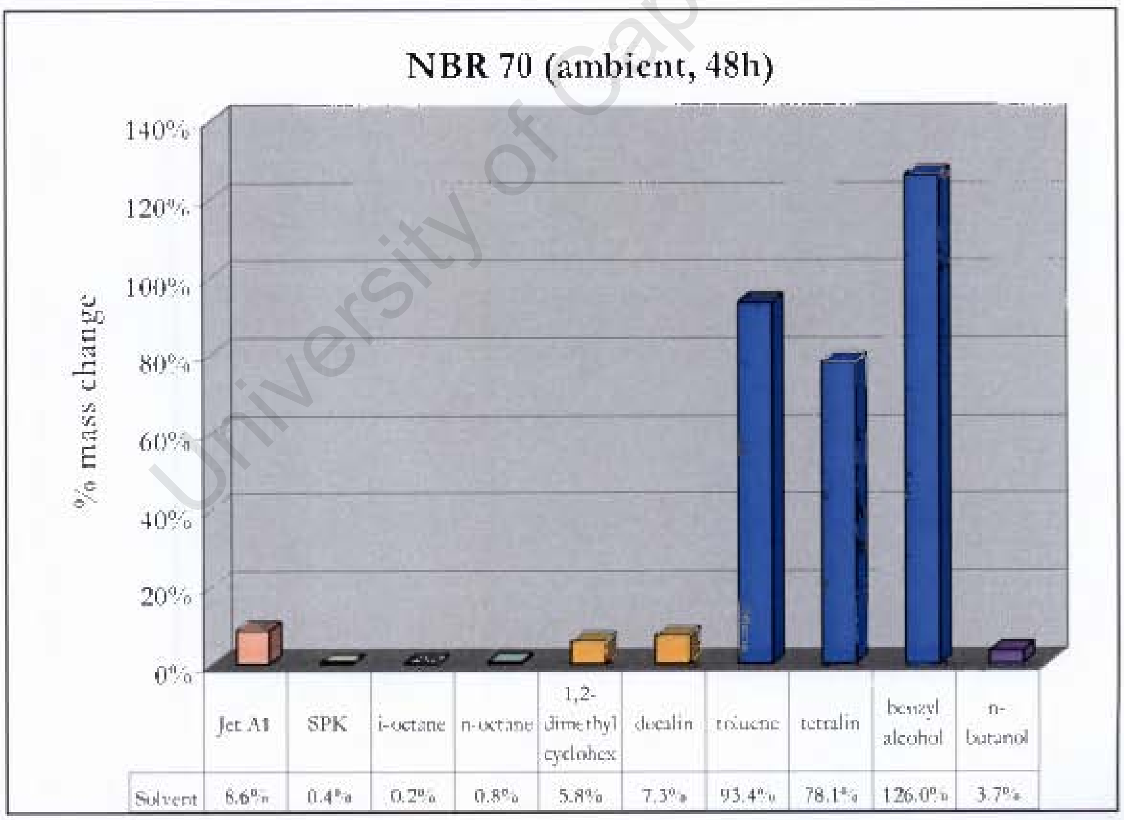

Figure 5.2: Mass percentage change of NBR O-rings immersed in pure solvents at room temperature and for 48 hours

5.1.3 Additised SPK

SPK was additised with the pure solvents in section 5.1.2 that displayed significantly more swell than Jet A-1. A hexylbenzene solvent (a mixture of isomers) was also blended to investigate the effect of the type and concentration of aromatics that would provide similar swell to Jet A-1. These aromatics are believed to be present in a typical commercial Jet A-1 [15]. A solvent concentration of 8% was used because of the total aromatic limit of 8% in DEF STAN [1]. Figure 5.3 shows the percentage mass change of NBR O-rings in additised SPK.

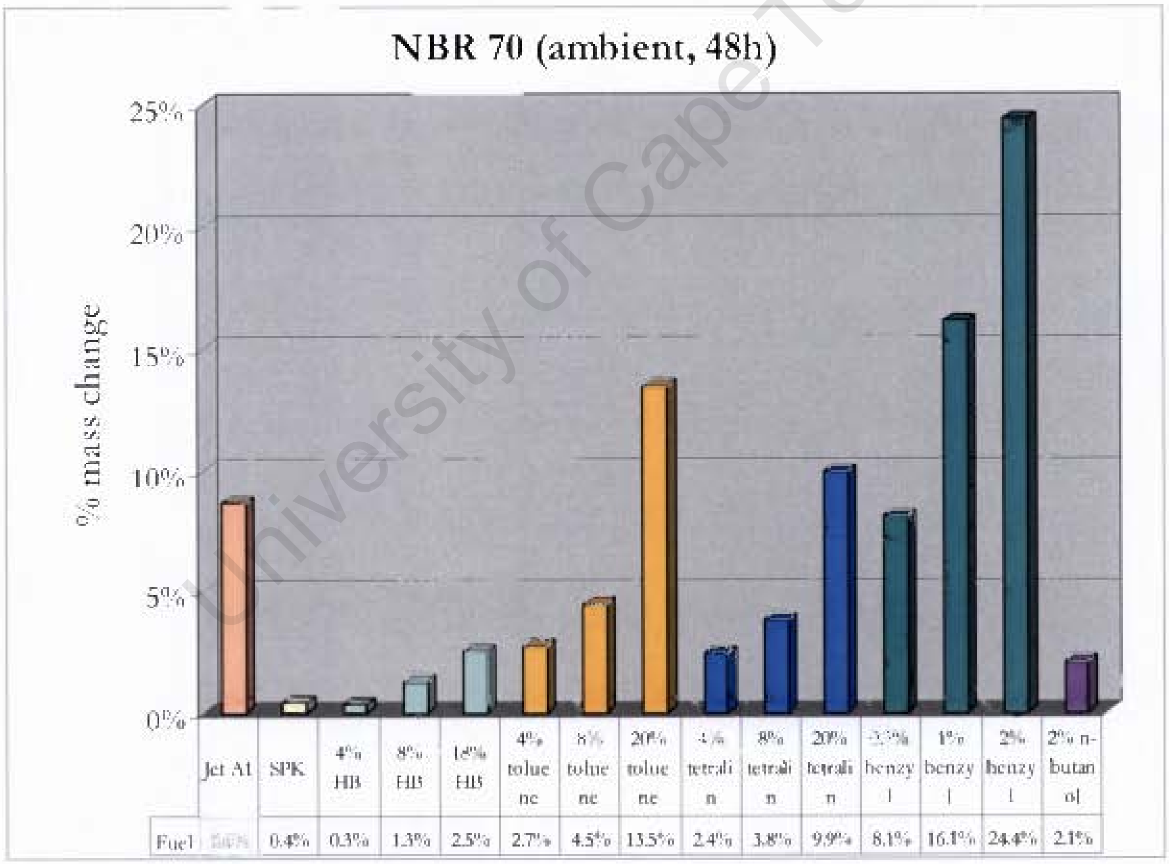

Figure 5.3: Comparing swelling behaviour of additised SPK blends to Jet A-1

It was shown that SPK containing 8% toluene and tetralin do not swell as much compared to Jet A-1. Nevertheless, SPK containing 20% toluene swelled considerably more than Jet A-1. On the other hand, SPK containing 20% tetralin swelled to a similar extent as Jet A-1. SPK additised with 1-2% benzyl alcohol was shown to swell more than Jet A-1. It was also illustrated that SPK additised with hexylbenzene did not swell as much as Jet A-1 but swelled more than neat SPK. This result indicated that the type of aromatic compounds used is significant. Nevertheless in all cases, it can be seen that increasing concentration of aromatics increases swell. In the case of the hexylbenzene (HB) blend, significantly more than 18% aromatics would be required to achieve the same swell at Jet A-1.

Figure 5.4 shows that SPK required at least 0.5% benzyl alcohol, between 10-15% toluene and between 15-18% tetralin to be added to be able to swell as much as Jet A-1. Tetralin has a higher solubility parameter than toluene [41]. It is thus expected to swell more than toluene provided that the difference in solubility parameter between the rubber and the tetralin is small. Toluene, however has a smaller molar volume [41] counterbalancing the solubility parameter effect and hence leading to a greater swell than tetralin. The result of toluene is in agreement with Westbrook and French [55]. They suggested that toluene exhibited a non-ideal behaviour in a toluene/iso-octane blend. In contrast, hexylbenzene has a very small effect on the overall swelling, with even SPK additised with 18% hexylbenzene not comparable to Jet A-1. It was inferred that the aromatics with a significant paraffinic structural component has shown little influence on the swelling behaviour of NBR O-rings as opposed to aromatics with a small paraffinic component such as toluene.

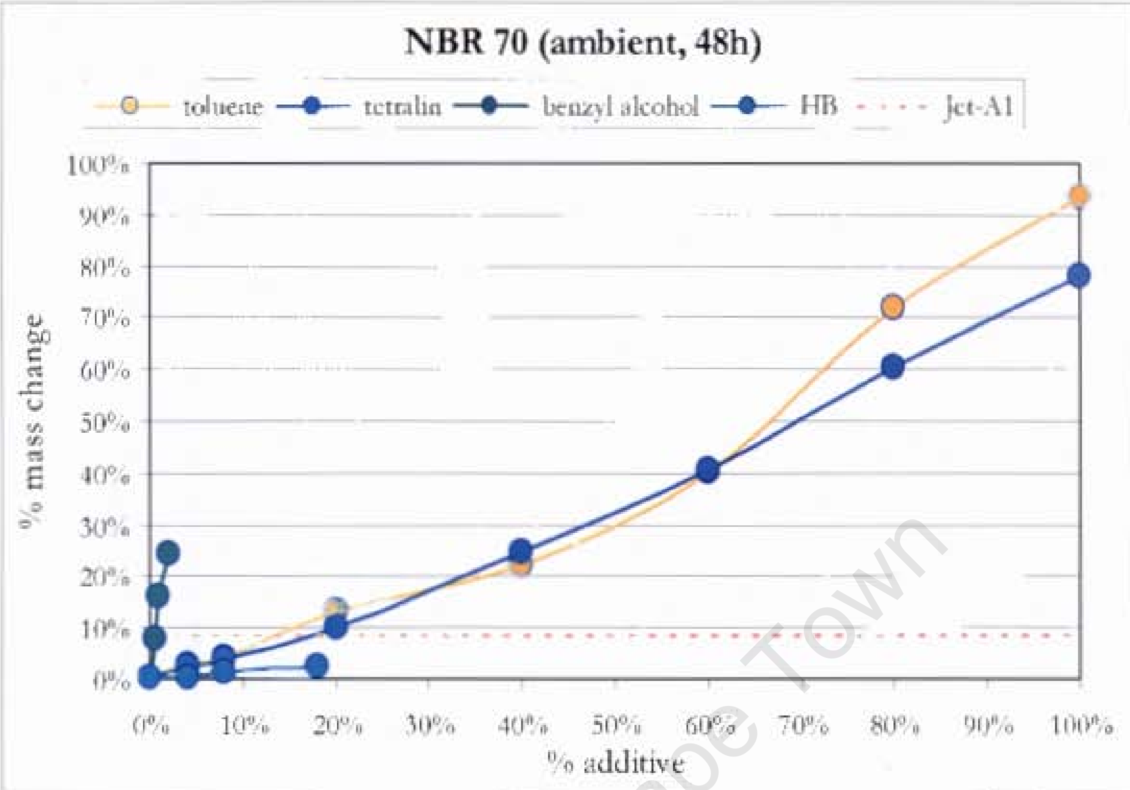

Figure 5.4: Relationship of percentage additive in SPK to change in mass percentage

The solubility parameters of the various blends of SPK were calculated using the solubility blending rule suggested by Beerbower and Dickey [43]. Figure 5.5 below shows the relationship of solubility parameter of blended SPK and percentage mass change. The solubility parameter of SPK blended with tetralin exhibited a proportional relationship with percentage mass change, while toluene has shown a different trend. The results are in good agreement with Flory [52, 57] reporting that swelling increases with increase in solubility parameter. However, tetralin has a higher solubility parameter than toluene but it was showed to swell less compared to toluene. This suggests that molar volume also has an effect on swelling.

It can also be inferred that a high percentage of hexylbenzene is needed to achieve relatively small difference in solubility parameters between NBR and hexylbenzene. Solubility parameter values in Hansen [41] indicated that aromatics with less paraffinic components have larger solubility parameters. Since hexylbenzene has a smaller solubility parameter, more would be required to achieve an amount to swell comparable to Jet A-1. Refer to the Appendix A for detailed calculations of the solubility parameters of SPK and Jet A-1.

On the other side, blends of benzyl alcohol were shown to swell significantly more than Jet A-1 despite their lower total solubility parameter. This result suggests that a specific kind of interaction might be observed between the polar groups of benzyl alcohol and nitrile rubber. This would suggest that benzyl alcohol is preferentially entering the nitrile rubber rather than the SPK.

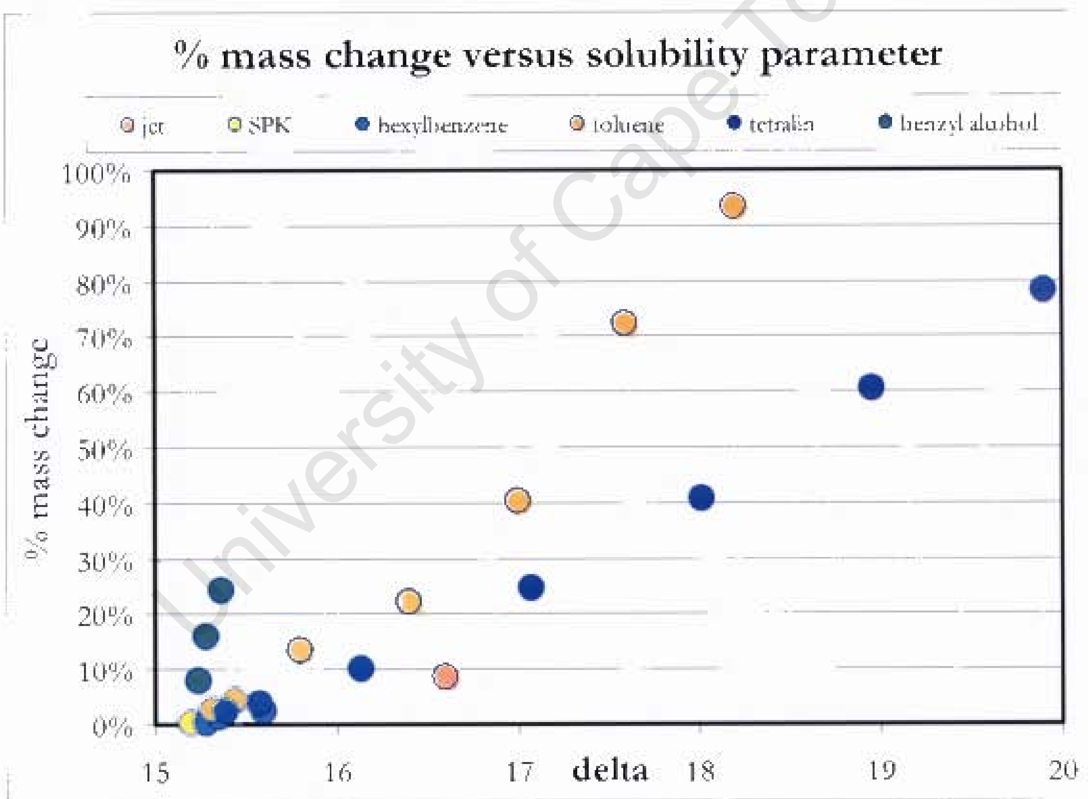

Figure 5.5: Volume change versus total solubility parameter of the SPK blends

5.2 Statistical Analysis

Statistical analysis shown in Table 5.1 illustrates repeatability of mass measurements for Jet A-1 and additised SPK fuels. Some measurements have displayed larger variability especially volatile solvents such as toluene. Toluene is likely to evaporate during mass measurements and therefore, caution must be taken such as performing the measurement quicker to reduce any solvent evaporation. Also, a high value of coefficient of variation (CV) was observed with low percentages of mass change. Otherwise the mass measurements were consistent, suggesting very good repeatability.

Table 5.1: Tabulated values of mean mass % change, standard deviation of the mean and coefficient of variation of Jet A-1 and SPK additised blends fuels

Solvent	Mean mass % change	Standard deviation of the mean	CV
Jet A1	8.6%	0.4%	4.6%
SPK	0.4%	0.1%	15.2%
4% HB	0.3%	0.0%	5.7%
8% HBB	1.3%	0.2%	15.2%
18% HBB	2.5%	0.0%	0.0%
4% toluene	2.7%	0.0%	0.8%
8% toluene	4.5%	0.1%	3.3%
20% toluene	13.5%	1.0%	7.1%
4% tetralin	2.4%	0.1%	2.1%
8% tetralin	3.8%	0.2%	6.1%
20% tetralin	9.9%	0.0%	0.1%
0.5% benzyl alcohol	8.1%	0.7%	8.5%
1% benzyl alcohol	16.1%	1.0%	6.3%
2% benzyl alcohol	24.4%	3.3%	13.7%
2% n-butanol	2.1%	0.3%	16.1%

Table 5.2: Tabulated values of mean mass % change, standard deviation of the mean and coefficient of variation of Jet A-1 and SPK and pure solvents

Solvent	Mean mass % change	Standard deviation of the mean	CV
Jet A1	8.6%	0.4%	4.6%
SPK	0.4%	0.1%	15.2%
i-octane	0.2%	0.0%	6.8%
n-octane	0.8%	0.4%	48.2%
1,2-dimethylcyclohexane	5.8%	0.1%	1.6%
decalin	7.3%	0.6%	7.9%
toluene	93.4%	1.1%	1.2%
tetralin	78.1%	0.3%	0.4%
benzyl alcohol	126.0%	1.3%	1.1%
n-butanol	3.7%	0.0%	1.1%

5.3 Interaction Energies of Model Rubber and Model Fuel Solvent

The binding energies of pure solvent molecules interacting with the isobutylnitrile model compound are shown in Figure 5.6. The least energy value (minimum value) indicates the most stabilised interaction between two molecules of interest. Benzyl alcohol was shown to have more negative energy (least energy), followed by toluene and tetralin. Dimethylcyclohexane and isooctane were both shown to have significant interaction with isobutylnitrile. Dimethylcyclohexane was shown to have lower energy value compared to normal and iso paraffins. This would suggest that cyclic-paraffins interact better than straight chain paraffins. However, it was reported by Alfonso and Cugini [37] that density functional theory provides poor energy prediction for weak interaction complexes.

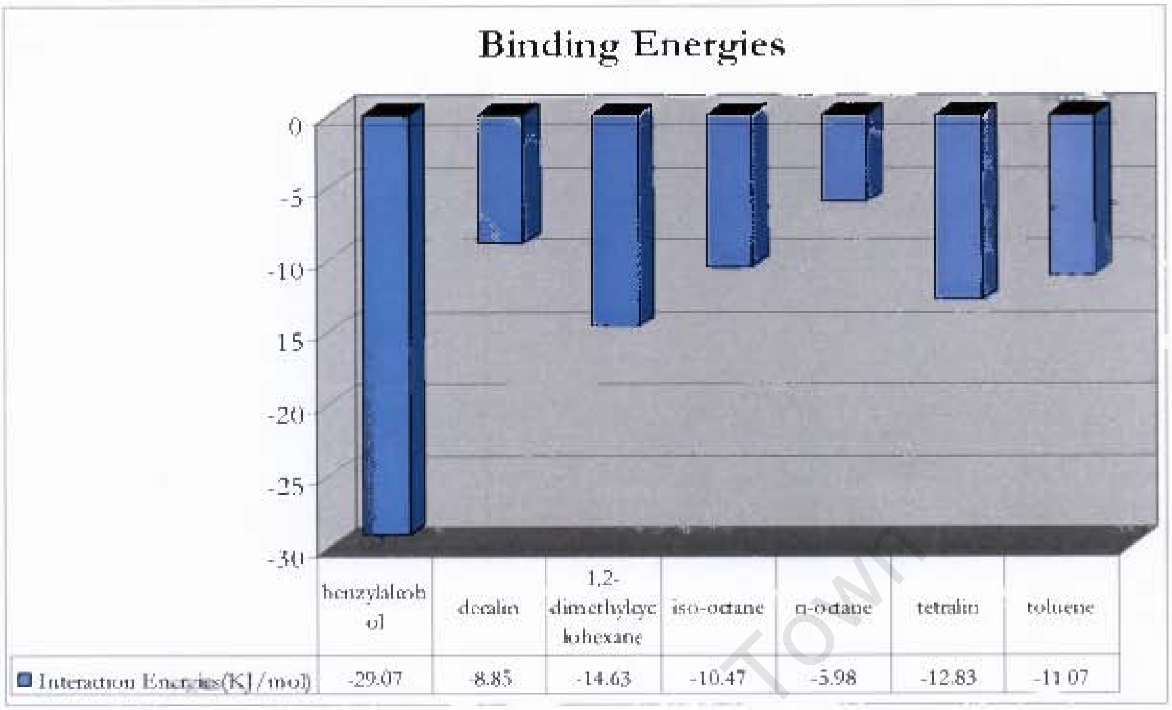

Figure 5.6: Interaction energies of pure solvents bonded with nitrile rubber

Referring to the Figure 5.7 below, the optimised geometries of these structural molecules indicated possible interactions between the solvents and the isobutylnitrile compound. The molecules orient themselves in a direction which gives the most stable (optimised) geometry. The proximity of certain functional groups between two molecules indicates a tendency of a very strong interaction.

Benzyl alcohol displayed strong interaction with the isobutylnitrile compound. It was shown with the proximity of the hydroxyl group of benzyl alcohol to the nitrile group of the polymer. It can be inferred that a specific interaction such as hydrogen bonding is possible between the two compounds. On the other hand, it can be inferred that dipole-dipole interaction might be present between the nitrile group of the polymer and either toluene or tetralin.

Alkanes (paraffins) are non-polar compounds and generally have very weak interaction such as dispersive forces. Hence, they interact very weakly with the nitrile group of the polymer compared to polar compounds. Also, it should be noted that the butadiene monomer of the NBR polymer was ignored due to the complexity of the calculation. The polybutadiene segment contains double bonds which would interact preferentially with the aromatic double bonds and hence, give better energy estimation and possible stable geometries.

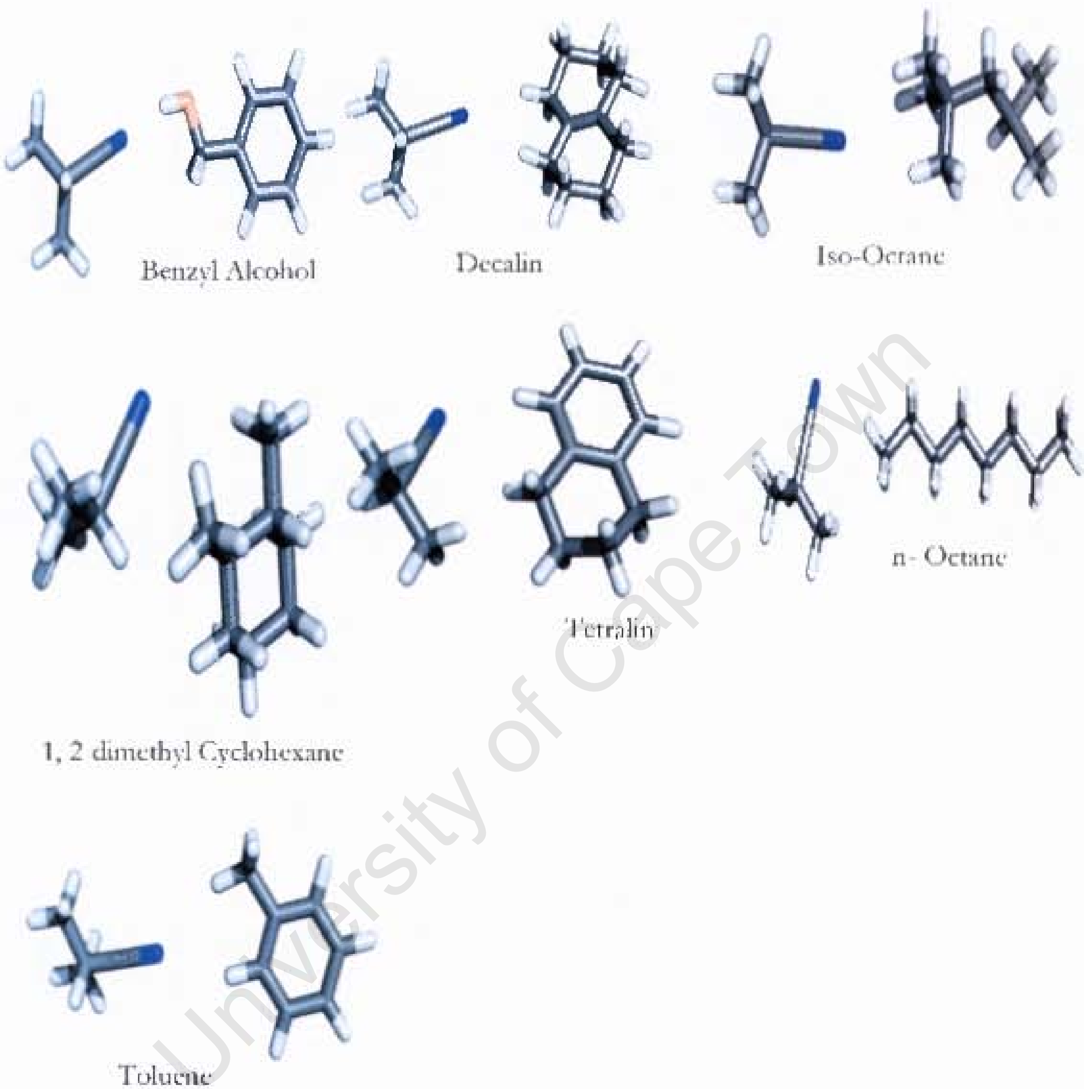

Figure 5.7: Optimised geometries of model fuel molecules and model polymer. White, red, blue and grey are hydrogen, oxygen, nitrogen and carbon atoms respectively

5.4 Static Switch Load Experiments

5.4.1 Switch Load Between Jet A-1 and SPK for NBR 70 and 90 O-rings

Figure 5.8 shows the percentage mass change of NBR 70 O-ring immersed in Jet A-1 and SPK. The graph displayed a decrease in percentage mass change when the O-rings were switched from Jet A-1 to SPK. The amount of swell when switched to SPK was higher compared to the swell if it was initially immersed in SPK. This indicated that some residual amount of Jet A-1 might not have diffused out from the rubber causing it to swell more than expected when switched to SPK.

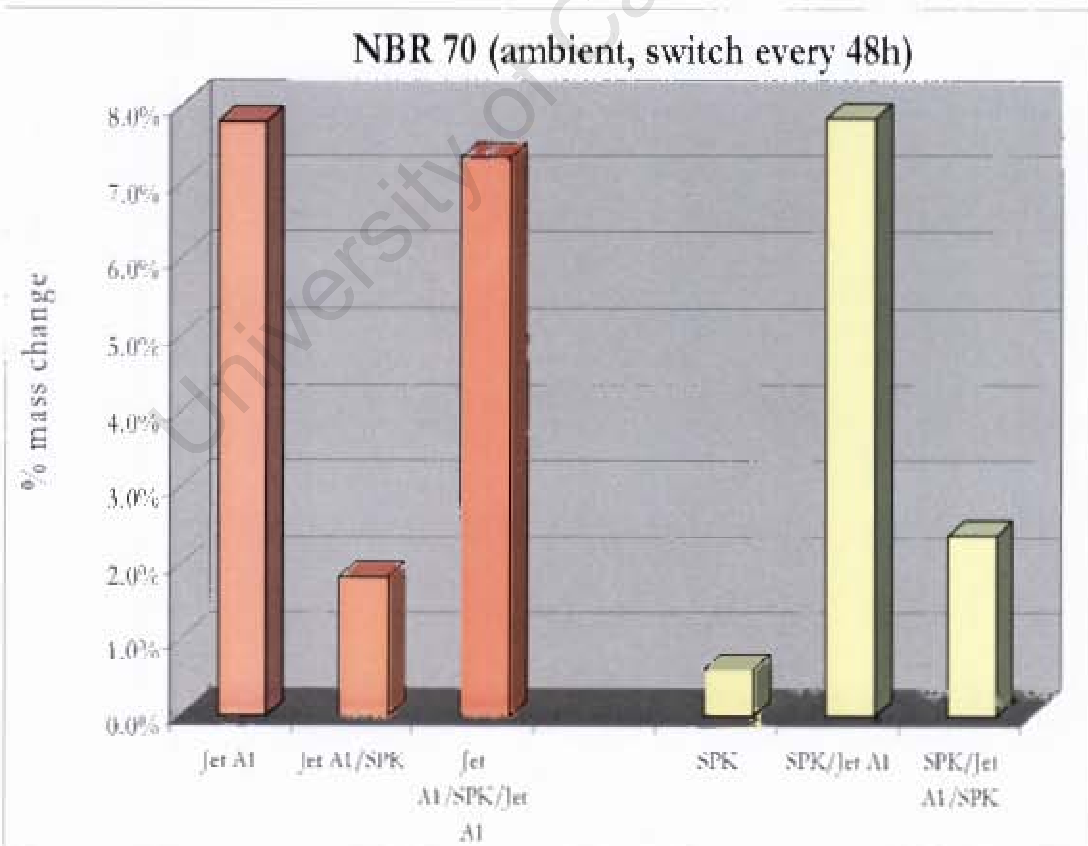

Figure 5.8: Switch load NBR 70 O-ring between Jet A-1 and SPK

An opposite effect was observed when NBR O-rings were immersed initially in SPK and then switched to Jet A-1. An increase in percentage mass change was expected when the O-rings were switched from SPK to Jet A-1. However, switching the O-rings back to SPK resulted in an increase in percentage mass change compared to the swell in neat SPK before the switching of fuels for the same reason mentioned above.

Similar behaviour was observed for NBR 90 O-rings when switched from Jet A-1 to SPK and vice versa as shown in Figure 5.9.

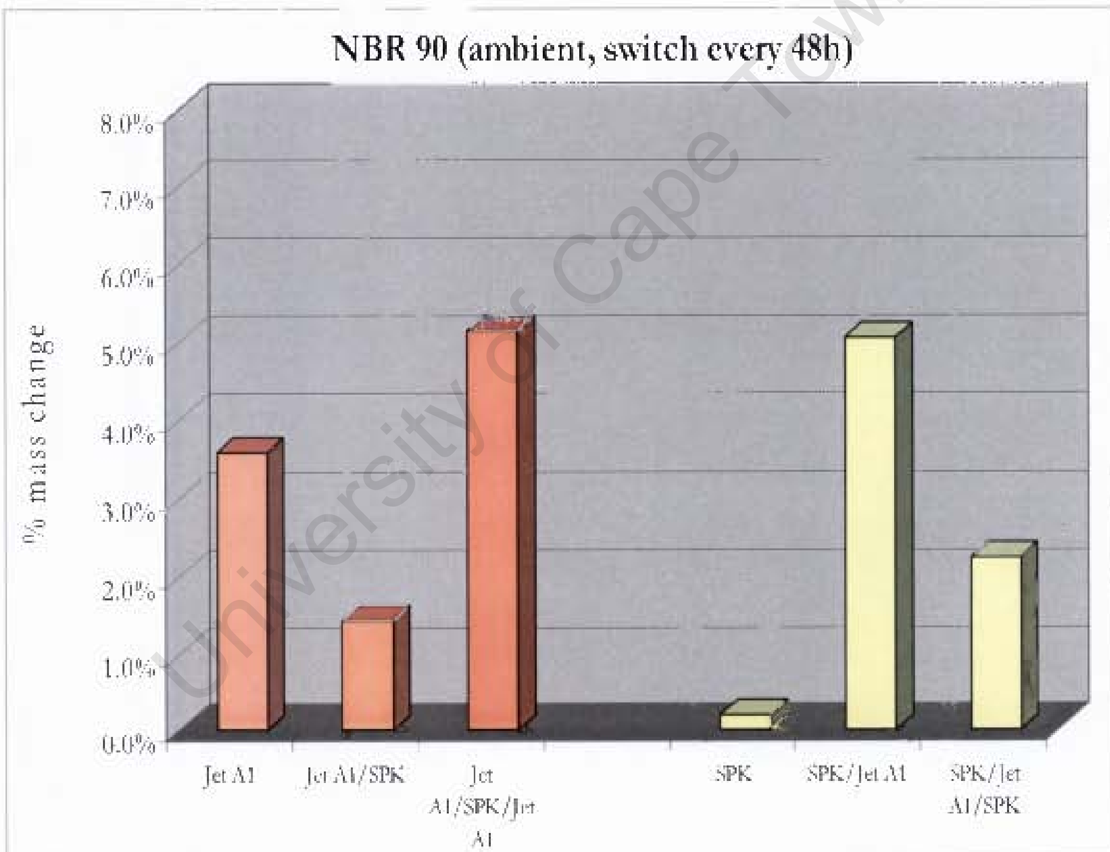

Figure 5.9: Switch load NBR 90 O-ring between Jet A-1 and SPK

NBR 90 is a harder O-ring with typically less plasticisers than NBR 70 O-rings. It is known that harder materials have higher amount of carbon black as their compounding ingredient but this does not necessarily results in increase hardness but displays resistance to deterioration. The reinforcing fillers restrict the mobility of rubber chains and hence, make it difficult for the solvent molecules to diffuse into the gaps between the rubber molecules. This results in a decrease in the amount of swelling [58]. NBR 90 O-rings swell less in both the experiments which is in agreement with Mosafa *et al.* [58].

5.4.2 Switch Load Between Jet A-1 and Additised SPK

Figure 5.10 shows a switch load between Jet A-1 and SPK additised with 8% toluene. SPK containing 8% toluene swelled less compared to Jet A-1.

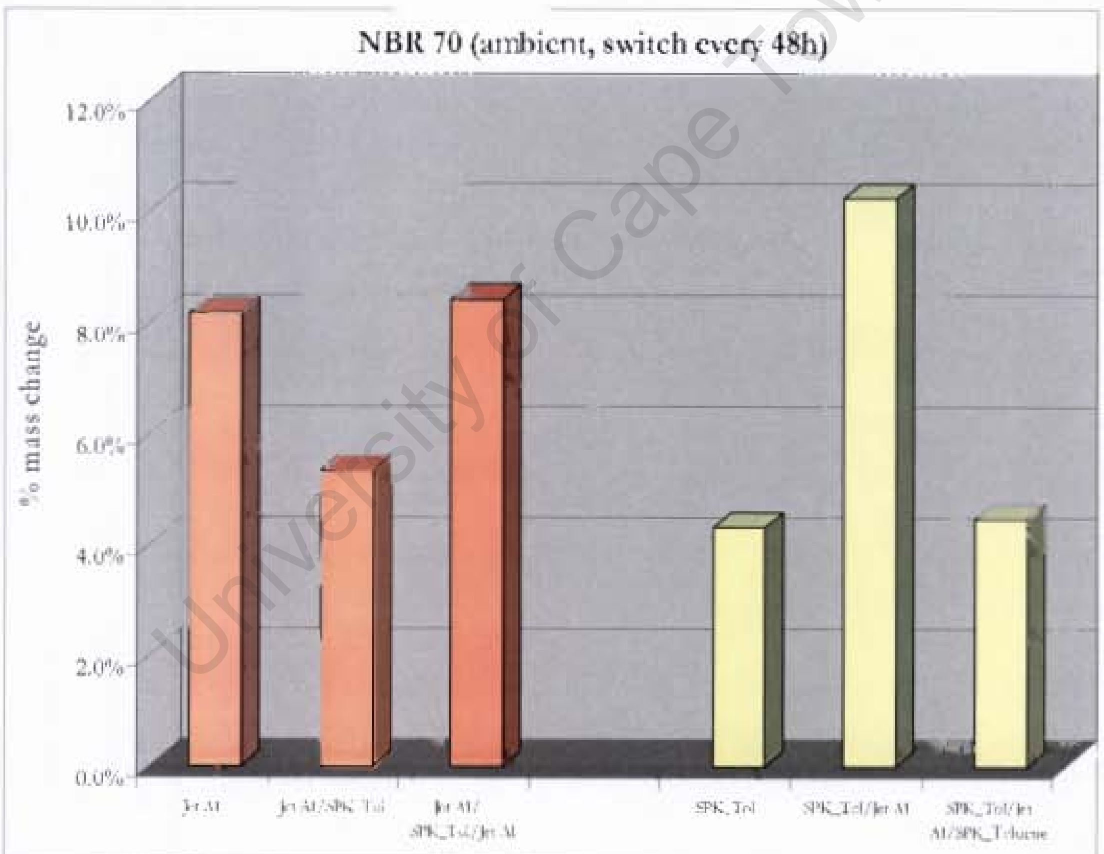

Figure 5.10: Switch load NBR 70 O-ring between Jet A-1 and SPK additised with 8% toluene

This caused the NBR O-ring to shrink when switched from Jet A-1. It is suggested that Jet A-1 diffused out from the rubber. It is known that diffusion occurs from high to low concentration and therefore, a concentration gradient of Jet A-1 had developed between the rubber and SPK additised with 8% toluene. However, switching back to Jet A-1 from SPK additised with 8% toluene resulted in an increase in mass. On the other hand, the O-ring swelled extensively upon switching from SPK additised with 8% toluene to Jet A-1. The rubber eventually shrinks upon switching back to additised SPK for the reasons mentioned above.

Figure 5.11 shows a switch load between Jet A-1 and SPK additised with 0.5% benzyl alcohol. SPK containing 0.5% benzyl alcohol was shown to swell slightly less than Jet A-1. However, the decrease in mass upon switching from Jet A-1 was small compared to neat SPK. From this it may be inferred that SPK containing 0.5% benzyl alcohol may not be enough to match the swelling of Jet A-1. An opposite effect was shown with SPK additised with 0.5% benzyl alcohol switched to Jet A-1.

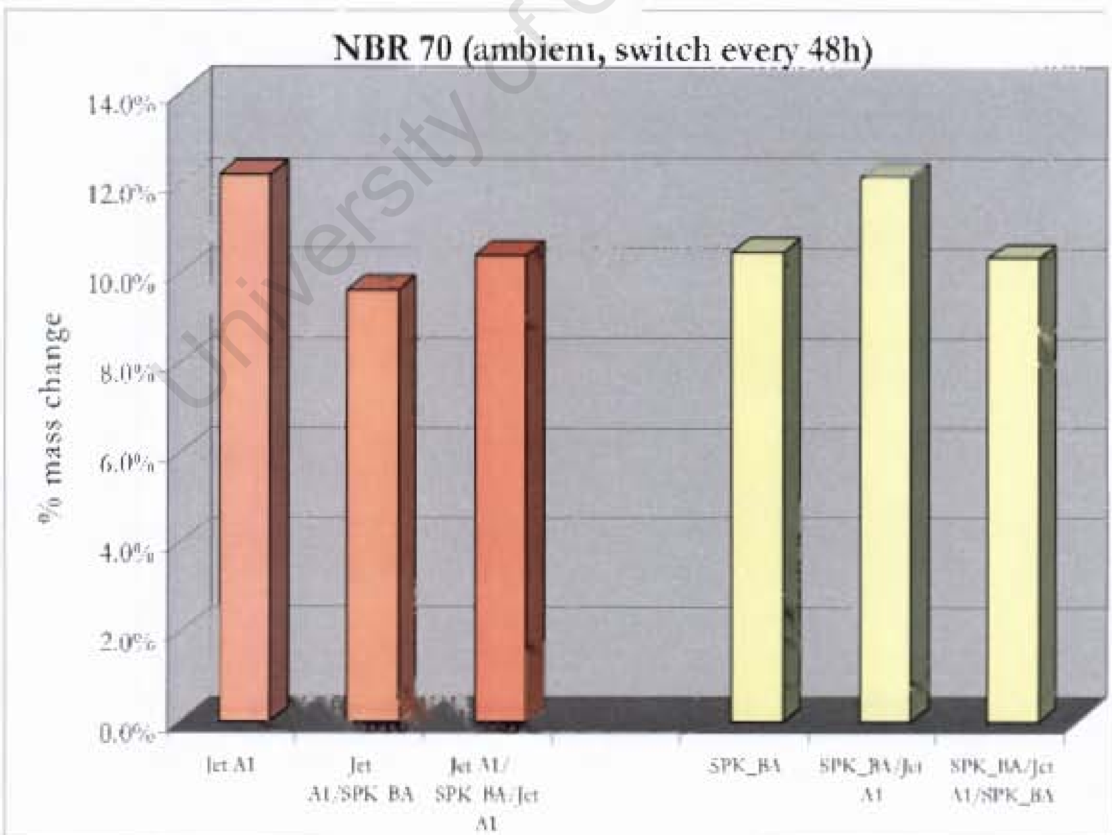

Figure 5.11: Switch load NBR 70 O-ring between Jet A-1 and SPK additised with 0.5% benzyl alcohol (BA)

Referring to Figure 5.12 and 5.13, both figures show switch load behaviour between SPK containing 1% and 2% benzyl alcohol and Jet A-1. The result displayed a significant increase in percentage mass change when switched from Jet A-1 to both SPK additised with 1% and 2% benzyl alcohol. SPK additised with 2% benzyl alcohol showed an even greater amount of swelling compared to Jet A-1. When SPK containing 1% or 2% benzyl alcohol was switched to Jet A-1, there was a decrease in percentage mass change. This result suggested that concentrations of 1-2% benzyl alcohol could be blended in SPK to provide the fuel with adequate swelling ability compared to Jet A-1.

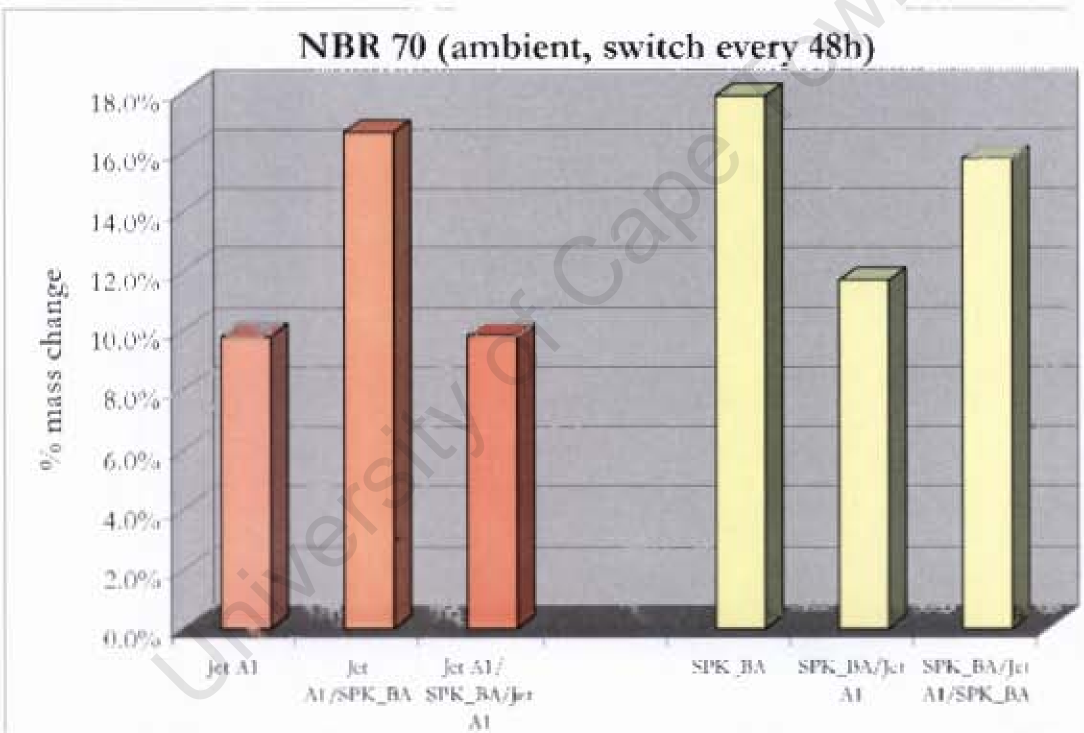

Figure 5.12: Switch load NBR 70 O-ring between Jet A-1 and SPK additised with 1% benzyl alcohol (BA)

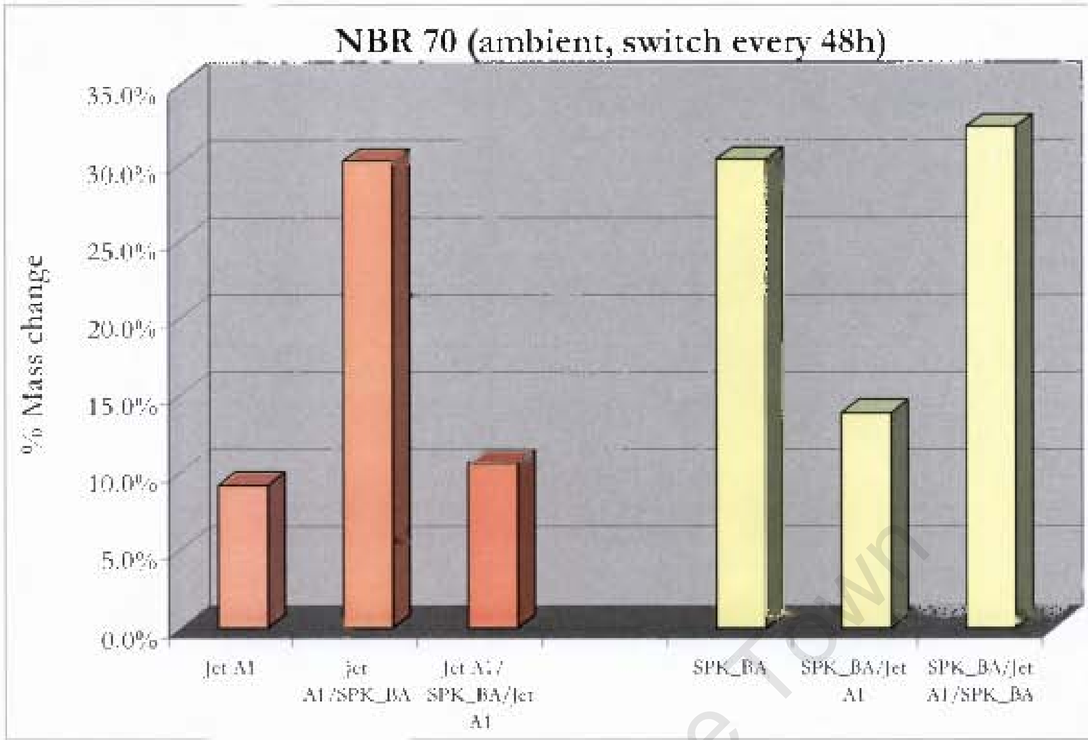

Figure 5.13: Switch load NBR 70 O-ring between Jet A-1 and SPK additised with 2% benzyl alcohol (BA)

5.5 Elastomer Rig Compression Experiments

5.5.1 Normalised Expansion of NBR O-rings in Jet A-1 and SPK

The seal swelling parameter in an O-ring compression test was determined by using the normalised ratio of thickness (T) at any given point in time to the estimated thickness at the test temperature at time zero (T_0). Thickness, T_0, was calculated by extrapolating an exponential curve to determine the thickness at 50°C (test temperature). The equation below was used to extrapolate the thickness at 50°C.

$$T = T_0 + \beta(1 - e^{-kt})$$

This ratio is called normalised expansion, λ (lambda). The graph in Figure 5.14 shows the change in lambda with time for nitrile O-rings of the same type immersed in Jet A-1 and SPK. The thicknesses of the O-ring increases to a maximum for Jet A-1 followed by a decrease in thickness (contraction). Experimental results obtained from the compression rig test were shown to agree with the time swell experiment conducted for a static swell experiment in terms of the swelling behaviour i.e. both tests showed similar trend of swelling and shrinking as a function of time. However, with time the thickness of the O-ring in Jet A-1 stabilises to give a constant lambda value. The change in thickness for the SPK fuel was very minimal indicating poor swelling behaviour. On the other side, SPK continues to contract at extended periods of time. It was suggested that the decrease in thickness of O-rings was caused by plasticiser extraction from the rubber. This behaviour is shown in Jet A-1 and SPK, with Jet A-1 removing plasticiser faster than SPK.

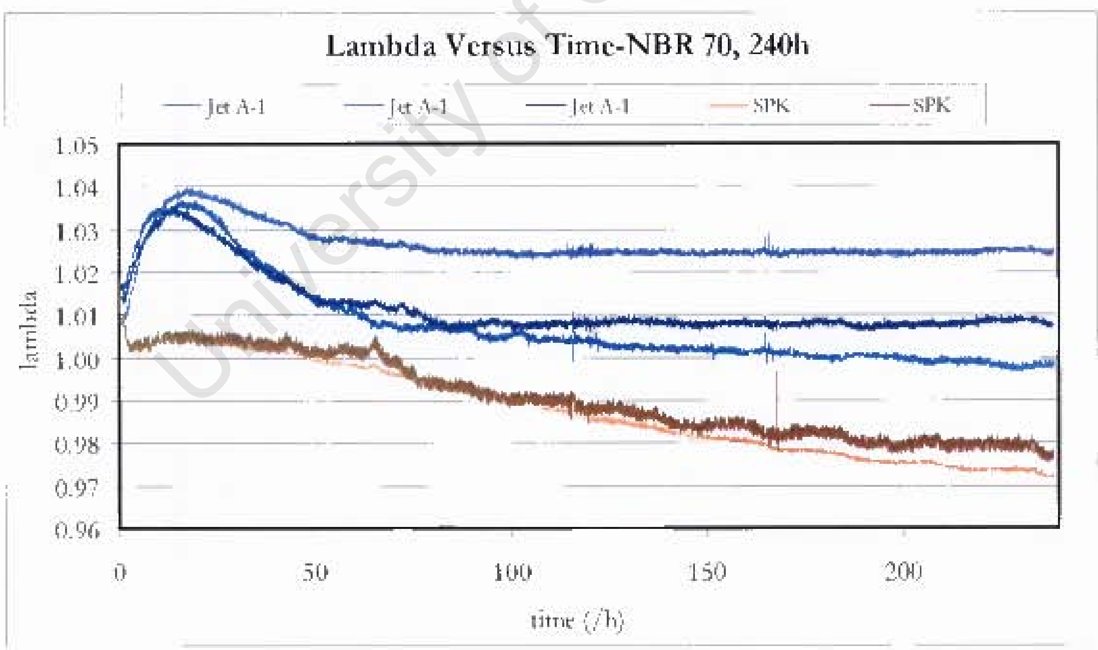

Figure 5.14: Thickness change of NBR 70 O-rings with time in SPK and Jet A-1 for 240h and 50°C

Figure 5.15 shows changes in breakaway pressure with time. The breakaway pressures presented on the Figure indicate the measured pressure plus an offset in order to show clarity within the trends. The result displayed a similar trend to changes in lambda. The breakaway pressure increases to a maximum for Jet A-1 as a result of O-ring swelling, i.e. it requires more pressure to compress a swollen O-ring. On the other hand, small changes in breakaway pressure were observed for SPK. However, the breakaway pressure decreases as a result of rubber contraction before it reaches a constant value. Breakaway pressure appears to be less sensitive than the displacement measurements which are sensitive to temperature changes during start-up where not only does the seal contract but the rig apparatus expands on heating.

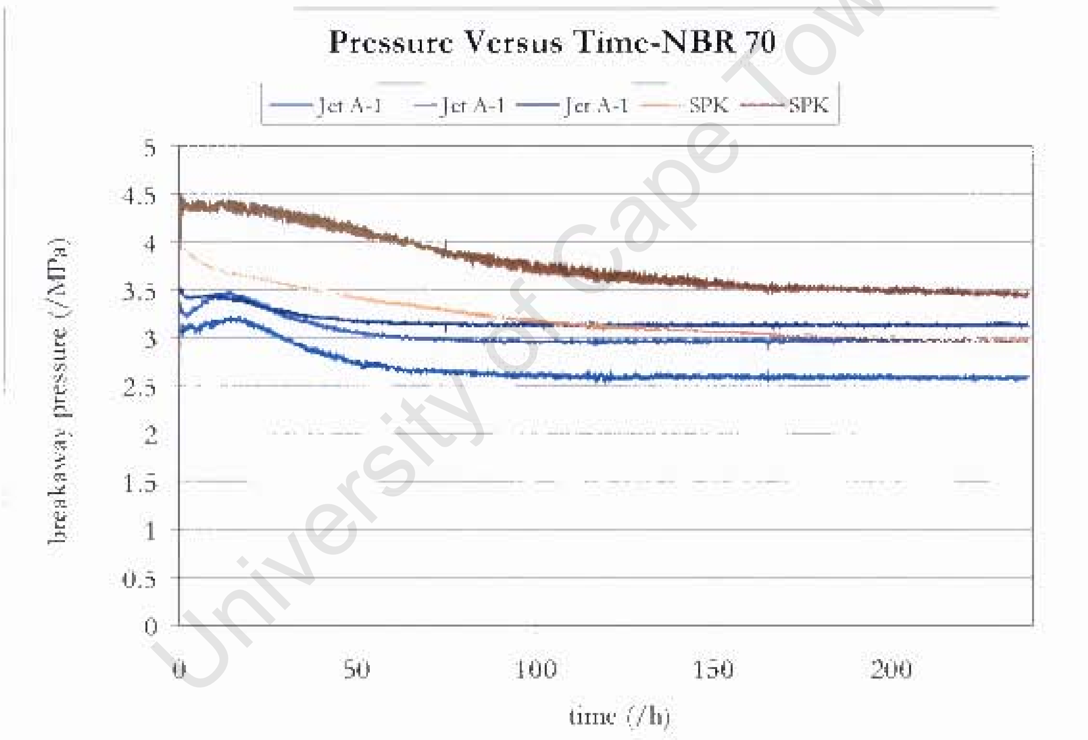

Figure 5.15: Breakaway pressure versus time for NBR 70 O-rings

Figure 5.16 shows thickness change in nitrile 90 O-rings. Nitrile 90 is a harder O-ring containing less plasticiser than nitrile 70 O-ring. The graph has indicated that no decrease in thickness could be observed for both the fuels. It is suggested that NBR O-ring might not have any plasticisers (or very little) to begin with or the little plasticisers that were present initially were extracted from the rubber during the initial swelling process. The breakaway pressure displays a similar trend to λ with no decrease in thickness of the O-ring.

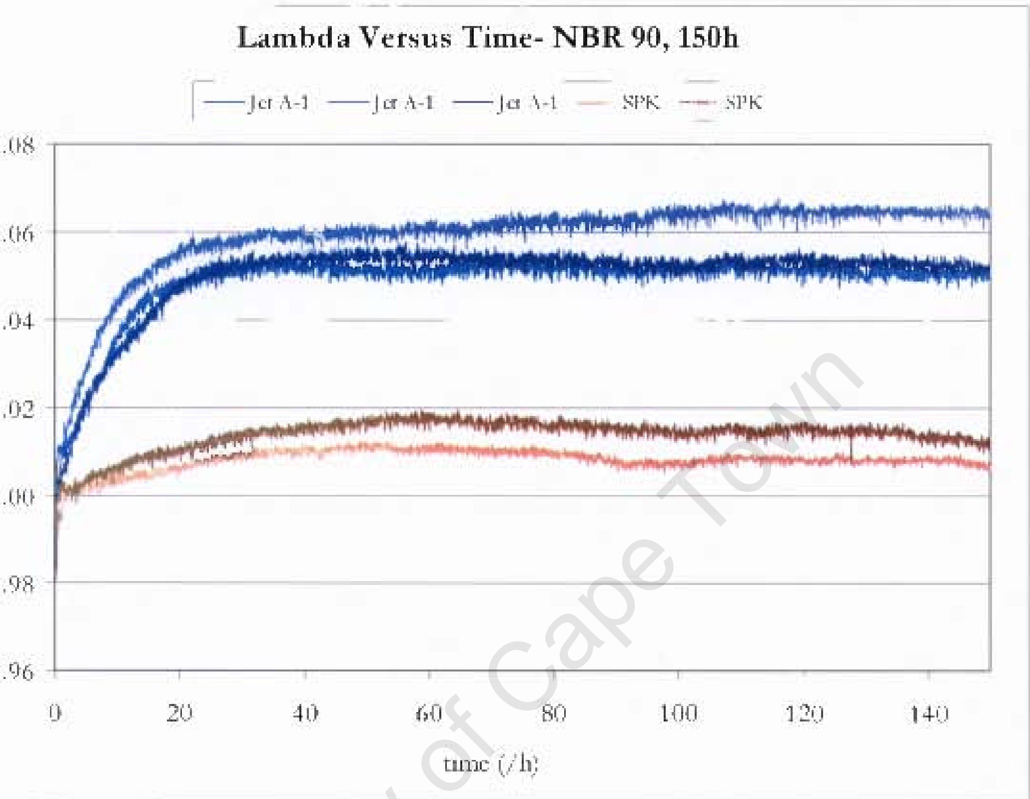

Figure 5.16: Thickness change of nitrile 90 O-ring with time in SPK and Jet A-1

5.5.2 Normalised Expansion of NBR O-rings in Jet A-1 and Additised SPK

Referring to Figure 5.17, SPK additised with 8% toluene displayed similar maximum swelling compared to Jet A-1. On the other hand, both fuels showed a decrease in thickness to a certain extent after which Jet A-1 reached a constant thickness while SPK additised with 8% toluene decreased further in thickness. This result suggested that SPK additised with 8% toluene had slower diffusion kinetics in terms of plasticiser removal compared to Jet A-1. However, referring to Section 5.1.3, SPK additised with 8% toluene was shown to swell less compared to Jet A-1. This result further suggested that there is a temperature effect on the diffusion kinetics of solvent and plasticiser molecules.

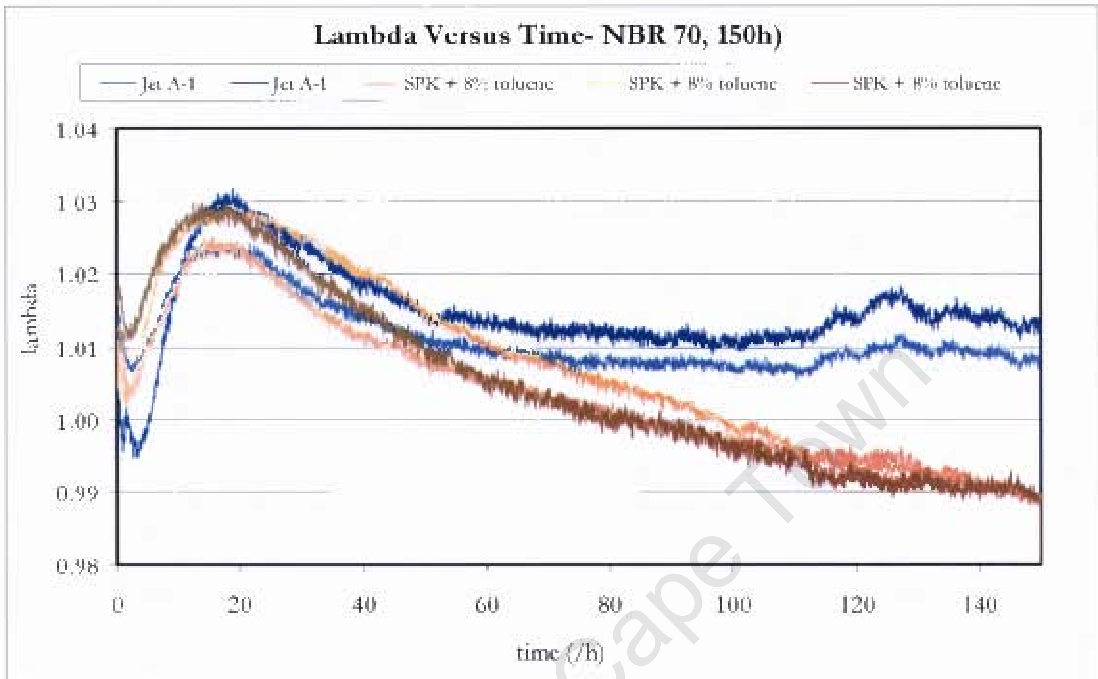

Figure 5.17: Thickness change of nitrile 70 O-rings with time in 8% toluene additised SPK

Results displayed in Figure 5.18 with SPK additised with 4% and 8% tetralin showed that SPK additised with 8% tetralin has better swelling performance compared to SPK containing 4% tetralin. The results suggested that swelling of NBR O-rings in SPK can be enhanced depending on the concentration of tetralin in the final blend. However, concentration effect of tetralin in the final blend also has an effect on the diffusion kinetics of plasticiser extraction. The result also suggested that SPK additised with 8% tetralin swell to a similar extent to Jet A-1 (albeit possibly slightly less). The maximum thickness for SPK containing 8% tetralin is delayed relative to Jet A-1 suggesting that tetralin diffuses more slowly into the rubber than Jet A-1. This result was confirmed by observing the breakaway pressure graph (not shown).

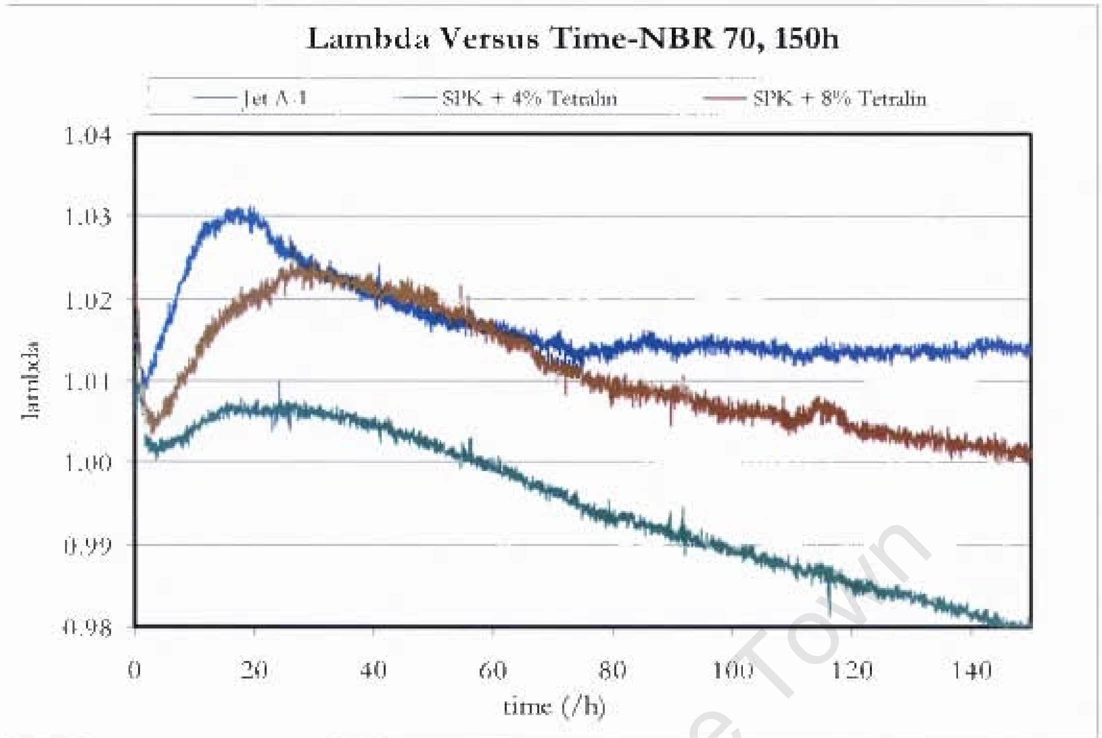

Figure 5.18: Thickness change of NBR 70 O-rings with time in SPK additised with 4% and 8% tetralin

Figure 5.19 shows the graph of SPK additised with 4% and 8% hexylbenzenes. The result illustrates that SPK additised with hexylbenzenes show little additional swelling compared to neat SPK. SPK containing 8% hexylbenzenes showed greater amount of swell compared to SPK additised with 4% hexylbenzenes. The results suggested that swelling was dependent on the total concentration of hexylbenzenes in the final blend. The results agreed with static swelling experiment shown in Section 5.1.3 inferring that the type of aromatics used in this particular experiment have little influence on swelling NBR O-rings.

In a similar experiment shown in Figure 5.20, SPK additised with 18% hexylbenzenes displayed less swelling compared to Jet A-1. However, swelling performance of 18% hexylbenzenes has shown to increase significantly compared to the lower concentrations shown in Figure 5.19.

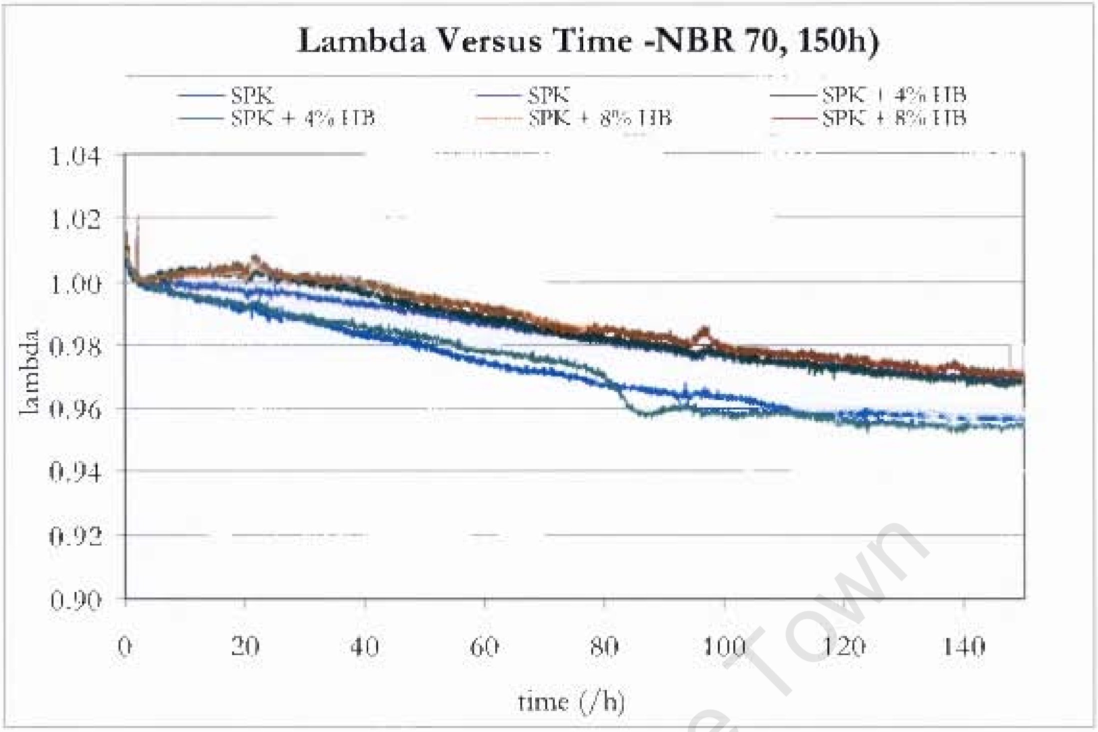

Figure 5.19: Thickness change of NBR 70 O-rings with time in 4% and 8% hexylbenzenes additised SPK

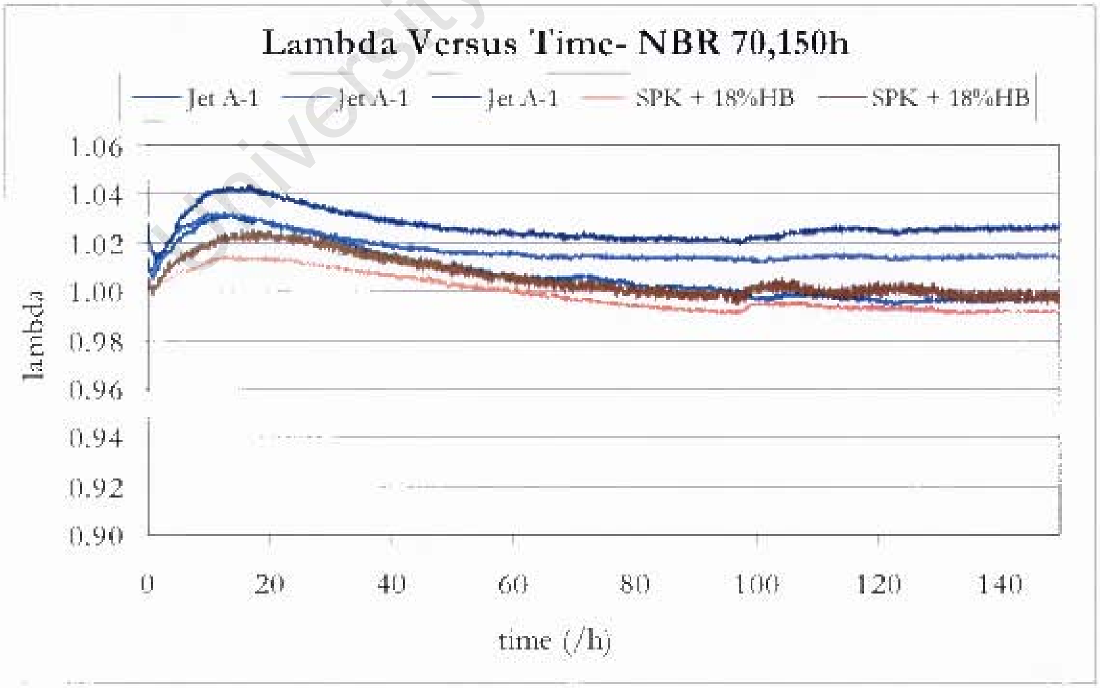

Figure 5.20: Thickness change of NBR 70 O-rings with time in SPK additised with 18% hexylbenzenes

Referring to Figure 5.21, SPK additised with 0.5% benzyl alcohol was shown to swell less compared to Jet A-1. On the other hand, referring to Figure 5.22 and 5.23, SPK additised with 1%, and 2% benzyl alcohol respectively show similar maximum thickness change compared to Jet A-1. However, SPK additised with 2% benzyl alcohol shows much closer behaviour to Jet A-1 as opposed to the lower concentrations of benzyl alcohol. The results also illustrated that change in thickness for SPK additised with benzyl alcohol is much slower suggesting that the diffusion of benzyl alcohol into the rubber occurs at a slower rate compared to Jet A-1

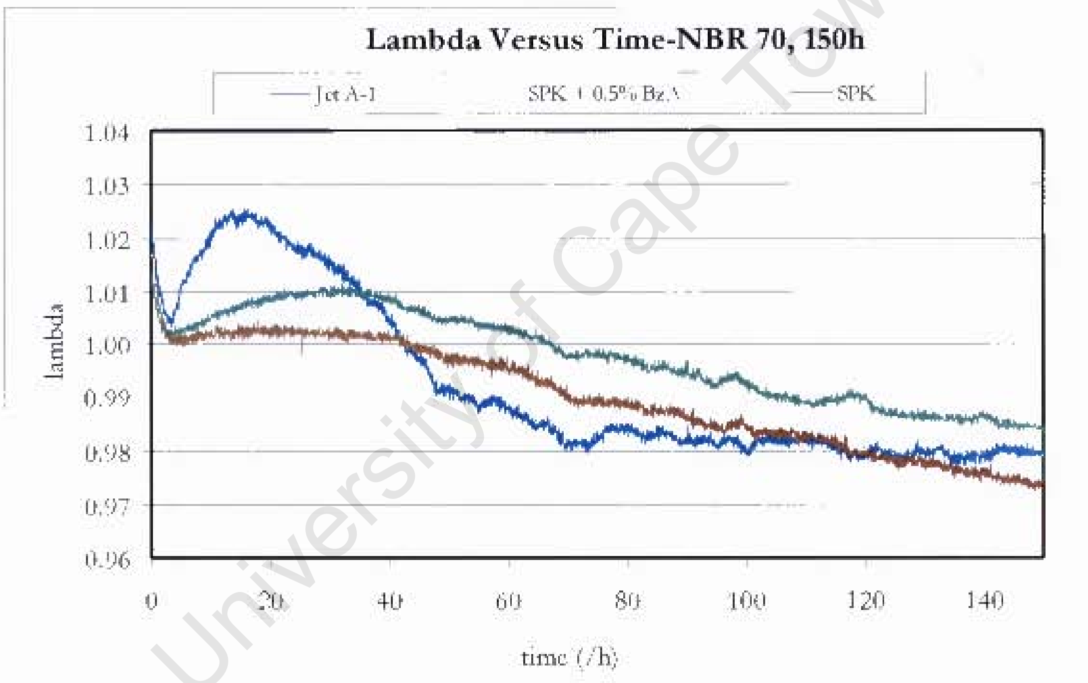

Figure 5.21: Thickness change of NBR 70 O-rings with time in 0.5% benzyl alcohol additised SPK

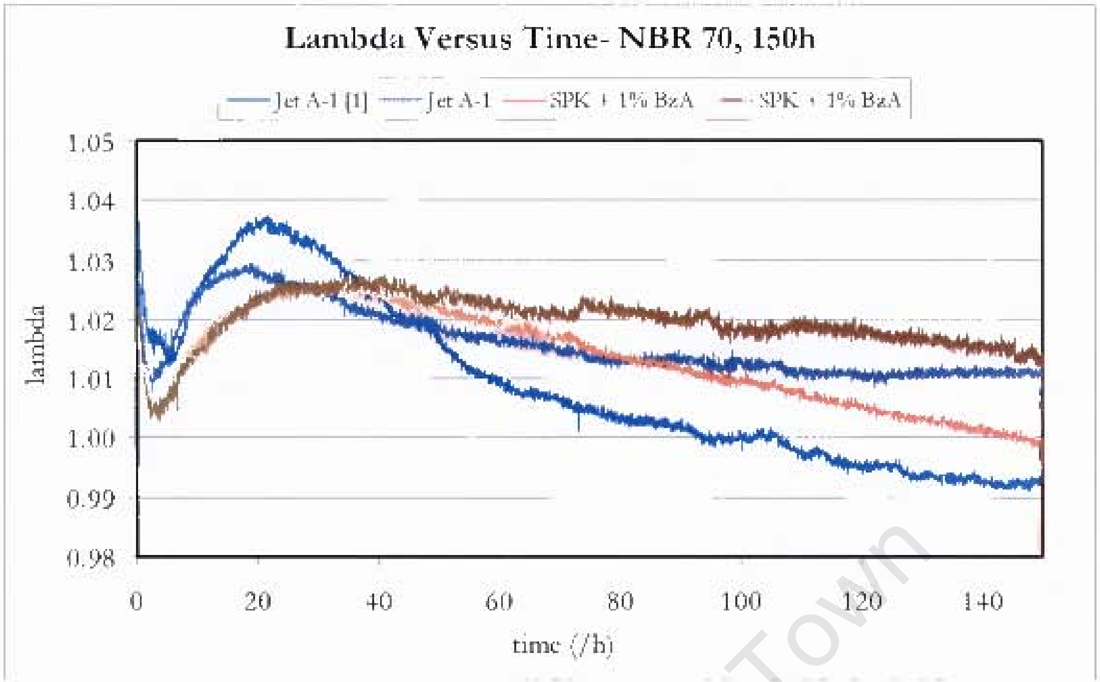

Figure 5.22: Thickness change of NBR70 O-rings with time in 1% benzyl alcohol additised SPK

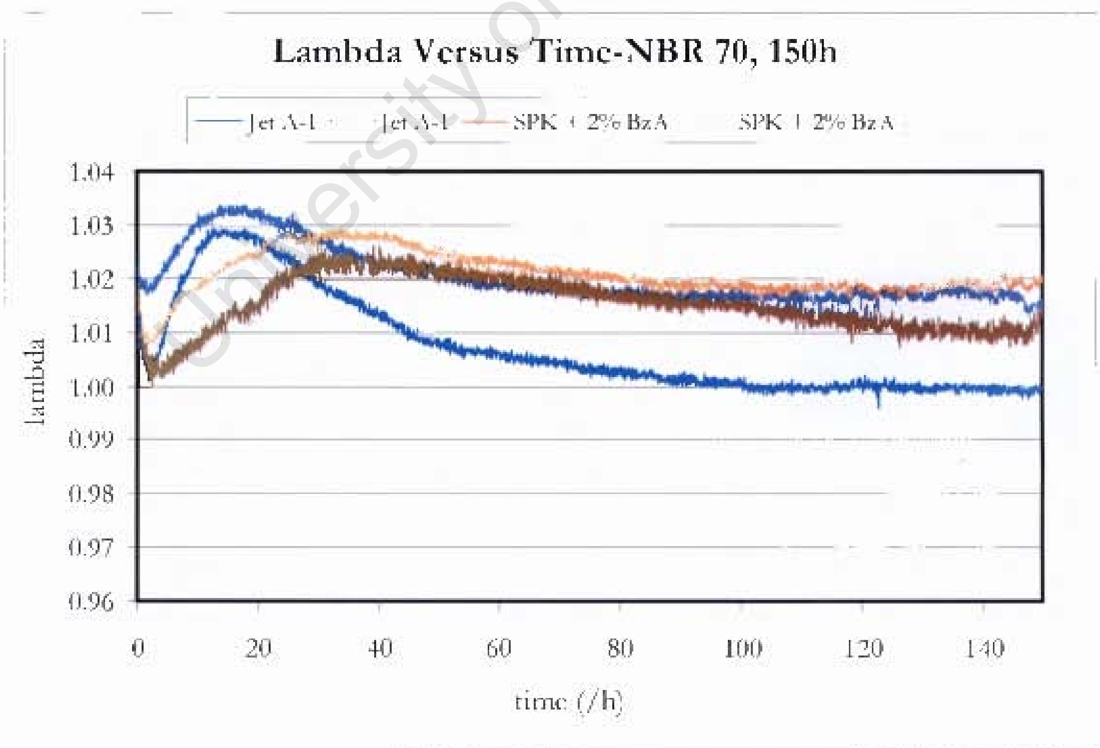

Figure 5.23: Thickness change of NBR 70 O-rings with time in 2% benzyl alcohol additised SPK

5.6 Rig Compression Switch Load Experiments

5.6.1 Switch Load Compliance Test

The compliance of the rig for a switch load test was done using the same fuel for every switch load. Figure 5.25 shows the switch load experiment with Jet A-1 and SPK switched with itself. The breakaway pressure was shown to have no effect upon switching the fuels suggesting that the rig is working in accordance with the post design modifications mentioned in section 4.1.3. These post design modifications were required in order to develop an experimental procedure for the switch load experiment.

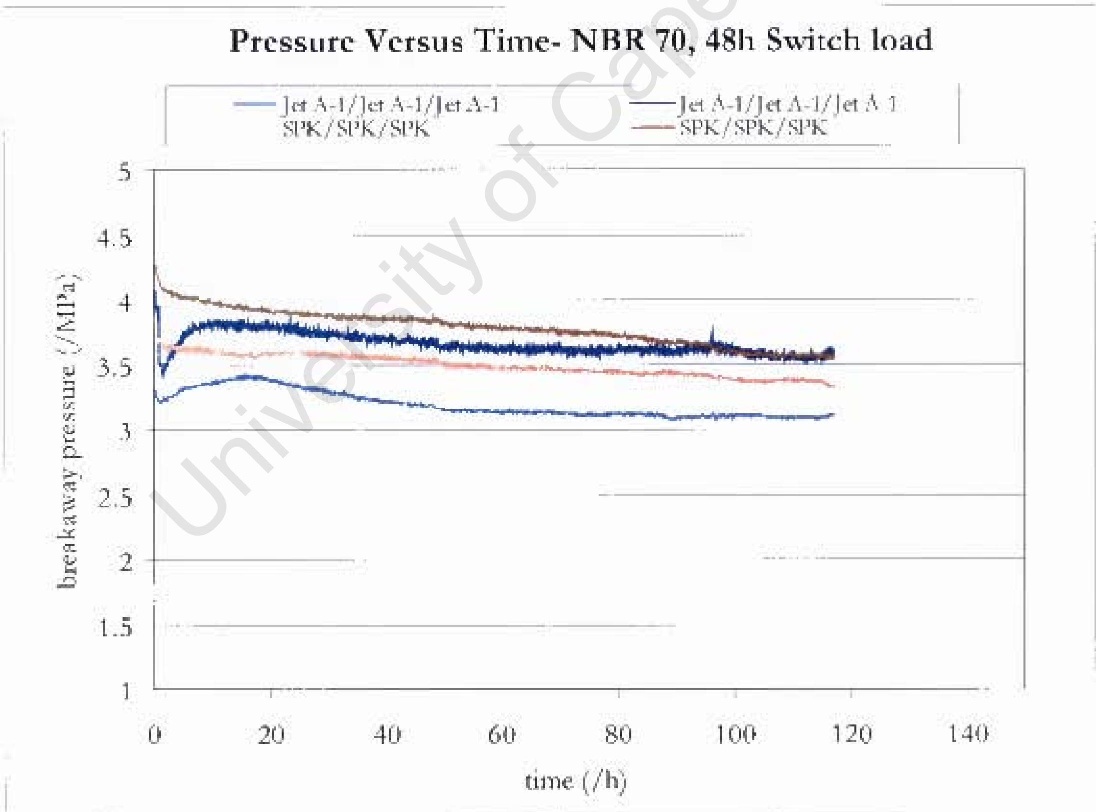

Figure 5.24: Switch load between the same fuels to check the compliance of the rig

5.6.2 Switch Load Between Additised SPK and Jet A-1

Figure 5.26 shows a switch load test between SPK additised with 8% toluene. Jet A-1 was kept as a baseline fuel for comparison. The first switch load pair between Jet A-1 and SPK additised with 8% toluene resulted in a decrease in thickness of the O-ring upon switching to additised SPK. The thickness increased again after switching back to Jet A-1. The result correlated well with the static (bench) switch load shown in Section 5.2.2 for the two pair of fuels. An opposite effect was observed with SPK additised with 8% toluene switched to Jet A-1.

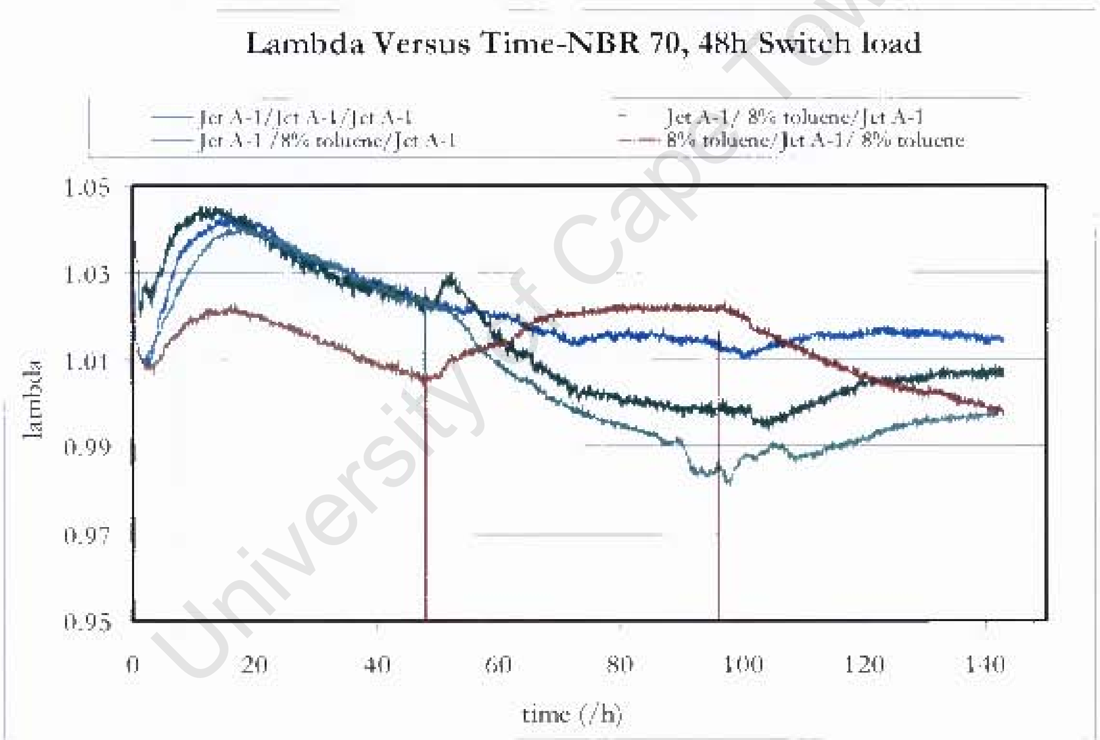

Figure 5.25: Switch load between SPK, SPK with 8% toluene and Jet A-1

Break away pressure shown in Figure 5.26 displayed similar trends to changes in lambda. However, there were some step changes in some of the curves in Figure 5.25 which were observed for lambda in the switch load results when switch loading took place. It is possible that the fuel might have been dirty causing the particles in the dirty fuel to affect the sensor readings when the anvil is bottoming out.

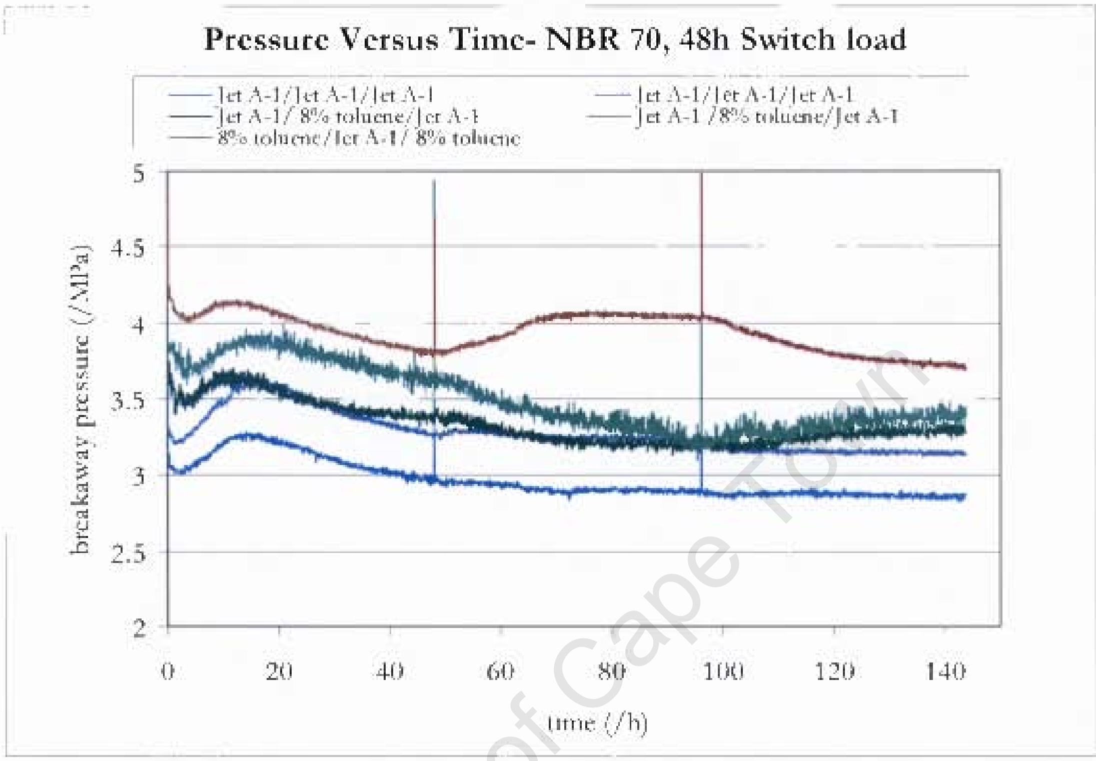

Figure 5.26: Break away pressure versus time for NBR O-ring in a 8% toluene switch load

Figure 5.27 shows the switch load experiment conducted between Jet A-1, SPK and SPK additised with 0.5% benzyl alcohol. The first switch load pair between Jet A-1 and SPK resulted in a significant decrease in thickness of the O-ring upon switching to SPK. The thickness increased again after switching back to Jet A-1. The result correlated well with the static (bench) switch load shown in Section 5.22 for the two pair of fuels. The second switch load pair was between Jet A-1 and SPK additised with 0.5% benzyl alcohol. The result also showed a decrease in thickness upon switching to 0.5% benzyl alcohol SPK. However, the change in thickness was smaller compared to switching to SPK. The third switch load pair was between Jet A-1 switched to SPK and then switched to 0.5% benzyl SPK. SPK additised with 0.5% benzyl alcohol swells the O-ring after it was switched from Jet A-1 to SPK. This result suggested that 0.5% benzyl alcohol does not match the swelling of Jet A-1.

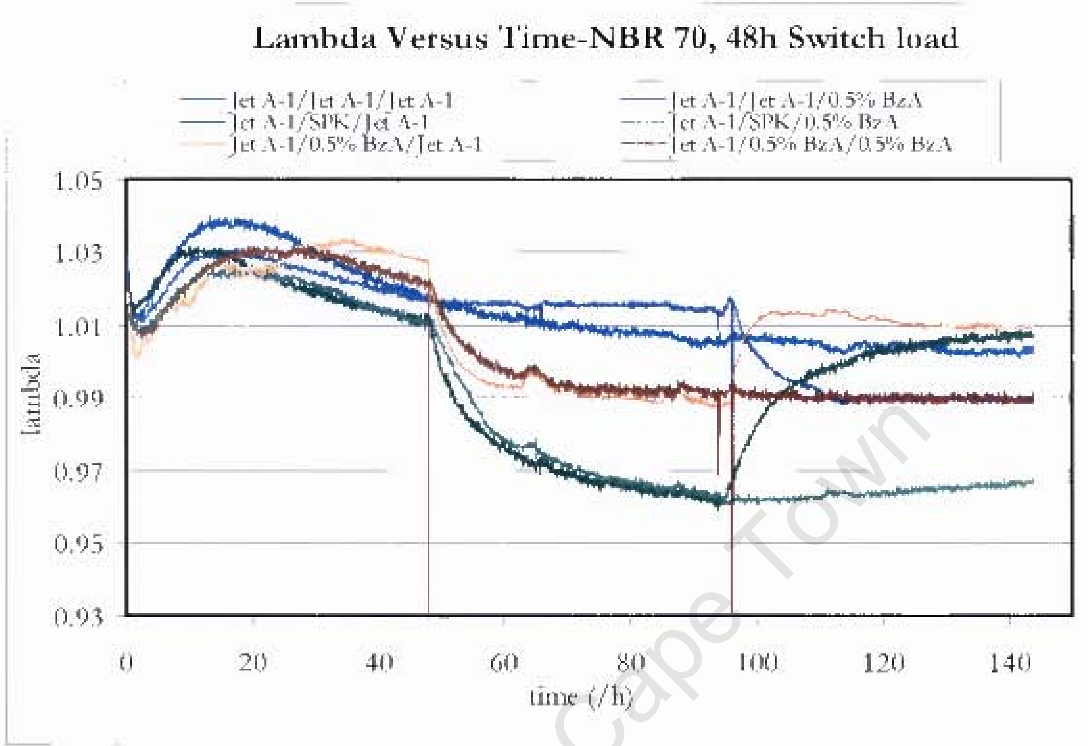

Figure 5.27: Switch load between SPK additised with 0.5% benzyl alcohol and Jet A-1

Similar switch load experiments shown in Figure 5.28 were conducted between Jet A-1 and SPK additised with 0.5% and 1% benzyl alcohol. Referring to Figure 5.29, the graph further confirmed the deductions that were made earlier on SPK additised with 0.5% benzyl alcohol. The results also show that when Jet A-1 was switched to SPK containing 1% benzyl alcohol, a decrease in thickness was observed inferring that SPK additised with 1% benzyl alcohol has not matched the swelling of Jet A-1. However, the result suggested that SPK with 1% benzyl alcohol displayed a small decrease in thickness compared to SPK with 0.5% benzyl alcohol.

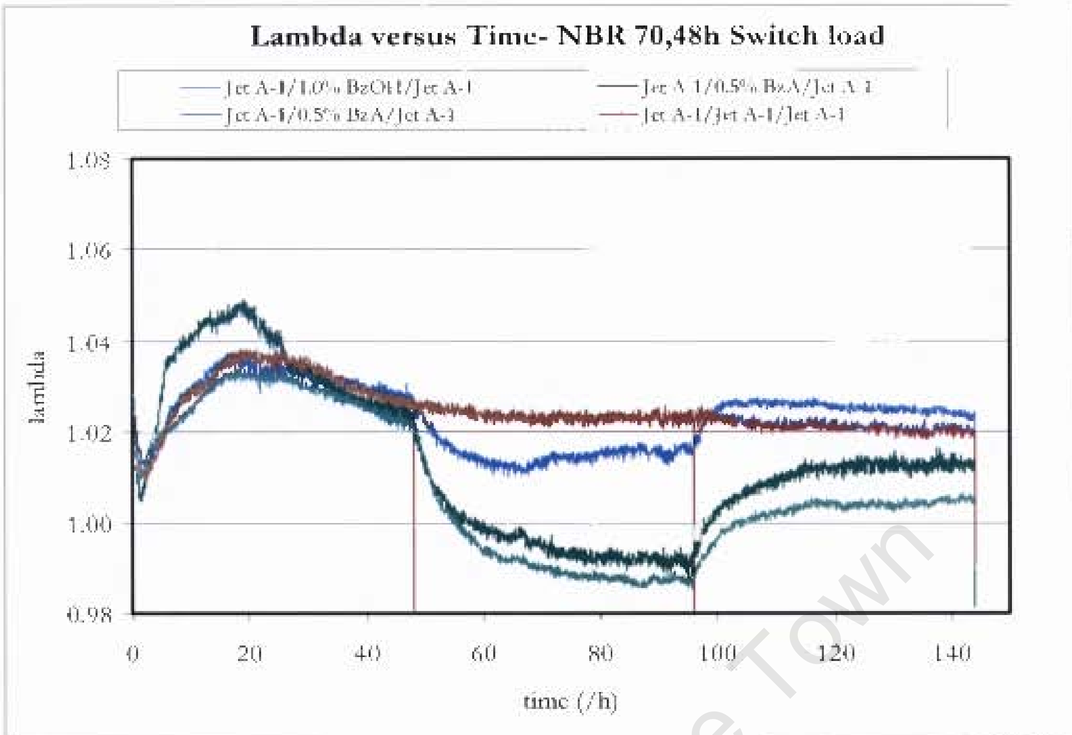

Figure 5.28: Switch load between 0.5% and 1% benzyl alcohol additised SPK and Jet A-1

Figure 5.29 shows that SPK with 2% benzyl alcohol resulted in a further increase when switched from Jet A-1 followed by a decrease in thickness upon switching back to Jet A-1. It is believed that concentration of 2% benzyl alcohol in the final SPK blend would result in excessive swell compared to Jet A-1 resulting in no difference in the swelling performance when switched interchangeably. Similar results were observed for breakaway pressure for SPK additised with 0.5%, 1% and 2% benzyl alcohol. The breakaway pressure graphs can be found in appendix D.

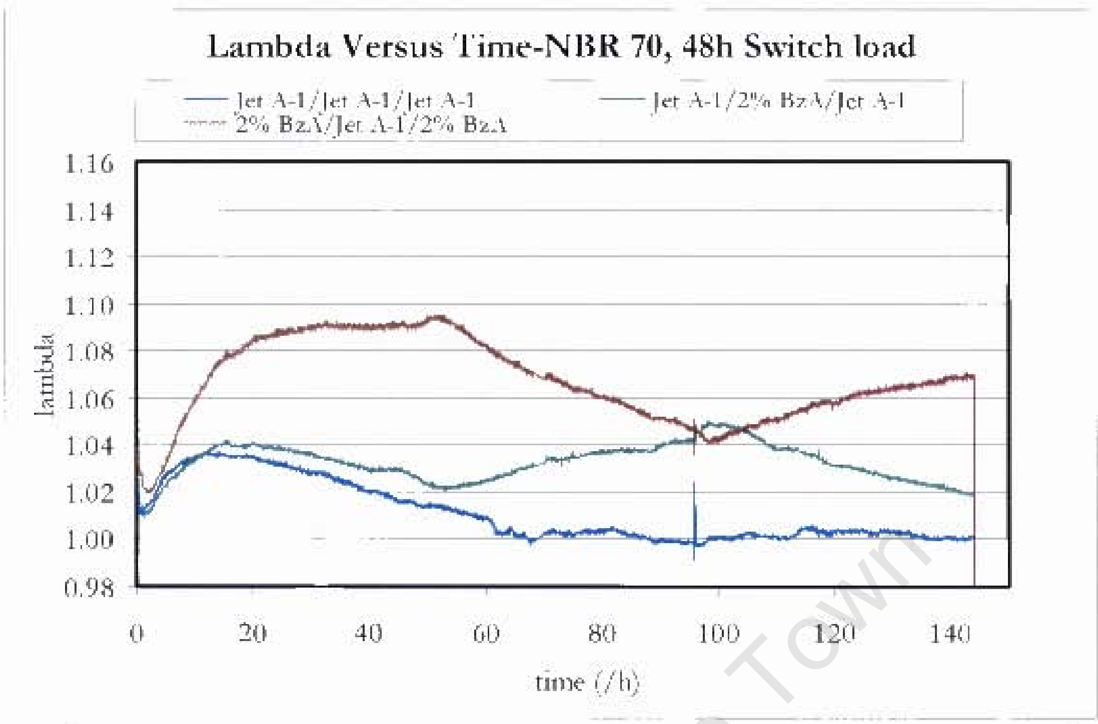

Figure 5.29: Switch load between SPK, SPK additised with 2% benzyl alcohol and Jet A-1

CHAPTER 6

DISCUSSION OF RESULTS

6.1 Volume Swelling in Pure Solvents

Measurements in pure solvents that were tested in the current study revealed that benzyl alcohol produced the highest percentage mass change, even higher than aromatic and hydroaromatic hydrocarbons (tetralin and toluene).

This result was consistent with binding energies predicted by molecular modelling (cf. Figure 5.2). The optimised geometry of benzyl alcohol with isobutylnitrile showed a specific interaction (hydrogen bonding) between the hydroxyl group (-OH) of benzyl alcohol and the nitrile group (-CN) of isobutylnitrile. On the other hand, optimised geometries of tetralin and toluene with isobutylnitrile showed some interactions between the equatorial hydrogen atoms i.e. the hydrogen atoms on the aromatic ring and the nitrile group of isobutylnitrile. The equatorial hydrogen atoms in toluene and tetralin are polar enough due to the delocalisation of electrons (partial charge) in the aromatic ring.

n-Butanol on the other hand displayed poorer swelling behaviour despite its polar nature suggesting that the straight chain paraffins attached to the polar end reduces the polarity of this molecule. For this reason, it was suggested that solvents with an aromatic-like ring attached to a polar group would result in a better interaction with the isobutylnitrile molecule compared to a saturated paraffinic chain attached to a polar group. Nevertheless, it should be borne in mind and has been also stated by Alfonso and Cugini [37] that density functional theory predicts poorly for interaction energies between molecules with fairly weak interactions. It is known to predict more accurately for systems which involves hydrogen bonding interactions [37].

Straight chain paraffinic solvents such as n-octane and iso-octane displayed poor swelling characteristics compared to cyclic paraffinic solvents such as decalin and dimethylcyclohexane. This observation explains the poor swelling characteristics of SPK fuel which is entirely dominated by isoparaffins. In contrast, Jet A-1 contains monocyclic and bicyclic paraffins among their fuel components.

Graham and Striebich [59] reported that bulk of aromatic compounds present in Jet A-1 such as toluene have solubility parameters fairly close to the solubility parameters of NBR. Therefore, the difference in the solubility parameters would be minimal, explaining the observed volume swell of NBR O-rings in Jet A-1.

Hansen [41] has also shown that straight chain paraffins have a lower solubility parameter compared to cyclic paraffins present in a typical Jet A-1. This suggests further need of higher amount of cyclic paraffinic components in SPK. On the other hand, Hansen [41] has also reported that oxygenates have a high solubility parameter but this alone cannot explain the results observed here. n-Butanol displayed low swell whereas benzyl alcohol swelled NBR to a large extent. It is rather the difference in the solubility parameters between the oxygenate and the NBR that determines high volume swell. Uncertainties in the available Hansen solubility parameters for nitrile rubber make it difficult to draw firm conclusions about which of the Hansen terms drives the observed swelling of NBR by benzyl alcohol. Such an analysis based on Hansen solubility parameters is further complicated by the fact that NBR is a copolymer, with highly polar polyacrylonitrile segments and less polar polybutadiene segments.

Nevertheless the high swelling observed is indicative of a specific interaction between benzyl alcohol and nitrile rubber.

6.2 Volume Swelling in Jet A-1 and Additised SPK

The swelling phenomena of nitrile elastomers involve diffusion of fuel molecules and rubber compounding molecules along a concentration gradient between the fuel and the elastomer [22]. Diffusion of fuel and rubber compounding molecules takes place in two directions, the elastomer compounding molecules (plasticisers and processing oil) into the fuel and fuel molecules into the elastomer. The overall change in free energy of mixing depends of the concentration gradient and the enthalpy of mixing between the fuel molecules and the elastomer [41]. However, using the equation suggested by Hansen [41], the smaller the difference in the solubility parameters between the fuel molecules and the elastomer, the smaller the enthalpy of mixing and hence, the more negative free energy of mixing. It was suggested that the difference in the solubility parameters between the fuel molecules and the elastomer is much smaller compared to the difference between the elastomer and the compounding aids. Therefore, the overall increase in volume is the result of diffusion kinetics between the fuel molecules diffusing into the rubber compared to the rubber compounding components such as plasticisers diffusing out.

With time a stage is reached when the diffusion rate of the rubber compounding molecules is faster than the fuel molecules diffusion into the rubber suggesting that although the chemical potential for diffusion of solvent molecules into the rubber has reach equilibrium, the chemical potential for plasticiser extraction is still driving these molecules out.

Experimental results in terms of static volume swell measurements revealed that nitrile elastomers swelled more in Jet A-1 when compared to SPK. The rate of shrinkage in SPK was slow suggesting that the polar plasticisers diffuse out more slowly into the less polar SPK fuel. On the other hand, Jet A-1 was shown to have a faster rate of λ decrease suggesting that the polar plasticisers diffuse out at a faster rate into the Jet A-1. Furthermore the fact that λ stabilises in the case of Jet A-1 would suggest that the equilibrium for plasticiser extraction is reached far sooner.

It is known from Campion *et al.* [23] that the percentage mass changes of plasticised polymers increase to a maximum when exposed to solvent, thereafter decreasing as opposed to de-plasticised rubber which merely increase to their equilibrium value. A similar effect was observed in the current study using NBR rubbers.

Experimental results expressed in terms of normalised expansion also revealed that Jet A-1 has a better swelling performance compared to SPK. However, the normalised expansion indicated that with time, both the seals shrink. Equilibrium at different times suggesting Jet A-1 and SPK have different diffusion rates of absorption and extraction of fuel molecules and rubber compounding molecules (plasticisers).

Measurement of static volume swell with additised SPK revealed that concentrations of benzyl alcohol as low as 1-2% could be required to achieve greater swell comparable to Jet A-1. The result was in agreement with Link *et al.* [33]. This is indicative of the specific interaction that occurs between benzyl alcohol and the nitrile rubber. This specific interaction which is likely hydrogen bonding is more important than the difference in the solubility parameters between the two compounds. The concentration of the components (additive) in the SPK blend also plays a major role in determining swell of nitrile rubbers.

The results relating to percentage toluene in SPK were in agreement with Westbrook and French [55]. Higher amount of high solubility parameter components in the blend will provide more of the component (additive) to interact with the elastomer and hence greater volume swell. Diffusion phenomena of substituted aromatics in nitrile rubbers was explained by DeWitt *et al.* [5] and Joseph *et al.* [25]. This was one of the reasons used to explain the poor swelling behaviour of hexylbenzenes blended in SPK. The results were shown to be consistent with Joseph *et al.* [25] indicating that molar volume has an effect. It was also suggested that aromatic ring with a longer saturated group attached to the ring in the case of hexylbenzene, have a tendency to behave more like normally saturated paraffins. Not only is this a molar volume effect but aromatics with longer alkyl chains attached (hexylbenzenes as opposed to toluene) tend to have a smaller solubility parameters. Hence, the overall difference in the solubility parameter between the NBR and the longer chain alkylbenzene would be larger compared to the shorter alkylbenzene. This is indicative of solubility parameter effect in addition to the molar volume effect. Furthermore, it was suggested that shorter alkylbenzenes would require lower concentration to swell NBR O-ring than the longer hexylbenzenes used in the current study.

Normalised expansion measurements of SPK additised with 8% toluene indicated similar swelling to Jet A-1 suggesting that toluene has a significant effect on the swelling performance of SPK. Coleman and Gallop [34] indicated that toluene is typically present in commercial Jet A-1. Toluene has small molar volume and a high solubility parameter contributing towards the swelling behaviour in NBR O-rings. SPK additised with tetralin also displayed similar seal performance to Jet A-1. The swelling performance of SPK is dependent on the concentration of tetralin. Tetralin has a higher solubility parameter than toluene and was shown to interact strongly with the nitrile polymer. On the other hand Hansen [41] reported that tetralin has a higher molar volume suggesting that it would diffuse more slowly into the rubber compared to toluene.

6.3 Switch Load in Jet A-1 and Additised SPK

The switch load experiments highlighted certain differences when switching from Jet A-1 to SPK and vice versa. Nitrile O-ring behaves differently in fuels with different hydrocarbon composition. Shrinkage of an O-ring switching from Jet A-1 to SPK was suggested to be caused by the concentration gradient of high solubility parameters compounds such as aromatics present in Jet A-1 as opposed to low solubility parameter paraffins present in SPK. These aromatics diffuse into the polymer during the initial Jet A-1 immersion followed by removal of the same aromatics together with some plasticisers when switched to SPK. The results are in good agreement with Muzzell *et al* [18, 31]. However, Muzzell *et al.* performed the switch load experiment at 40°C as opposed to 23°C in this project. Nevertheless, it does show the overall trend of swelling when switched from a high aromatic fuel to a low aromatic fuel. SPK additised with 0.5% benzyl alcohol also resulted in shrinkage of O-rings when switched from Jet A-1 to SPK additised with 0.5% benzyl alcohol. This suggests that 18% aromatics present in Jet A-1 swell more than the 0.5% benzyl alcohol present in SPK. Nonetheless, SPK containing 2% benzyl alcohol has an opposite effect to 0.5% benzyl alcohol suggesting that concentration of 2% benzyl alcohol in SPK showed greater swell than the aromatics present in Jet A-1.

6.4 Static Versus Elastomer Compression Volume Swelling

Results from the elastomer rig displayed some differences in seal performance measurements for additised SPK compared to static measurements. The following ideas may be used to provide explanation for the difference in the sealing performances for the two different experimental methods:

- Mathai and Thomas [24] have shown that rubber/solvent ratio and sample geometry affects the diffusion rates of solvent molecules. Static swelling measurements were done on a cross section O-ring. This type of geometry allows more diffusion of solvent molecules compared to the elastomer rig which used an O-ring with no cross section exposed. Static measurements used rubber/solvent ratio of 0.025 while elastomer rig used a ratio of 0.004.
- Static measurements were done at 23°C and the overall swelling performance was based on the percentage mass change. This measurement enables one to determine the fraction of the mass that is extracted by the fuel in a static environment. On the other hand, elastomer rig measurements were done at 50°C and the overall swelling performance was based on thickness change of the O-ring. This measurement enables one to determine the swelling performance of an O-ring in a dynamic environment. However, the difference in the operating temperatures could affect the diffusion kinetics of various fuel and rubber compounding molecules.

CHAPTER 7

CONCLUSION

7.1 Seal Swell performance

- It was concluded that NBR O-ring swell extensively in Jet A-1. On the other hand, NBR O-rings displayed very poor swelling behaviour in SPK.

- It was suggested that 1-2% benzyl alcohol was enough to act as a potential swelling additive in SPK. Furthermore, it was concluded that SPK blended with low solubility parameter alkylbenzenes (long paraffinic chains attached to the O-rings) such as hexylbenzenes would not provide adequate swelling compared to higher solubility parameter alkylbenzenes (short paraffinic chain attached to the ring) such as toluene. Also, lower solubility parameter aromatics would require greater quantities of for equal amount of swelling.

- The swelling performance parameter lambda, also led to a similar conclusion on the swelling behaviour of Jet A-1 and additised SPK.

- Furthermore, it was concluded that elastomer rig measurements agreed with the static swelling measurements in pure SPK. However, they showed some disagreement with additised SPK. It was suggested that sample geometry, rubber-solvent ratio and temperature could cause a difference in the swelling performance of some solvents that were blended in SPK i.e.

some additives indicated to be more effective in rig measurements at lower levels than static measurements.

- It was concluded that bench seal swell measurements should be handled with caution when comparing them to the rig measurements. This is because rig measurements were done at different temperatures and different volumes of fuel. Also rig measurements were done in a dynamic environment compared to bench measurements which were conducted in a static environment.

7.2 Switch load performance

A novel method was developed which assesses the switch load performance of fuels in an elastomer compression rig. The switch load performance result suggested that 1-2% benzyl alcohol could be used as a potential swelling additive in SPK and could replace the need for aromatics in synthetic jet fuels. The static switch load measurements were in agreement with the elastomer switch load rig measurements. Nevertheless caution should also be taken when comparing the static switch load measurements to the rig switch load measurements especially if conditions such as solvent/rubber ratios and temperature differ.

CHAPTER 8

RECOMMENDATIONS AND FUTURE WORK

8.1 Experimental Apparatus and Procedures

The following are some guidelines that should be considered for further seal swell experiments:

- It is important to consider a range of temperatures to investigate the swelling behaviour of rubber O-rings at different temperatures. However, the rig displays a temperature dependence for calculated O-ring thickness during the early stages of the experiment due to O-ring contraction and rig expansion. Thus, it is recommended to pre-condition the O-rings to the required temperature before inserting them into the rig i.e. run the rig dry for a couple of hours before inserting the fuel via a syringe. Alternatively, one could possibly calculate the lambda value as the ratio of the actual thickness at any given point in time to the minimum thickness observed during the initial hours of testing. However, referring to Figure 5.14 lambda values for SPK do not show any minimum thickness and therefore would have to be estimated at similar times to the Jet A-1 which shows a minimum thickness in the few initial hours of the test.

- The elastomer rig experiments could be performed at 23°C in order to be able to compare with static swell measurements. It is also recommended that similar rubber/solvent ratio and rubber geometry for static and rig measurements to avoid any complications relating to diffusion kinetics. Alternatively bench swell experiments could be performed at 50°C. Nevertheless a more detailed comparison at both temperatures could elucidate diffusion processes in more detail.

- It is also recommended that elevated temperatures between 60° and 80°C for static and rig swelling measurements be explored. Several degradation products and oxidation products from the rubber have been observed at these temperatures [60]. This would provide insight into accelerated age hardening effects upon seal swell. These temperatures can be attained by using an oven for static swell measurements.

- It is advised to conditions the O-rings for a longer period of time (4-6 weeks) at the same temperatures used in the current study before taking mass measurements. This will provide some insight about the effects of thermal/oxidation ageing process on the swelling and switch load performance of nitrile rubbers.

- It is also recommended to age the O-rings in fuels at temperatures typical to the test temperature prior to inserting them in the rig. This will remove almost all plasticiser and processing oil from the rubber after which the O-ring can be tested for switch load performance and volume swell.

8.2 Alternative method to measure seal swell

There is a need for accurate static volumetric measure for seal swell. Firstly, the mass measurements ignores the density of the solvents in the blend i.e. it is difficult to measure the density of the solvent in the blend exactly. Secondly, the volumetric measurements will take into account the mass of plasticisers that is removed during the swelling process. The following is a detailed calculation of the percentage volume estimate including the volume of plasticiser extracted.

$$\%Vol.change = (V_{final} - V_0)/V_0$$
$$= (((M_{deswollen}/\rho_{rubber}) + ((M_{swollen} - M_{deswollen})/\rho_{solvent})))/(M_{original}/\rho_{original}) - 100$$

where M is the mass and ρ is the density.

An optical dilatometry apparatus would be recommended for volume swell measure as a function of time. This system consists of a fuel reservoir fitted in an optical window. A digital camera could be mounted above the fuel reservoir to photograph the sample over a certain period of time. The photograph will provide the cross sectional area of the sample as a function of time [6]. However, the apparatus measures the volume swell at room temperature and therefore a heated chamber is required for heating the fuel reservoir if more representative results of real seal swell conditions are to be obtained. The figure below shows a schematic diagram of an optical dilatometry set-up.

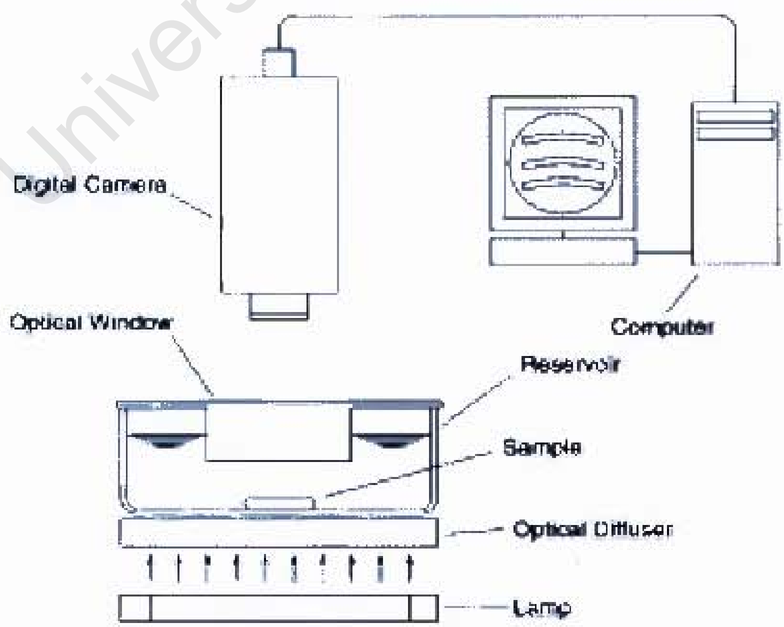

Figure 8.1: Schematic of the optical dilatometry apparatus used to measure volume swell as a function of time [6]

Alternatively O-rings could be deswollen after completion of mass swell measurements. Deswelling experiments could be performed using a vacuum oven. This experiment allows one to analyse the amount of plasticisers extracted by a particular kind of fuel. From such measurements one could not only obtain information about how much plasticiser was extracted in experiments but one could also estimate volume expansion.

8.3 Computational Modelling

DFT was used for computing optimised interaction energies between the solvent and the rubber molecules. This computational software yielded reliable estimations of stabilisation energies of hydrogen bonded complexes. However, it is recommended Moller-Plesset (MP2) theory be used as alternative computational software. This software predicts accurate energies of complex which contain weak interactions [37]. Furthermore, the theory can be used to carry out simulations involving complex structures of nitrile polymer as opposed to the model isobutylnitrile molecule used in this research. There is a need for further computational investigations into other possible additives containing an aromatic ring attached to a polar group such as aromatic ethers before considering them to be blended in fuels.

8.4 Further Swell Performance and Switch load Test with Different Solvents

It is recommended that further seal performance and switch load test be conducted on different aromatics solvents that could blended in SPK. This allows further investigation on the type and concentration of aromatics which might have a bigger influence of seal swelling performance than those used in the current study.

Recommendations and Future Work

The following are the aromatic solvents to be considered blended in SPK:

- Disubstituted benzene such as xylene. Xylene is known to be present in a typical Jet A-1 fuel [15]. This would also provide information about the effect of higher degrees of substitution on swell.
- Highly diaromatic solvent such as naphthalene and alkylnaphthalenes. These are also known to be present in Jet A-1 [15]. Nevertheless it needs be borne in mind that these compounds are more likely to cause soot emissions problems and so are more likely to be of academic interest in terms of explaining swelling phenomena.

Further experiments could be conducted for other types of fuels such as JP-900. Balster *et al.* [13] reported that JP-900 has similar swelling characteristics as Jet A-1 and therefore tests on JP-900 fuel could be conducted to verify the above statement by Balster *et al.* [13]. This could be compared to swelling behaviour in pure decalin.

There has been a concern over usage of biofuels such as fatty acid methyl esters (FAMEs). FAMEs are polar fuel components and therefore could interact with the polar nitrile group in NBR. The effect of biofuels blended in SPK could also have importance given the possible mandatory inclusion of such fuels in the future. Note, however, that biofuels based on hydrogenated vegetable oils (HVOs) are expected to behave similarly to SPK in terms of seal swell although being n-paraffinic there may be slight differences, e.g w.r.t. the rate of plasticiser extraction.

It is also recommend that investigations of the effect of various fuels on fluorocarbon (Viton) seals be initiated. This is especially true of SPK additised with benzyl alcohol. It is known that methanol swells Viton seals [19] significantly Because benzyl alcohol is also an alcohol a specific interaction cannot be ruled out and might warrant further investigation.

REFERENCES

[1] "ASTM D471-06 Standard Test Method for Rubber Property-effects of Liquids," West Conshohocken, PA: American Society for Testing and Materials, 2006.

[2] C. A. Moses and P. N. J. Roets, "Properties, Characteristics and Combustion Performance of Sasol Fully Synthetic Jet Fuel," in *Proceedings of the ASME Turbo Expo 2008: Power for Land, Sea and Air GT2008*, Berlin, Germany, 2008.

[3] C. A. Moses, L. L. Stavinoha, and P. Roets, "Qualification of Sasol Semi-Synthetic Jet A-1 as Commercial Jet Fuel," SwRI-8531, San Antonio, TX: South West Research Institute, 1997.

[4] "DEF STAN 91-91, Issue 6, Turbine Fuel, Aviation Kerosine Type, Jet A-1," Glasgow, UK: Defense Equipment and Support, UK Defence Standardization, 2008.

[5] M. J. DeWitt, E. Corporan, J. Graham, and D. Minus, "Effects of Aromatic Type and Concentration in Fischer-Tropsch Fuel on Emissions Production and Material Compatibility," *Energy & Fuels,* vol. 22, pp. 2411-2418, 2008.

[6] J. L. Graham, R. C. Striebich, K. J. Myers, D. K. Minus, and W. E. Harrison, "Swelling of Nitrile Rubber by Selected Aromatics Blended in a Synthetic Jet Fuel," *Energy & Fuels,* vol. 20, pp. 759-765, 2006.

[7] C. Forest and P. Muzzell, "Fischer-Tropsch Fuels: Why are They of Interest to the United States Military?," *SAE Technical Paper Series,* 2005-01-1807, 2005.

[8] D. Lamprecht, "Fischer-Tropsch Fuel for Use by the U.S Military as Battlefield-Use Fuel of the Future," *Energy & Fuels,* vol. 21, pp. 1448-1453, 2007.

[9] D. Lamprecht, L. P. Dancuart, and K. Harrillal, "Performance Synergies Between Low Temperature and High Temperature Fischer-Tropsch Diesel Blends," *Energy & Fuels,* vol. 21, pp. 2846-2852, 2007.

[10] D. J. O'Rear, "Distillate Fuel Blends from Fischer-Tropsch Products with Improved Seal Swell Properties," US patent US6890423, 2005.

[11] C. A. Moses, "Comparative Evaluation of Semi-Synthetic Jet Fuels," CRC Project No. AV-02-04a, Alpharetta, GA: Coordinating Research Council, 2008.

[12] P. A. Muzzell, L. L. Stavinoha, and R. Chapin, "Synthetic Fischer-Tropsch JP-5/JP-8 Aviation Turbine Fuel Elastomer Compatibility," TARDEC Report No. 15043, Warren, MI: U.S Army Tank-Automotive Research, Development, and Engineering Centre, 2005.

[13] J. P. Balster, E. Corporan, M. J. DeWitt, T. J. Edwards, J. S. Ervin, J. L. Graham, S.-Y. Lee, S. Pal, D. K. Phelps, L. R. Rudnick, R. J. Santoro, H. H. Schobert, L. M. Shafer, R. C. Striebich, Z. J. West, G. R. Wilson, R. Woodward, and S. Zabarnick, "Development of an Advanced, Thermally Stable, Coal-based Jet Fuel," *Fuel Proc. Technol.,* vol. 89, pp. 364-378, 2008.

[14] "Handbook of Aviation Fuel Properties," CRC report No.635, Alpharetta, GA: Coordinating Research Council, 2004.

[15] W. C. Lai and C. Song, "Temperature-Programmed Retention Indices for G.C and G.C-M.S Analysis of Coal- and Petroleum-Derived Liquid Fuels," *Fuel,* vol. 74, pp. 1436-1451, 1995.

[16] J. M. G. Cowie and V. Arrighi, *Polymers: Chemistry and Physics of Modern Materials.*, 3rd edn. Boca Raton, LA: CRC Press, 2008.

[17] www.parkerorings.com, "Parker O-Ring Handbook," Lexington, KY: Parker Hannifin Corporation, 2007.

[18] P. A. Muzzell, B. J. McKay, E. R. Sattler, L. L. Stavinoha, and R. A. Alvarez, "The Effect of Switch-Loading Fuels on Fuel-Wetted Elastomers," *SAE Technical Paper Series,* 2007-01-1453, 2007.

[19] A. O. Patil and T. S. Coolbaugh, "Elastomers: A Literature Review with Emphasis on Oil Resistance," *Rubber Chem. Technol.*, vol. 78, pp. 516-535, 2005.

[20] R. F. Ohm, Ed. *Rubber Handbook*, 13th edn., Norwalk, CT: R.T Vanderbilt Company, 1990.

[21] S. O'Rourke, "High Performance Ester Plasticizers," presented at *160th Technical Meeting of the Rubber Division, American Chemical Society*, Cleveland, OH: 2001.

[22] S. C. George and S. Thomas, "Transport Phenomena through Polymeric Systems," *Prog. Polym. Sci.*, vol. 26, pp. 985-1017, 2001.

[23] R. P. Campion, B. Thomson, and J. A. Harris, *Elastomers for Fluid Contaminent in Offshore Oil and Gas Production: Guidelines and Review*. Hertford, UK: HSE Books, 2005.

[24] A. E. Mathai, R. P. Singh, and S. Thomas, "Transport of Substituted Benzenes through Nitrile Rubber/Natural Rubber Blend Membranes," *J. Membrane Sci.*, vol. 202, pp. 35-54, 2002.

[25] A. Joseph, A. E. Mathai, and S. Thomas, "Sorption and Diffusion of Methyl Substituted Benzenes through Cross-Linked Nitrile Rubber/Poly(Ethylene Co-vinyl Acetate) Blend Membranes," *J. Membrane Sci.*, vol. 220, pp. 13-30, 2003.

[26] A. E. Mathai and S. Thomas, "Transport of Aromatic Hydrocarbons through Crosslinked Nitrile Rubber," *J. Macromolec. Sci.*, vol. B35, pp. 229-253, 1996.

[27] S. D. Robertson, D. R. Price, P. E. Wolveridge, H. C. Grigg, D. Holmes, M. R. West, R. J. Butterfield, and G. Stewart, "Effect of Automotive Gas Oil Composition on Elastomer Behaviour," *SAE Technical Paper Series*, 942018, 1994.

[28] C. A. Moses, G. Wilson, and P. Roets, "Evaluation of Sasol Synthetic Kerosene for Suitability as Jet Fuel," SwRI 08-04438, San Antonio, TX: Southwest Research Institute, 2003.

[29] www.jameswalker.biz, "O-ring Materials," Crewe: UK: James Walker Group, 2009.

[30] R. J. Gormley, D. D. Link, J. P. Baltrus, and P. H. Zandhuis, "Interaction of Jet Fuel with Nitrile O-rings: Petroleum-Derived versus Synthetic Fuels," *Energy & Fuels,* vol. 23, 2, pp. 857-861, 2009.

[31] P. A. Muzzell, L. L. Stavinoha, E. Sattler, A. Terry, and L. Villahermosa, "Elastomer Impact when Switch-Loading Synthetic Fuel Blends and Petroleum Fuels," TARDEC Report No. 16028, Warren, MI: U.S Army Tank-Automotive Research, Development, and Engineering Centre, 2006.

[32] D. Lamprecht, "Elastomer Compatibility of Blends of Biodiesel and Fischer-Tropsch Diesel," *SAE Technical Paper Series,* 2007-01-0029, 2007.

[33] D. D. Link, R. J. Gormley, J. P. Baltrus, R. R. Anderson, and P. H. Zandhuis, "Potential Additives to Promote Seal Swell in Synthetic Fuels and their Effect on Thermal Stability," *Energy & Fuels,* vol. 22, 2, pp. 1115-1120, 2008.

[34] J. R. Coleman and L. D. Gallop, "Effects of Fuels on the Physical Properties of Nitrile Rubber O-Rings," DREO Technical Note 82-41, Ottawa: Department of National Defence, Canada, 1983.

[35] C. M. Cusano, R. W. Flaherty, and A. N. Roush, "Survey of Winter '93 Low Sulphur Diesel Fuels in the U.S.," *SAE Technical Paper Series,* 942013, 1994.

[36] T. Yamada, J. L. Graham, and M. K. Donald, "Density Functional Theory Investigation of the Interaction Between Nitrile Rubber and Fuel Species," *Energy & Fuels,* vol. 23, pp. 443-450, 2009.

[37] D. R. Alfonso and A. V. Cugini, "Ab Initio Study of Interactions of a Model Nitrile Polymer with Various Model Fuel Molecules," *Prepr. Pap. - Am. Chem. Soc., Div. Fuel Chem,* vol. 48, 2, pp. 508-509, 2003.

[38] D. D. Link, R. J. Gormley, P. H. Zandhuis, and J. P. Baltrus, "Effects of Potential Additives to Promote Seal Swelling on the Thermal Stability of Synthetic Jet Fuels," IR-2008-008, South Park, USA: DOE-NETL, 2008.

[39] J. Hildebrand and R. L. Scott, *The Solubility of Nonelectrolytes*, 3rd edn. New York, NY: Reinhold, 1950.

[40] J. Hildebrand and R. L. Scott, *Regular Solutions.* Englewood Cliffs, NJ: Prentice-Hall, 1962.

[41] C. M. Hansen, *Hansen Solubility Parameters: A User's Handbook*, 2nd edn. Boca Raton, LA: CRC Press, 2007.

[42] M. K. Buckley-Smith and C. J. Fee, "The Use of Solubility Parameters for the Selection of Materials for Organic/Organic Separations by Pervaporation," in *Proceedings of the 9th APCChe Congress and CHEMECA*, Christchurch, NZ, 2002.

[43] A. Beerbower and J. R. Dickey, "Advanced Methods for Predicting Elastomer/Fluid Interactions," *Tribology Transactions,* vol. 12, 1, pp. 1-20, 1969.

[44] P. J. Flory, *Principles of Polymer Chemistry.* Ithaca: Cornell University Press, 1953.

[45] P. J. Flory, "Statistical Mechanics of Swelling of Network Structures," *J. Chem. Phys.,* vol. 18, pp. 108-111, 1950.

[46] F. T. Wall and P. J. Flory, "Statistical Thermodynamics of Rubber Elasticity," *J. Chem. Phys.,* vol. 19, pp. 1435-1439, 1951.

[47] H. M. James and E. Guth, "Theory of the Increase in Rigidity of Rubber During Cure," *J. Chem. Phys.,* vol. 15, pp. 669-683, 1947.

[48] L. R. G. Treloar, "The Elasticity of a Network of Long Chains-I," *Trans. Faraday. Soc.,* vol. 39, pp. 36-40, 1943.

[49] L. R. G. Treloar, "The Elasticity of a Network of Long Chains-II.," *Trans. Faraday. Soc.,* vol. 39, pp. 241-246, 1943.

[50] J. J. Hermans, "Statistical Thermodynamicsof Swollen Polymer Networks," *J. Polym. Sci.,* vol. 59, pp. 191-208, 1962.

[51] J. A. Brydson, *Rubber Chemistry.* London, UK: Applied Science Publishers, 1978.

[52] P. J. Flory and J. Rehner, "Statistical Mechanics of Crosslinked Polymer Networks II. Rubberlike Elasticity " *J. Chem. Phys.,* vol. 11, pp. 512-520, 1943.

[53] L. R. G. Shvarts, "Evaluation of Rubber-Solvent Interaction," *Rubber Chem. Technol,* vol. 31, pp. 691-698, 1958.

[54] T. Lindvig, M. L. Michelson, and G. M. Kontogeorgis, "Thermodynamics of Paint Related Systems with Engineering Models," *AICheE J.,* vol. 47, pp. 2573-2584, 2001.

[55] P. A. Westbrook and R. N. French, "Elastomer Swelling in Mixed Solvents," *Rubber Chem. Technol.,* vol. 72, pp. 74-90, 1999.

[56] J. P. Baltrus, D. D. Link, P. H. Zandhuis, R. J. Gormley, and R. R. Anderson, "Screening of Potential O-ring Swelling Additives for Ultraclean Transportation Fuels," in *Ultraclean Transportation Fuels* Oxford, UK: Oxford University Press, 2007, pp. 197-207.

[57] P. J. Flory and J. Rehner, "Statistical Mechanics of Crosslinked Polymer Networks II. Swelling," *J. Chem. Phys.,* vol. 11, pp. 521-526, 1943.

[58] A. Mosafa, A. Abouel-Kasem, M. R. Bayoumi, and M. G. El-Sebaie, "Effect of Carbon Black Loading on the Swelling and Compression Set Behaviour of SBR and NBR Compounds," *Materials and Design,* vol. 30, pp. 1561-1568, 2009.

[59] J. L. Graham and R. C. Striebich, "The Swelling of Selected O-ring Materials in Jet Propulsion and Fischer-Tropsch Fuels," *Prepr. Pap. - Am. Chem. Soc., Div. Pet. Chem.,* vol. 49, pp. 435-439, 2004.

[60] M. Hakkarainen, A. C. Albertsson, and S. Karlsso, "Migration and Emission of Plasticizer and its Degradation Products During Thermal Aging of Nitrile Rubber," *Int. J. Polym. Anal. Charact.,* vol. 8, pp. 279-293, 2003.

[61] A. E. B. Bailey, E. J. Gilham, E. F. G. Herington, and B. Rose, Eds., *Tables of Physical and Chemical Constants and Some Mathematical Functions, Originally Compiled by Kaye and Laby.*, 14th edn., London: Longman, UK, 1973.

[62] J. Brandrup, E. H. Immergut, E. A. Grulke, and D. Bloch, Eds., *Polymer Handbook*, 4th edn., New York, NY: Wiley-Interscience, 1999.

[63] D. W. v. Krevelen and P. J. Hoftyzer, *Properties of Polymers*, 2nd edn. Amsterdam, Netherlands: Elsevier, 1976.

APPENDICES

APPENDIX A

MOLAR VOLUME AND SOLUBILITY PARAMETER ESTIMATIONS

A.1 The Estimation of Molar Volumes and Solubility Parameters for Fuel Blends

Fuel blends are complex systems containing a wide variety of components across a wide concentration range. Because molar volumes and solubility parameters are key determinants of the degree of swelling of elastomers in fuels, it is important to have estimates of these parameters for fuel blends.

Molar volumes and solubility parameters may be estimated as volume fraction weighted averages of the molar volumes and solubility parameters of the individual components such that

$$V_{blend} = \sum \phi_i V_i \qquad \text{and} \qquad \delta_{blend} = \sum \phi_i \delta_i$$

where ϕ_i, V_i and δ_i are the volume fraction, molar volume and solubility parameter of component (i) respectively.

Unfortunately, molar volumes and solubility parameters are not available for all components in fuel blends. In these cases, they need to be estimated as weighted sums of the contributions of the constitutive groups of the component under consideration.

As an example, the molar volume of ethane (CH_3CH_3) could be estimated as twice the contribution of a methyl group ($-CH_3$). Propane ($CH_3CH_2CH_3$) would be obtained by adding twice the contribution of a methyl group to that of one methylene ($-CH_2-$) group.

A.1.1 Estimating the Functional Group Contributions to Molar Volume

Molar volume data for pure compounds were used to estimate the functional group contributions at 25°C. The primary data was obtained from Bailey *et al.* [61], Brandrup *et al.* [62]and Hansen [41].

Compounds used were linear alkanes (n-pentane; n-hexane; n-heptane; n-octane; n-nonane; n-decane; n-undecane; n-dodecane; n-tridecane; n-tetradecane; n-hexadecane; n-heptadecane and n-octadecane), branched alkanes (2-methylbutane; 2,2-dimethylpentane; 2,3-dimethylpentane; 2,4-dimethylpentane; 3,3-dimethylpentane; 3-ethylpentane; 2-methylhexane; 3-methylhexane; 2,2,3-trimethylbutane; 2,2-dimethylhexane; 2,3-dimethylhexane; 2,4-dimethylhexane; 2,5-dimethylhexane; 3,3-dimethylhexane; 3,4-dimethylhexane; 3-ethylhexane; 3-ethyl-2-methylpentane; 2-methylheptane; 3-methylheptane; 4-methylheptane; 2,2,3-trimethylpentane; 2,2,4-trimethylpentane; 2,3,3-trimethylpentane; 2,3,4-trimethylpentane and 2,2,5-trimethylpentane), cyclic alkanes (cyclopentane, cyclohexane and methylcyclohexane), substituted aromatics (toluene; 1,2-dimethylbenzene; 1,3-dimethylbenzene; 1,4-dimethylbenzene; ethylbenzene; i-propylbenzene; n-propylbenzene; 1,4-diethylbenzene and 2-isopropyltoluene), bicyclic aromatics (1-methylnaphthalene and 1-bromonaphthalene), tricyclic aromatics (anthracene and phenanthrene) and brominated compounds (bromoethane; 1,2-dibromoethane; 1-bromopropane; 1-bromobutane; 2-bromobutane; 1-bromopentane; bromobenzene; 2-bromotoluene, 4-bromotoluene).

Although brominated compounds are not fuel components, they were included so that a molar volume for the naphthyl group could be estimated using 1-bromonaphthalene). The molar volumes for the group contributions were using least square regression according to the following equation

$$V = n_{-CH3}V_{-CH3} + n_{-CH2-}V_{-CH2-} + n_{>CH-}V_{>CH-} + n_{>C<}V_{>C<} + n_{ring}V_{ring} + n_{-Ph}V_{-Ph} + n_{-Ph-}V_{-Ph-} + n_{-Naph}V_{-Naph} + n_{-Br}V_{-Br} + n_{tri}V_{tri}$$

Where n_X is the number of a particular group in a particular reference compound and V_X is the optimized V_X for that particular group, solved over all the reference compounds. $-CH_3$ is a methal group, $-CH_2-$ a methylene group, >CH- a tertiary carbon, >C< a quaternary compound, ring refers to the additional contribution brought about by aliphatic ring closure, -Ph is a monosubstituted phenyl ring, -Ph- a disubstituted phenyl ring, -Naph a naphthyl group, -Br a bromine and tri indicates a trisubstituted aromatic compound.

The optimized group molar volume contributions are tabulated below

Table A1.1: Tabulated values of molar volumes of functional groups

Group	Group contribution (/cm^3 mol^{-1})
$-CH_3$	32.6
$-CH_2-$	16.3
>CH-	-0.3
>C<	-16.1
Ring	12.7
-Ph	75.3
-Ph-	59.0
-Naph	109.2
-Br	27.3
Tri	164.2

For components for which molar volumes were unavailable, molar volumes were then estimated using

$$V_{compound} = \sum n_X V_X$$

The value for pure naphthalene (unsubstituted) was set equal to the value in Hansen [41]. The value of bisubstituted naphthyl was estimated from monostubsituted and the difference between a di- and monosubstituted benzene

$$V_{-Naph-} = V_{-Naph} + (V_{-Ph-} - V_{-Ph})$$

For substituted tricyclic aromatics a similar methodology was employed to obtain the molar volume of the aromatic ring component

$$V_{tricyclic,\ monosubstituted} = V_{tri} + (V_{-Ph} - V_{benzene})$$

$$V_{tricyclic,\ disubstituted} = V_{tri} + (V_{-Ph-} - V_{benzene})$$

The value for pure decalin (unsubstituted) was set equal to the value in Hansen [41]. To account for substitution in decalin, the following equations accounted for the replacement of a methylene group by a tertiary carbon

$$V_{decalin,\ monosubstituted} = V_{decalin} + (V_{>C-} - V_{-CH2-})$$

$$V_{decalin,\ dinosubstituted} = V_{decalin} + 2\,(V_{>C-} - V_{-CH2-})$$

The value for pure tetralin (unsubstituted) was set equal to the value in Hansen [41]. Substitution in tetralin can occur on the aliphatic or the aromatic ring. Only disubstitution on the same was considered

$$V_{tetralin,\ monosubstituted\ aliphatic\ ring} = V_{tetralin} + (V_{>C-} - V_{-CH2-})$$

$$V_{decalin,\ dinosubstituted\ aliphatic\ ring} = V_{tetralin} + 2\,(V_{>C-} - V_{-CH2-})$$

$$V_{tetralin,\ monosubstituted\ aromatic\ ring} = V_{tetralin} + (V_{-Ph} - V_{benzene})$$

$$V_{tetralin,\ disubstituted\ aromatic\ ring} = V_{tetralin} + (V_{-Ph-} - V_{benzene})$$

Lastly molar volumes were estimated for acenapthenes (naphthalene bridged by 2 methylenes from positions 1-9)

$$V_{acenaphthene} = V_{disubstituted\ naphthyl} + 2\,V_{-CH2-} + V_{ring}$$
$$V_{acenaphthene\ monosubstituted} = V_{acenaphthene} + (V_{-Ph} - V_{benzene})$$
$$V_{acenaphthene\ disubstituted} = V_{acenaphthene} + (V_{-Ph-} - V_{benzene})$$

A.1.2 Estimating the Functional Group Contributions to Solubility Parameter

Group contributions were estimated not for solubility parameters themselves but rather for cohesive energy. In this regard the approach of van Krevelen and Hoftyzer [63] was followed.

This was obtained for the reference compounds from the solubility parameters and molar volumes

$$E_i = V_i\,\delta_i^2$$

The primary data was obtained from Brandrup *et al.* [62] and Hansen [41]. Fewer reference compounds are available for which accurate solubility parameters are known.

The reference compounds were linear alkanes (n-pentane; n-hexane; n-heptane; n-octane; n-nonane; n-decane; n-dodecane and n-hexadecane), branched alkanes (2-methylbutane and 2,2,4-trimethylpentane), cyclic alkanes (cyclopentane, cyclohexane and methylcyclohexane), substituted aromatics (toluene; 1,2-dimethylbenzene; 1,4-dimethylbenzene; ethylbenzene and 1,4-diethylbenzene), bicyclic aromatics (1-bromonaphthalene), tricyclic aromatics (anthracene and phenanthrene) and brominated compounds (1-bromopropane; 1-bromobutane; 2-bromobutane; bromobenzene; 2-bromotoluene, 4-bromotoluene).

The cohesive energy group contributions were using least square regression according to the following equation

$$E = n_{-CH3}E_{-CH3} + n_{-CH2-}E_{-CH2-} + n_{>CH-}E_{>CH-} + n_{>C<}E_{>C<} + n_{ring}E_{ring} + n_{-Ph}E_{-Ph} + n_{-Ph-}E_{-Ph-} + n_{-Naph}E_{-Naph} + n_{-Br}E_{-Br} + n_{tri}E_{tri}$$

The optimized group molar volume contributions are tabulated below:

Table A1.2: Tabulated values of solubility parameters of functional groups

Group	Group contribution (/kJ mol^{-1})
$-CH_3$	4756
$-CH_2-$	4928
>CH-	3408
>C<	903
Ring	774
-Ph	30680
-Ph-	30439
-Naph	46211
-Br	15908
Tri	66969

For components for which cohesive energies were unavailable, cohesive energies were then estimated using

$$E_{compound} = \sum n_X E_X$$

Energy contributions of disubstituted naphthyls, decalins, tetralins etc. were estimated in an analogous method to that detailed for molar volumes above.

Solubility parameters for non-reference compounds were then estimated using the cohesive energies and the molar volumes

$$\delta = \sqrt{\frac{E}{\delta}}$$

A.1.3 Solubility Parameters for Synthetic Paraffin Kerosene (SPK) and Jet A-1

Using chemical composition data for SPK and Jet A-1, the volume fraction weighted average for the solubility products for these two blends were found to be as follows:

Table A1.3: Total calculated solubility parameter of Jet A-1 and SPK

Blend	**δ (/kJ$^{1/2}$ cm$^{-3/2}$)**
Jet A-1	16.6
SPK	15.2

APPENDIX B

SAFETY CONSIDERATIONS

B.1 Fuel Handling

Gloves and safety glasses should be worn during fuel handling and solvent blending in with the laboratory policy to avoid any potential hazards. When handling pure solvents, reference should be made to appropriate MSDS information with regards to the specific solvent being blended. All solvent blending preparation should take place at the fuel station, with ventilation switched on to avoid any hazardous fumes being inhaled. Spills of pure solvents should be wiped immediately with a paper towel and disposed appropriately as some solvents are dangerous to the skin.

B.2 Glassware Handling

Glass vials should be disposed in appropriate containers with labels on them to avoid any chemical reaction. Measuring cylinder should be washed with the fuel to be used prior to measuring to ensure that used solvents (left over) are diluted with new solvents.

B.3 Fire and Explosions

The temperature controller should be switched off after completion of every test to avoid the fumes from the oil bath. These fumes can cause a fire or explosion with the solvents nearby or can even affect other apparatus which are in close proximity to the rig. These fumes generally appear when the temperature controller is switch on prior to inserting the modules in the oil bath.

B.4 Test modules and transducers

Transducers attached to each module are very sensitive to damage. They must be handled with care during rig assembly. Modules are tightened using a pipe range as they tend to loosen when inserting them inside the oil bath.

APPENDIX C

OPERATING PROCEDURES

C.1 Refuelling

1. Load the test module on the work bench and place the bottom in a vice, using a pipe wrench turn loose the cylinder.
2. Empty the test fuel from the bottom cylinder and discard into the slops drum.
3. Clean all internal components with a paper towel and refill with a new test fuel.
4. The fuel is filled into the cylinder to a limit where it is appropriate for the O-ring to be fully submerged.
5. During switch load experiments, the fuel is flushed out from the hose pipe attached to the cylinder using a syringe. The cylinder is refilled with a new test few for every switch load test.

C.2 Elastomer rig Operation

C.2.1 Start Up and Testing

- Put new test O-ring in the groove holder.
- Place the sleeve in the bottom cylinder and fill the bottom cylinder with the test fuel.

- Place the O-ring groove holder on top of the sleeve and tighten the top cylinder in to the bottom cylinder.
- Connect each test module up to the compressed air line.
- Connect each test module to its appropriate transducer.
- Insert all the modules in the oil bath, set the temperature of the oil bath.
- Ensure the thermocouple tip is submerged in the oil.
- Start the lab view Programme and edit the labels of fuel and rubber according to the test to be conducted and press start.

C.2.2 Shut Down

1. After testing has been completed, click the stop button in the Lab View programme.
2. Turn off the main switch.
3. Remove the test modules from the oil bath and place on the drainage grid.

APPENDIX D

BREAKAWAY PRESSURE GRAPHS

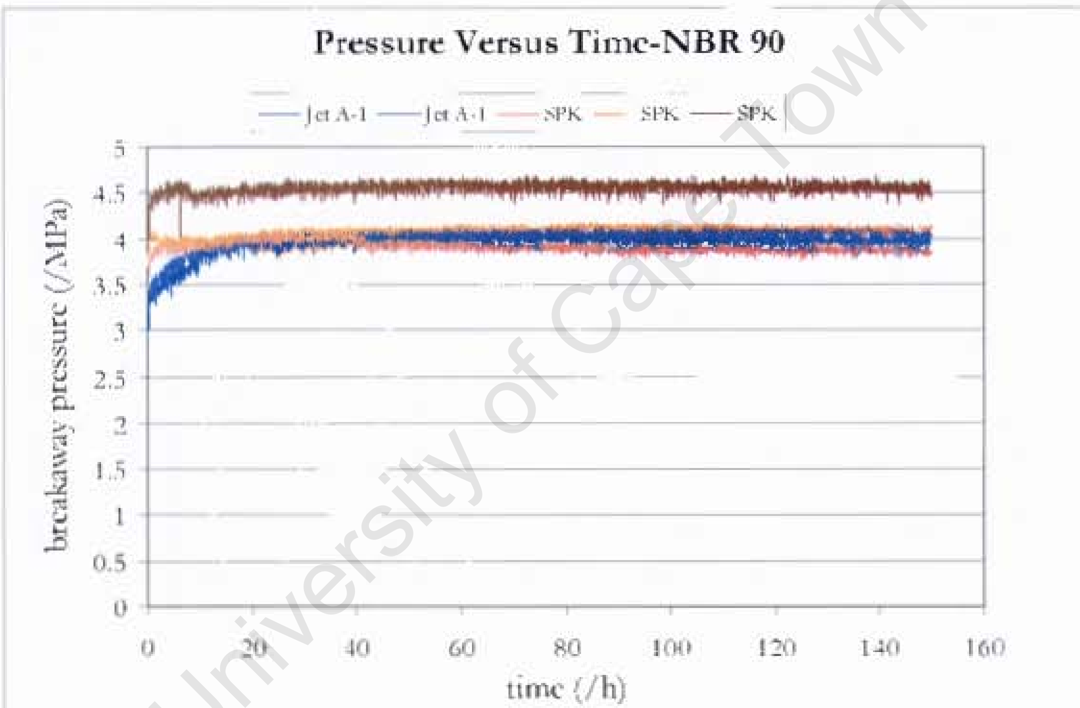

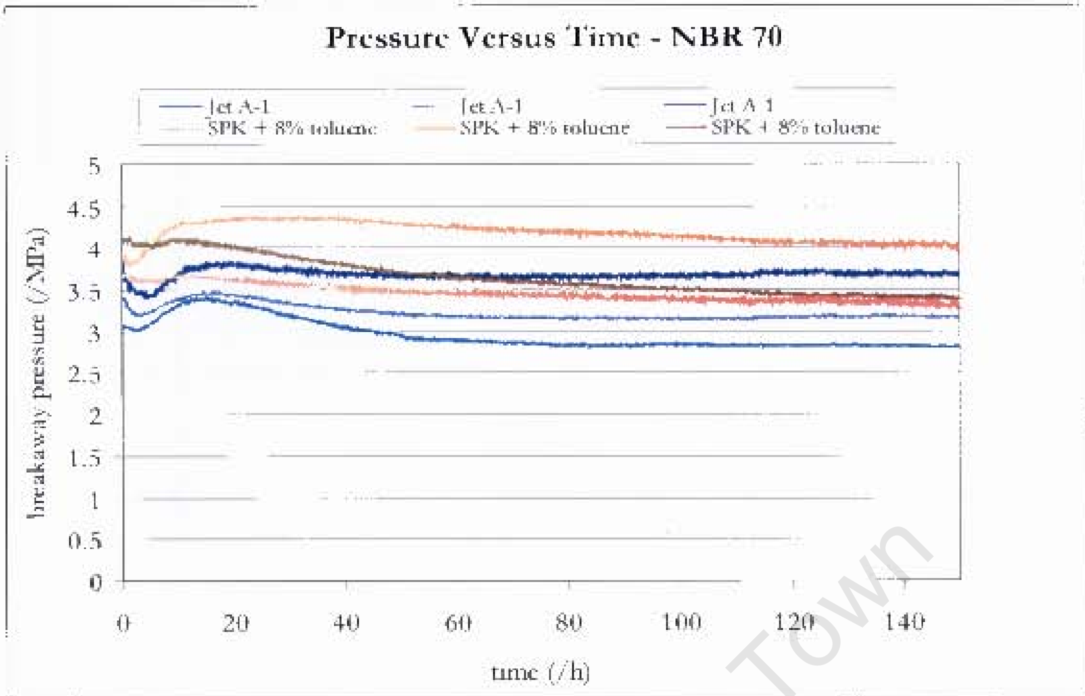
Pressure Versus Time - NBR 70
Jet A-1
SPK + 8% toluene
Jet A-1
SPK + 8% toluene
Jet A-1
SPK + 8% toluene
breakaway pressure (/MPa)
time (/h)

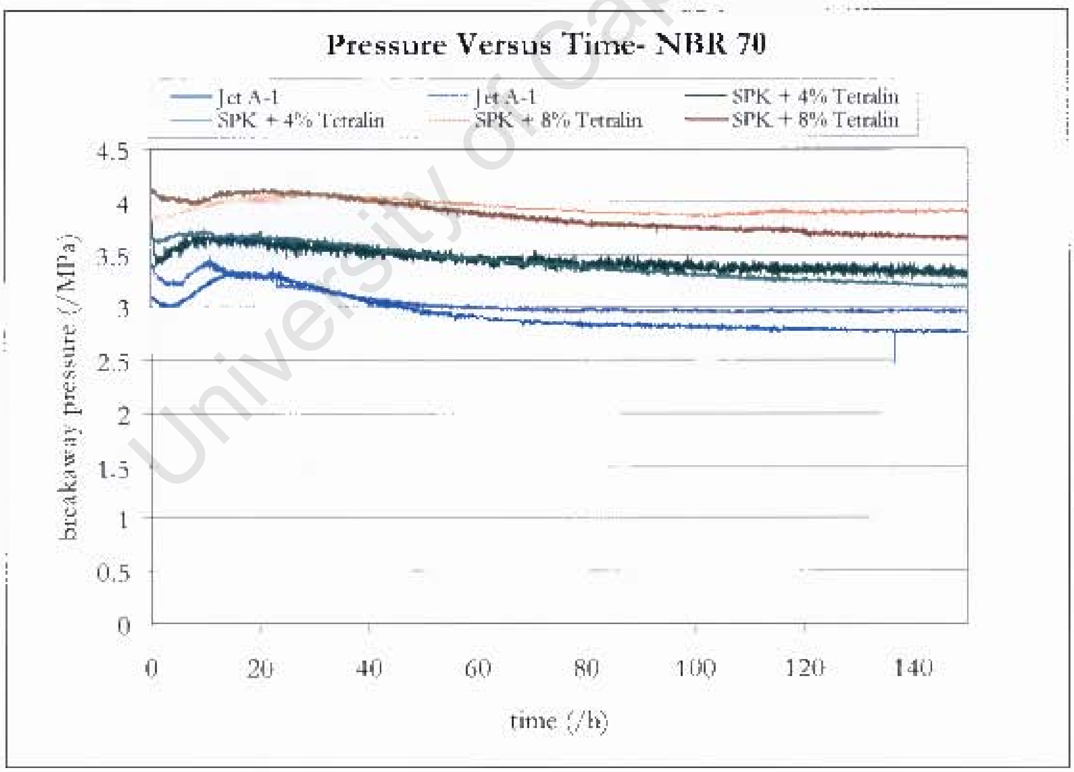
Pressure Versus Time- NBR 70
Jet A-1
SPK + 4% Tetralin
Jet A-1
SPK + 8% Tetralin
SPK + 4% Tetralin
SPK + 8% Tetralin
breakaway pressure (/MPa)
time (/h)

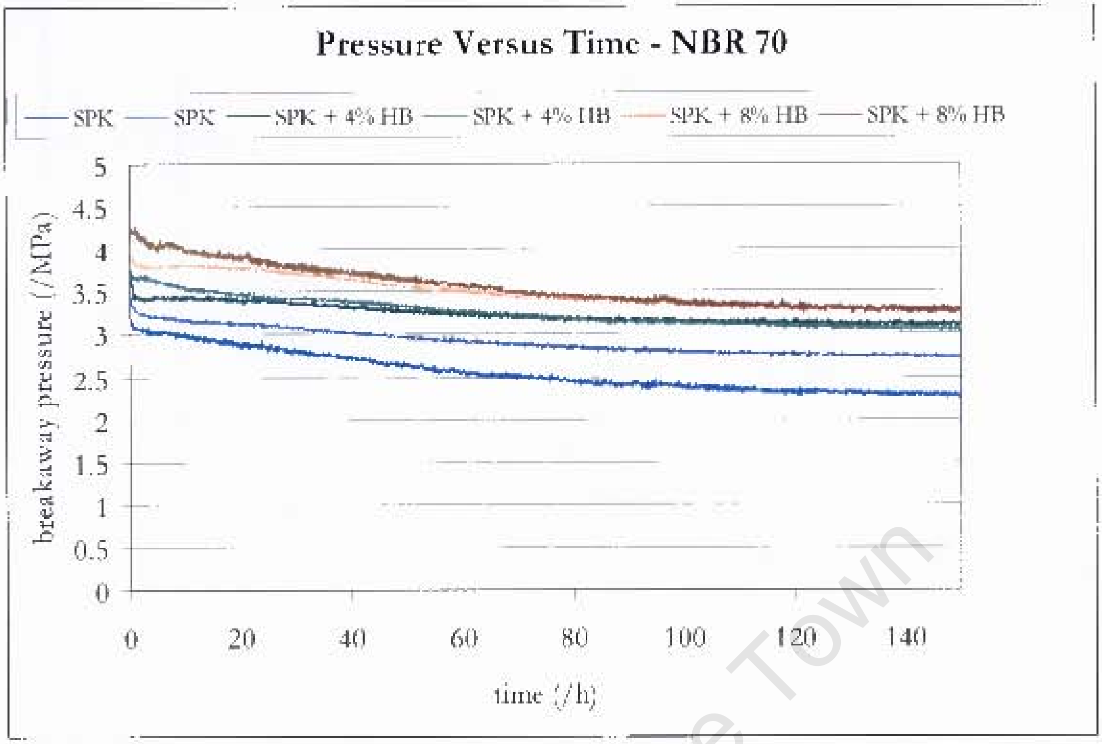
Pressure Versus Time - NBR 70
SPK
SPK
SPK + 4% HB
SPK + 4% HB
SPK + 8% HB
SPK + 8% HB
breakaway pressure (/MPa)
time (/h)

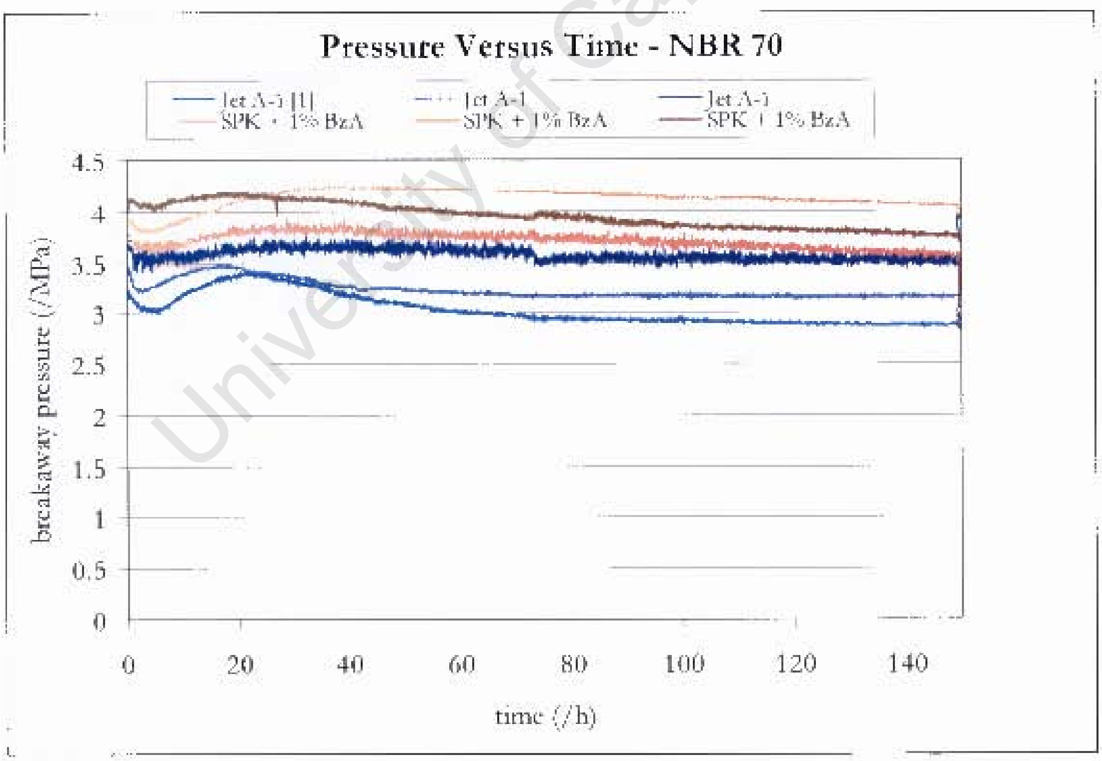
Pressure Versus Time - NBR 70
Jet A-1 [1]
Jet A-1
Jet A-1
SPK + 1% BzA
SPK + 1% BzA
SPK + 1% BzA
breakaway pressure (/MPa)
time (/h)

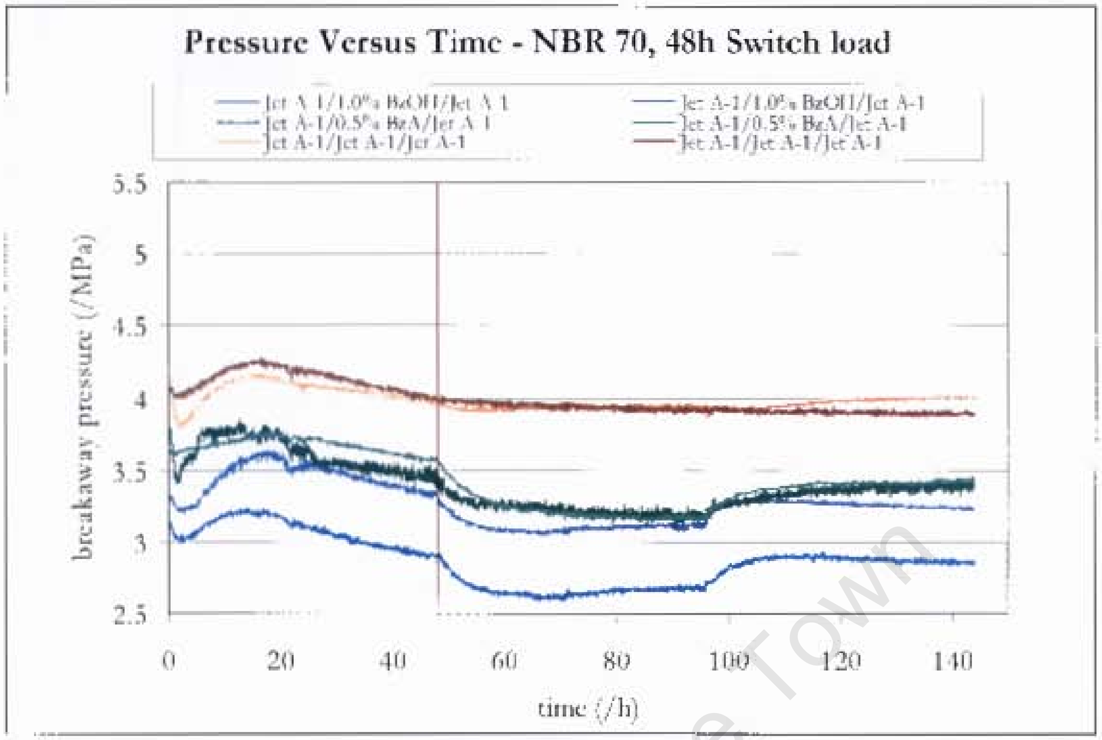
Pressure Versus Time - NBR 70, 48h Switch load
Jet A-1/1.0% BzOH/Jet A-1
Jet A-1/1.0% BzOH/Jet A-1
Jet A-1/0.5% BzA/Jet A-1
Jet A-1/0.5% BzA/Jet A-1
Jet A-1/Jet A-1/Jet A-1
Jet A-1/Jet A-1/Jet A-1
breakaway pressure (/MPa)
5.5
5
4.5
4
3.5
3
2.5
0
20
40
60
80
100
120
140
time (/h)